1.9 Oxygen-Centered Radicals
Zhang, J., Liu, D., Chen, Y., *Science of Synthesis: Free Radicals: Fundamentals and Applications in Organic Synthesis,* (2021) **1**, 323.

DOI 10.1055/sos-SD-234-00177

This chapter was published in
Science of Synthesis: Free Radicals: Fundamentals and Applications in Organic Synthesis 1

ISSN (print) 2510-5469
ISSN (online) 2566-7297

ISBN (print) 978-3-13-243552-0
ISBN (PDF) 978-3-13-244216-0
DOI 10.1055/b000000087

Structure searchable version available at:
sos.thieme.com

Copyright © 2021 Georg Thieme Verlag KG, Stuttgart, Germany
All rights reserved.
This document is for the personal use of **Professor Yiyun Chen**
only and may not be distributed to third parties.

Chinese Academy of Sciences
Shanghai Institute of Organic Chemistry
345 Lingling Road
Shanghai, 200032
China



Georg Thieme Verlag KG
Stuttgart · New York

1.9 Oxygen-Centered Radicals

J. Zhang, D. Liu, and Y. Chen

General Introduction

Oxygen-centered radicals ($R^1O^•$) are important reactive intermediates in organic synthesis and include carboxyl (R^1 = acyl), alkoxyl (R^1 = alkyl), phenoxyl (R^1 = aryl), and other related oxygen-containing radicals such as vinyloxy radicals (R^1 = vinyl).[1–8] One typical reactivity of oxygen-centered radicals is hydrogen-atom transfer (HAT), due to the high bond-dissociation energy of the O—H bond ($E_{(O\text{-}H)}$ = ~105 kcal/mol) (Scheme 1).[9] Another major reactivity of oxygen-centered radicals is β-fragmentation to form a C=O bond, which leads to either elimination of carbon dioxide from carboxyl radicals or elimination of ketones/aldehydes from alkoxyl radicals. Other reactivities of oxygen-centered radicals include radical addition to unsaturated carbon–carbon bonds and rearrangement reactions. Due to the high reactivity of oxygen-centered radicals, they easily undergo the typical reactivity described above to yield stable carbon-centered radicals, which can be further captured by radical acceptors or rearranged to construct carbon–carbon or carbon–heteroatom bonds.

Scheme 1 Typical Reactivity of Oxygen-Centered Radicals

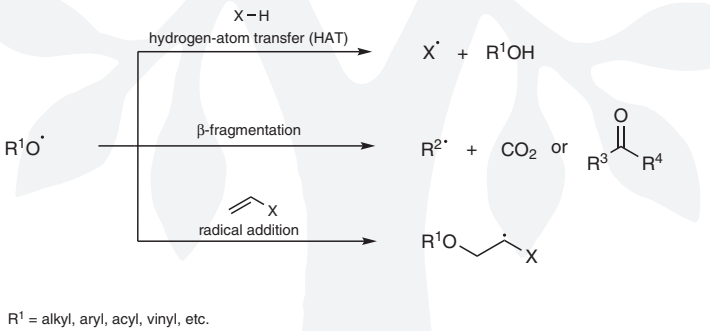

R^1 = alkyl, aryl, acyl, vinyl, etc.

Oxygen-centered radicals can be formed either by single-electron oxidation or single-electron reduction (Scheme 2). Widely used oxygen-centered radical precursors include O—H containing compounds, such as carboxylic acids, alcohols, and phenols, or O—X derivatives (X = N, O, I, etc.). Traditional methods for the generation of oxygen-centered radicals require ultraviolet light irradiation, 2,2′-azobisisobutyronitrile/tributyltin hydride/heat, or strong oxidants.[2,10] Although effective, these relatively harsh reaction conditions limit the chemoselectivity and functional-group compatibility. Recently, visible-light-induced reactions have emerged as a powerful radical initiation method and demonstrate excellent chemoselectivity, functional-group compatibility, and potential biomolecular compatibility due to the mild reaction conditions.[11–20] When a photocatalyst is present, under visible-light irradiation, the excited photocatalyst initiates electron-transfer or energy-transfer pathways with the oxygen-centered radical precursors to form the oxygen-centered radicals. In the absence of a photocatalyst, the oxygen-centered radical precursors may form electron donor–acceptor complexes and undergo electron-transfer reactions upon visible-light irradiation to yield oxygen-centered radicals. In addition, electro-

for references see p 377

Copyright © 2021 Georg Thieme Verlag KG, Stuttgart, Germany. All rights reserved. This document is for the personal use of – **Professor Yiyun Chen** – *Chinese Academy of Sciences, Shanghai, China,* only, and may not be distributed to third parties.

chemical methods have recently re-emerged for the generation of oxygen-centered radicals.[21] These novel methods for the generation of oxygen-centered radicals have enabled many new reactivities that have not been observed using the traditional reaction conditions.

Scheme 2 Generation of Oxygen-Centered Radicals

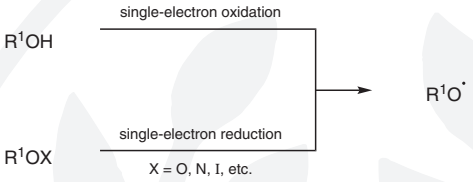

Because oxygen-centered radicals generated under traditional conditions have been extensively discussed in many excellent book chapters and review articles,[1–3,10,22–25] we will focus on recent advances in the generation of oxygen-centered radicals and their demonstrated reactivity, especially under visible-light-induced reaction conditions. As the nature of the substituent on oxygen dictates the reactivity of the oxygen-centered radicals, this chapter is divided into sections on carboxyl, alkoxyl, and other related oxygen-containing radicals. Each part provides a brief introduction to traditional methods for oxygen-centered radical generation, followed by the major advances in the reactivity enabled by visible-light-induced methods in chronological order. Peroxyl, hydroxyl, and cyclic nitroxyl radicals are not discussed (for nitroxyl radicals, see Section 1.2).

1.9.1 Carboxyl Radicals

1.9.1.1 Traditional Carboxyl Radical Generation and Functionalization

Radical decarboxylation has a long history in organic synthesis and is exemplified by the classical Hunsdiecker halogenative decarboxylation[26–28] and Barton decarboxylation reactions (Scheme 3).[29–31] Despite their elegant nature, these methods utilize either metal salts or the preactivated thiohydroxamate esters, for which starting materials, reagents, or waste production are costly. More importantly, the reaction conditions, such as the use of tributyltin hydride, limit further derivatization of the generated carbon-centered radicals.

Scheme 3 Traditional Carboxyl Radical Generation[26–31]

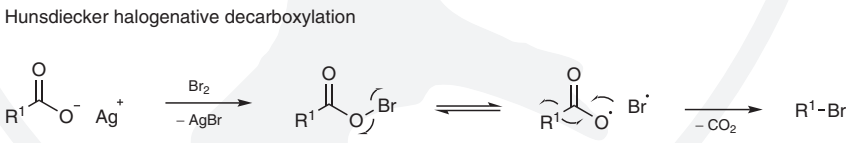

Copyright © 2021 Georg Thieme Verlag KG, Stuttgart, Germany. All rights reserved. This document is for the personal use of – Professor Yiyun Chen – Chinese Academy of Sciences, Shanghai, China, only, and may not be distributed to third parties.

Barton decarboxylation

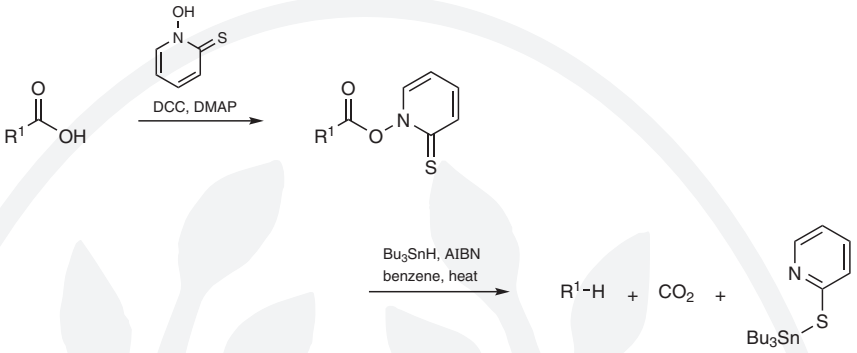

1.9.1.2 Visible-Light-Induced Carboxyl Radical Generation and Functionalization

Recently, a series of visible-light-induced decarboxylative cross-coupling reactions have been achieved. In general, the photocatalyst PC absorbs photons under visible-light irradiation to reach an excited state PC*. For photooxidative catalysis, the carboxylate anion is oxidized by PC* via single-electron transfer (SET). As a result, carbon dioxide elimination releases a carbon-centered radical and a proton; the reduced photocatalyst $PC^{\bullet -}$ reduces the electron acceptor A to regenerate the photocatalyst PC, simultaneously forming a radical anion $A^{\bullet -}$ (Scheme 4). Alternatively, in photoreductive catalysis, the excited state PC* is reduced by the electron donor D to generate the $PC^{\bullet -}$ species, which subsequently reduces a carboxylic acid derivative to generate a carbon-centered radical after the release of carbon dioxide and the anion X^- (Scheme 4).

Scheme 4 Visible-Light-Induced Carboxyl Radical Generation in Photooxidative and Photoreductive Catalysis

photooxidative catalysis

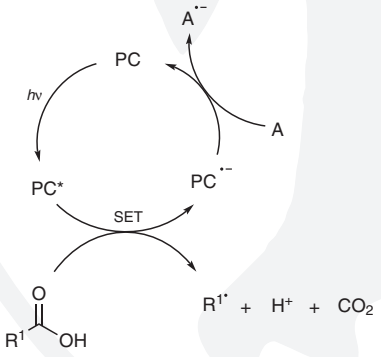

for references see p 377

Copyright © 2021 Georg Thieme Verlag KG, Stuttgart, Germany. All rights reserved. This document is for the personal use of – **Professor Yiyun Chen** – *Chinese Academy of Sciences, Shanghai, China,* only, and may not be distributed to third parties.

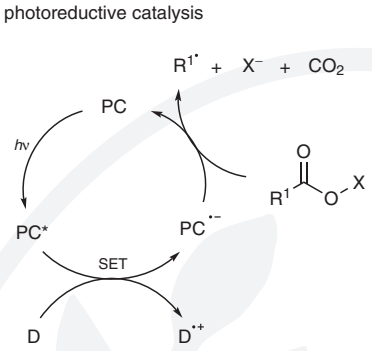

1.9.1.2.1 Alkyl Carboxyl Radicals

In 1991, the Okada group reported the first decarboxylative radical reaction enabled by visible-light photocatalysis.[32] Carbon-centered radical intermediates are generated from *N*-(acyloxy)phthalimides after decarboxylation in the presence of tris(2,2′-bipyridyl)ruthenium(II) chloride {[Ru(bipy)$_3$]Cl$_2$} under visible-light irradiation. For example, the reaction of *N*-(acyloxy)phthalimide **1** with methyl vinyl ketone (**2**) gives methyl ketone **3** in 68% yield (Scheme 5). Mechanistically, 1-benzyl-1,4-dihydronicotinamide first reduces the excited ruthenium(II) species to ruthenium(I), which then reduces the *N*-(acyloxy)phthalimide to form the radical anion **4**. Subsequently, carbon dioxide is eliminated from **4** to give carbon-centered radical **5**. This radical adds to the alkene to produce intermediate radical **6**, which is then reduced by 1-benzyl-1,4-dihydronicotinamide to form the product (Scheme 5).[32] In 2012, the Overmann group demonstrated a visible-light-induced decarboxylative addition as the key step for the synthesis of the complex molecule (−)-aplyviolene.[33]

Scheme 5 Decarboxylative Alkylation of *N*-(Acyloxy)phthalimides[32]

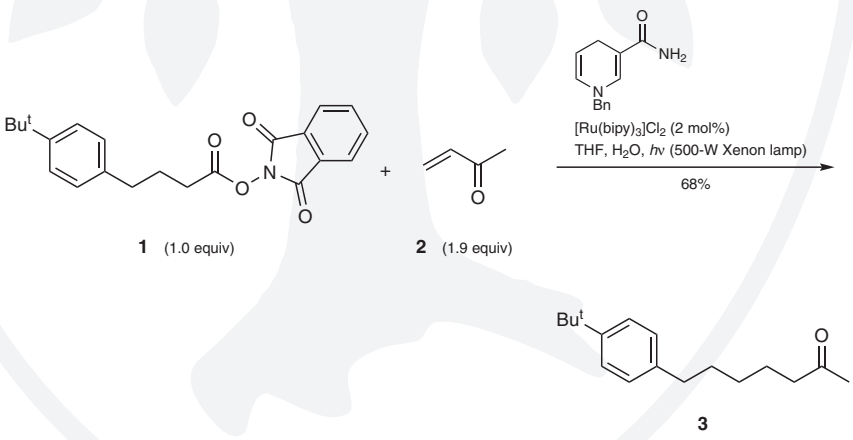

Copyright © 2021 Georg Thieme Verlag KG, Stuttgart, Germany. All rights reserved. This document is for the personal use of – Professor Yiyun Chen – *Chinese Academy of Sciences, Shanghai, China*, only, and may not be distributed to third parties.

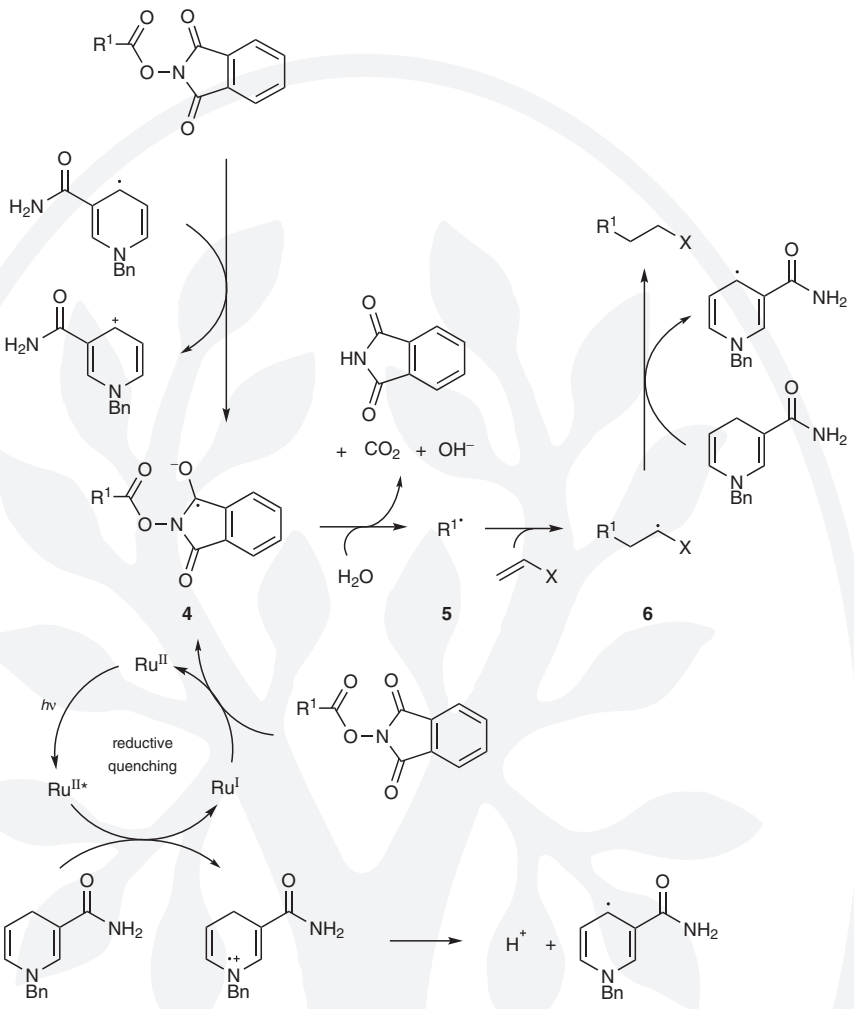

In 2013, the Zhu group reported the visible-light-induced decarboxylative tandem coupling reaction of phenyliodine(III) dicarboxylates in the presence of tris[2-(2-pyridyl)phenyl]iridium(III) [*fac*-Ir(ppy)$_3$]. For example, the reaction of *N*-methyl-*N*-phenyl-2-methylacrylamide (**7**) with (diacetoxyiodo)benzene gives 3-ethyl-1,3-dimethyl-2,3-dihydroindol-2(1*H*)-one (**8**) in 83% yield (Scheme 6). Mechanistically, the excited iridium(III) species is oxidized by a phenyliodine(III) dicarboxylate **9** to generate an iridium(IV) species and an iodine-centered radical **10**, which then undergoes a decarboxylation/radical C—H functionalization cascade to give cyclohexadienyl radical **11** after carbon dioxide and phenyl iodide extrusion and addition of the carbon-centered radical to the acrylamide. Subsequently, radical **11** is converted into cation **12** by single-electron transfer with iridium(IV) or a phenyliodine(III) dicarboxylate **9**, thus completing the catalytic cycle. Finally, cation **12** is deprotonated to generate the product **13** (Scheme 6).[34]

for references see p 377

Copyright © 2021 Georg Thieme Verlag KG, Stuttgart, Germany. All rights reserved. This document is for the personal use of – **Professor Yiyun Chen** – *Chinese Academy of Sciences, Shanghai, China,* only, and may not be distributed to third parties.

Scheme 6 Decarboxylative Tandem Coupling of Phenyliodine(III) Dicarboxylates[34]

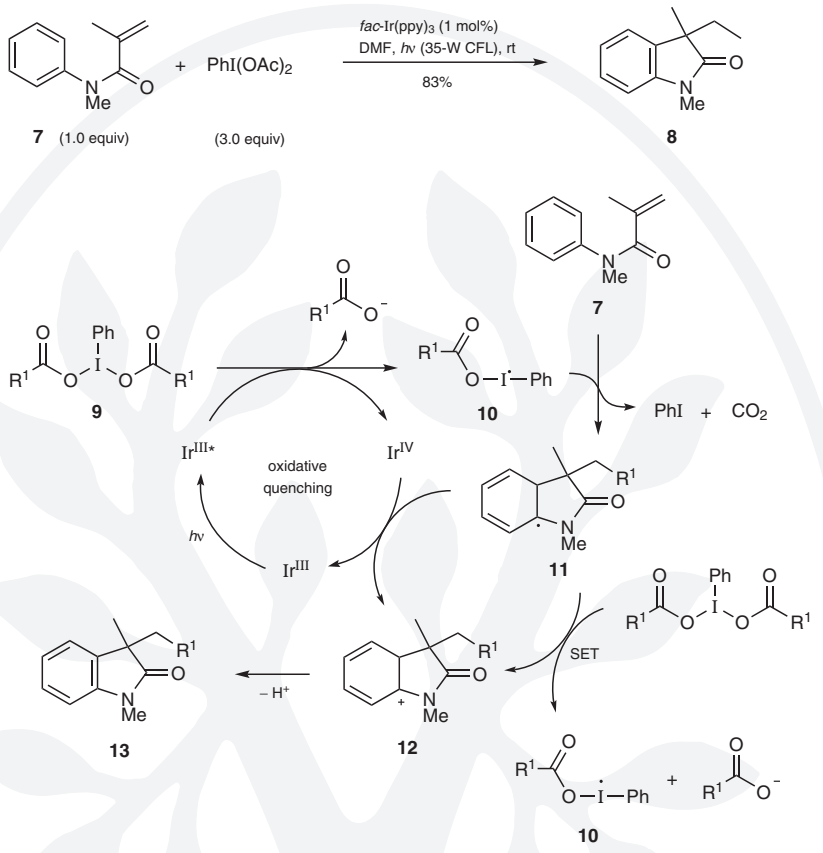

In 2015, the Chen group reported reductive decarboxylative alkynylation and allylation reactions with *N*-(acyloxy)phthalimide derivatives (e.g., **14** and **17**) and alkynyl/allyl sulfones (e.g., **15** and **18**; Scheme 7).[35,36] In both cases, the reactions proceed by reductive single-electron transfer, followed by radical addition and desulfonation to afford the decarboxylative coupling products (e.g., **16** and **19**). The functional-group tolerance and chemoselectivity of the reactions are excellent under the very mild reaction conditions. Notably, the reaction is biomolecule-compatible under neutral aqueous conditions without affecting the enzymatic activity of human carbonic anhydrase II (HCA II). Later, the Fu group employed a similar strategy for the coupling of bis[*N*-(acyloxy)phthalimides] and alkynyl sulfones to afford various substituted methylenecyclopentane analogues.[37]

Copyright © 2021 Georg Thieme Verlag KG, Stuttgart, Germany. All rights reserved. This document is for the personal use of – **Professor Yiyun Chen** – *Chinese Academy of Sciences, Shanghai, China,* only, and may not be distributed to third parties.

Scheme 7 Decarboxylative Alkynylation and Allylation of *N*-(Acyloxy)phthalimides under Biomolecule-Compatible Conditions[35,36]

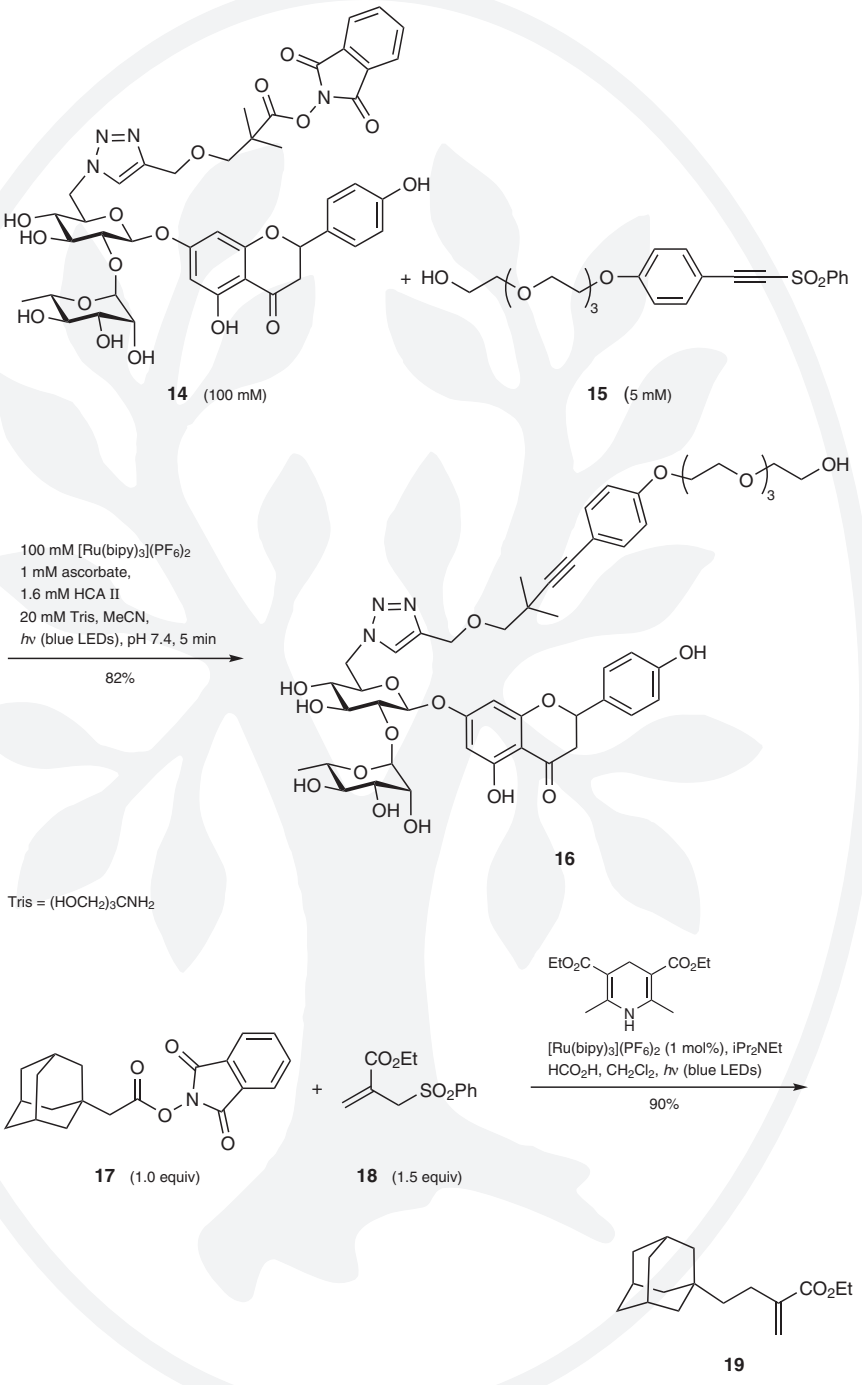

for references see p 377

Copyright © 2021 Georg Thieme Verlag KG, Stuttgart, Germany. All rights reserved. This document is for the personal use of – **Professor Yiyun Chen** – *Chinese Academy of Sciences, Shanghai, China*, only, and may not be distributed to third parties.

In comparison to phenyliodine(III) carboxylates and phthalamide esters, radical decarboxylation of carboxylic acids represents an attractive alternative. In 2014, the MacMillan group disclosed a visible-light-induced iridium/nickel dual catalysis approach for the radical cross coupling of α-heteroatom-substituted carboxylic acids with aryl halides. For example, in the presence of iridium complex **20** and cesium carbonate, the reaction of *N*-(*tert*-butoxycarbonyl)proline (**21**) and 4-iodotoluene furnishes *tert*-butyl 2-(4-tolyl)pyrrolidine-1-carboxylate (**22**) in 78% yield (Scheme 8). Mechanistically, in the photocatalysis cycle, the carboxylate is oxidized by the excited iridium(III) species to generate the radical **24** after decarboxylation. In the nickel catalysis cycle, oxidative addition of nickel(0) to the aryl halide delivers the arylnickel(II) complex **23**, which further reacts with radical **24** to yield the nickel(III) complex **25**. Finally, reductive elimination of the nickel(III) complex generates the cross-coupled product **22** and the nickel(I) species **26**, which re-oxidizes iridium(II) to iridium(III).[38]

Scheme 8 Decarboxylative Arylation of Carboxylic Acids by Dual Photoredox/Nickel Catalysis[38]

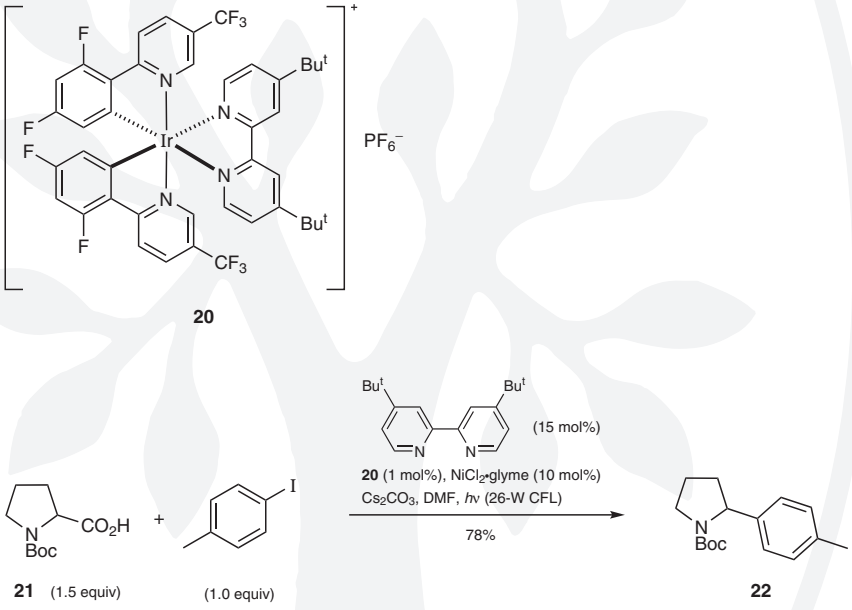

Copyright © 2021 Georg Thieme Verlag KG, Stuttgart, Germany. All rights reserved. This document is for the personal use of – **Professor Yiyun Chen** – *Chinese Academy of Sciences, Shanghai, China,* only, and may not be distributed to third parties.

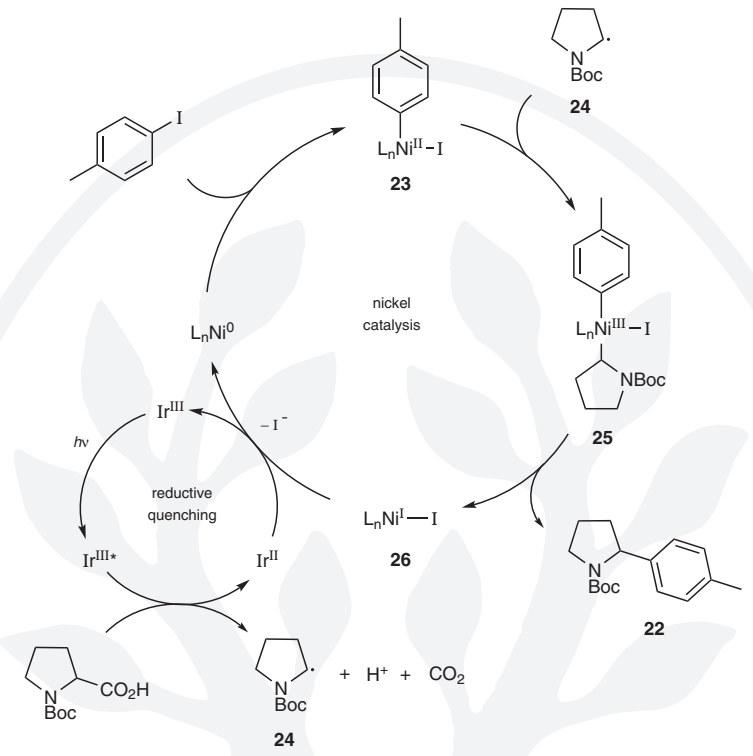

The Macmillan group later expanded the reaction to the cross coupling of alkyl carboxylic acids with vinyl halides and alkyl halides using iridium complex **20** or **27** as photocatalyst (Scheme 9).[39,40]

Scheme 9 Decarboxylative Alkenylation and Alkylation of Carboxylic Acids by Dual Photoredox/Nickel Catalysis[39,40]

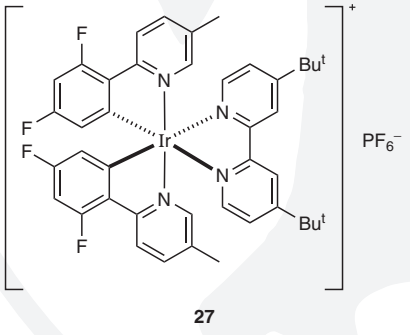

for references see p 377

Copyright © 2021 Georg Thieme Verlag KG, Stuttgart, Germany. All rights reserved. This document is for the personal use of – **Professor Yiyun Chen** – *Chinese Academy of Sciences, Shanghai, China*, only, and may not be distributed to third parties.

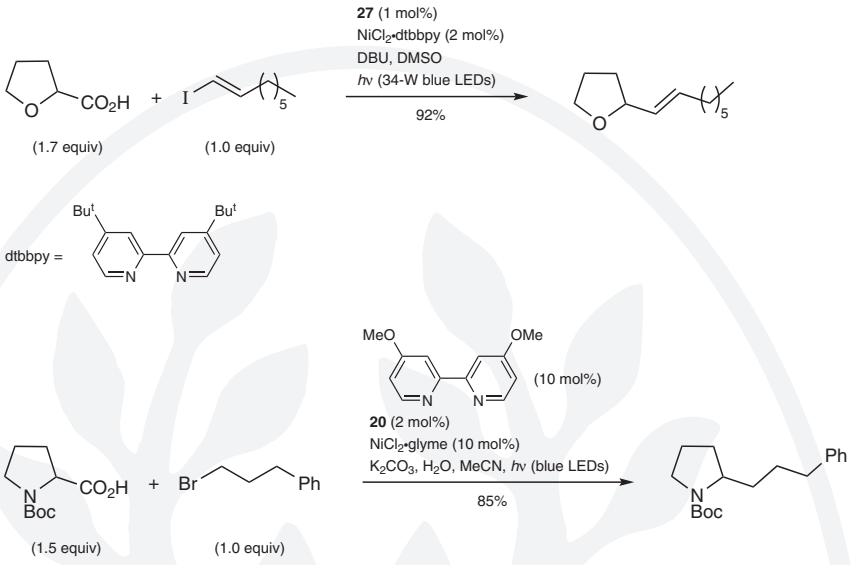

In 2015, the Xiao[16,41] and Waser[42] groups independently reported the radical decarboxylative alkynylation of alkyl carboxylic acids with alkynylbenziodoxole derivatives (Scheme 10). Interestingly, different bases (CsOBz vs. Cs_2CO_3) are used in combination with otherwise similar reaction conditions employing iridium complex **20** as photocatalyst. In addition, the Xiao group demonstrated the carbonylative addition to form the alkynone products (e.g., **28**) by conducting the reaction under 60 bar of carbon monoxide. In both cases, the catalytic cycles are proposed to involve initial oxidation of the carboxylate by the excited iridium(III) species, followed by an addition/elimination sequence with the alkynylbenziodoxole to produce the alkyne and the benziodoxole radical, which subsequently closes the catalytic cycle by oxidizing iridium(II).

Scheme 10 Decarboxylative Alkynylation of Alkyl Carboxylic Acids[41,42]

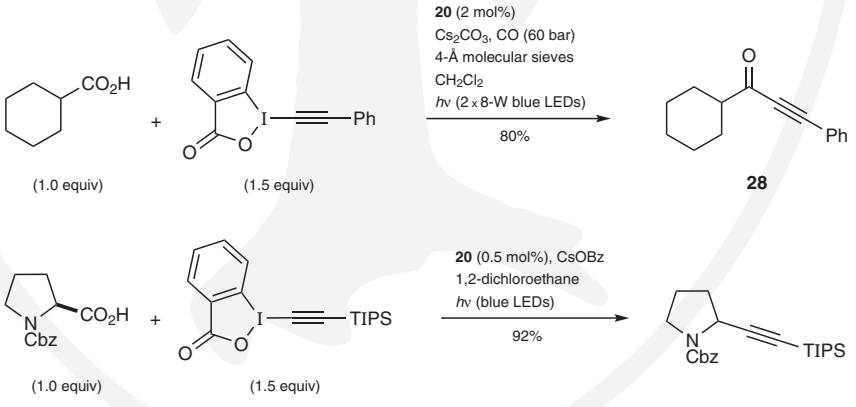

The Barton decarboxylation is a classical strategy for the hydrodecarboxylation of carboxylic acids; however, preactivation of carboxylic acids as activated esters is required. To this end, in 2015, the Nicewicz group reported a photocatalytic decarboxylation of carboxylic acids (e.g., **30** and **32**) to give hydrocarbons (e.g., **31** and **33**, respectively), in which the acridinium-derivative **29** (Mes-Acr-Ph) is used as the organic photocatalyst. Mechanistically, the carboxylic acid is deprotonated and single-electron oxidation by the excited photo-

Copyright © 2021 Georg Thieme Verlag KG, Stuttgart, Germany. All rights reserved. This document is for the personal use of – Professor Yiyun Chen – Chinese Academy of Sciences, Shanghai, China, only, and may not be distributed to third parties.

catalyst results in the formation of the carboxyl radical. Subsequent decarboxylation and hydrogen-atom abstraction from benzenethiol furnishes the hydrodecarboxylation product (Scheme 11).[43]

Scheme 11 Decarboxylative Hydrogenation of Carboxylic Acids[43]

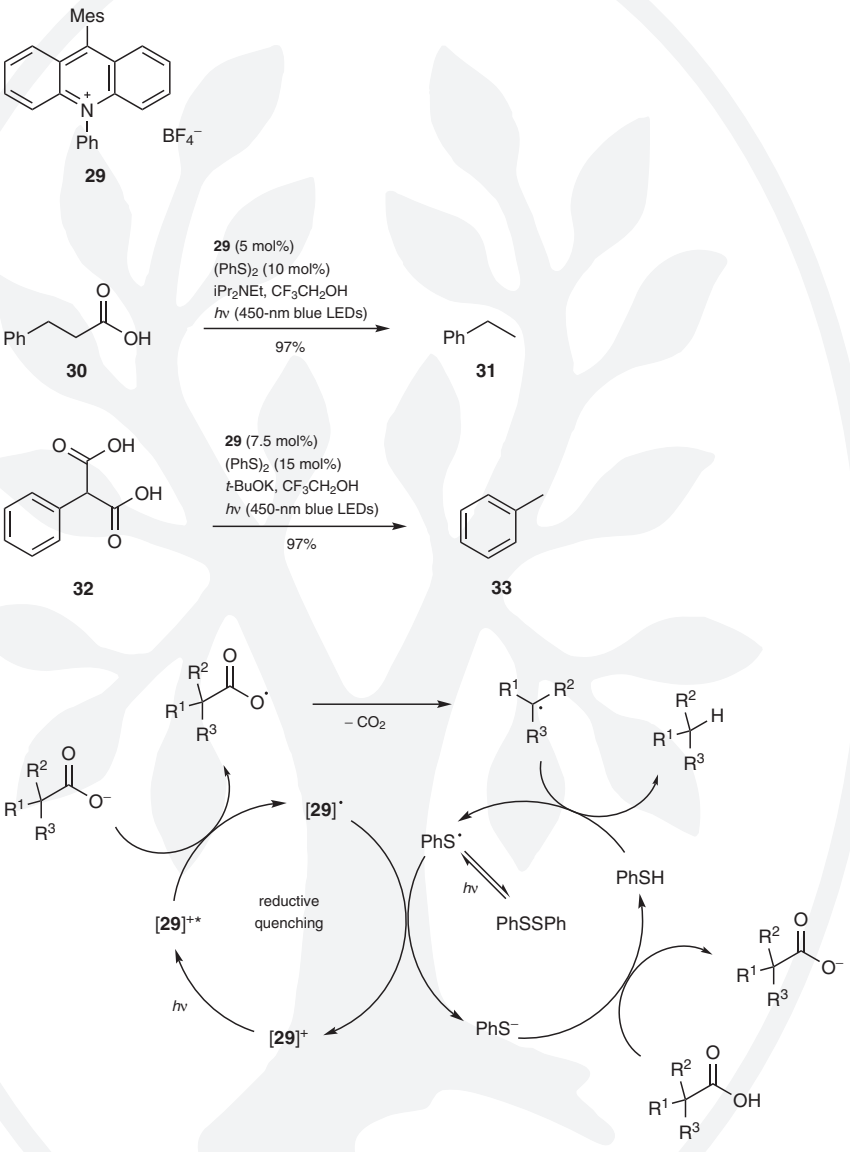

In 2015, the MacMillan group reported a decarboxylative fluorination of alkyl carboxylic acids (e.g., **34**) with 1-(chloromethyl)-4-fluoro-1,4-diazoniabicyclo[2.2.2]octane bis(tetrafluoroborate) (Selectfluor, **35**) as the electrophilic fluorine source (Scheme 12).[44] This reaction is a photocatalytic alternative to the Hunsdiecker halogenative decarboxylation. The excited iridium(III) species is first oxidized by Selectfluor to form an iridium(IV) species, which then oxidizes the carboxylate to form a carboxyl radical for the subsequent decarboxylative fluorination by Selectfluor. This concept was later utilized by the Glorius group to achieve radical chlorination, bromination, and iodination of alkyl carboxylic acids.[45]

for references see p 377

Copyright © 2021 Georg Thieme Verlag KG, Stuttgart, Germany. All rights reserved. This document is for the personal use of – **Professor Yiyun Chen** – *Chinese Academy of Sciences, Shanghai, China,* only, and may not be distributed to third parties.

Scheme 12 Decarboxylative Fluorination of Carboxylic Acids[44]

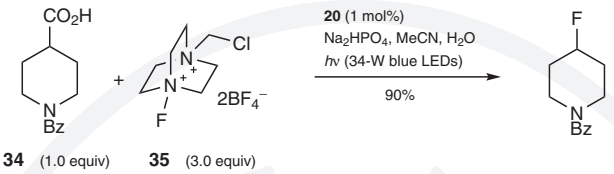

34 (1.0 equiv) **35** (3.0 equiv)

In 2019, the Baran group reported the synthesis of hindered ethers by electrochemical oxidation of simple carboxylic acids. For example, the reaction of 2-methyl-2-phenylpropanoic acid (**36**) and (*R*)-1-phenylethan-1-ol (**37**) gives (*R*)-[2-(1-phenylethoxy)propan-2-yl]benzene (**38**) in 77% yield (Scheme 13).[46] The mechanism is likely to involve a rate-limiting oxidation of carboxylates at the anode to generate a high-energy carbocation (e.g., **39**), followed by nucleophilic attack of the alcohol to afford the ether product.

Scheme 13 Decarboxylative Etherification of Carboxylic Acids by Electrochemical Oxidation[46]

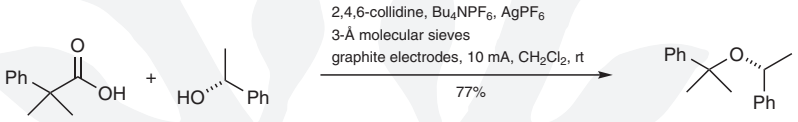

36 (1.0 equiv) **37** (3.0 equiv) **38**

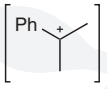

39

***tert*-Butyl 2-(4-Tolyl)pyrrolidine-1-carboxylate (22):**[38]
An oven-dried 40-mL vial equipped with a Teflon septum and magnetic stirrer bar was charged with iridium complex **20** (4.5 mg, 4.0 μmol, 1 mol%), $NiCl_2$•glyme (8.8 mg, 0.04 mmol, 10 mol%), 4,4′-di-*tert*-butyl-2,2′-bipyridyl (16.1 mg, 0.06 mmol, 15 mol%), 4-iodotoluene (89 mg, 0.40 mmol, 1.0 equiv), *N*-(*tert*-butoxycarbonyl)proline (**21**; 129 mg, 0.60 mmol, 1.5 equiv), Cs_2CO_3 (196 mg, 0.60 mmol, 1.5 equiv), and DMF (20 mL). The mixture was degassed by bubbling with a stream of argon for 20 min, then irradiated with two 26-W fluorescent lamps (at approximately 2-cm away from the light source) for 72 h, diluted with sat. aq $NaHCO_3$, and extracted with Et_2O (3 × 100 mL). The combined organic extracts were washed successively with H_2O and brine, dried ($MgSO_4$), filtered, and concentrated under reduced pressure. The crude product was purified by flash chromatography (silica gel, EtOAc/hexane 15:85); yield: 81 mg (78%).

(*R*)-[2-(1-Phenylethoxy)propan-2-yl]benzene (38):[46]
With no precautions to exclude air or moisture, the 5-mL ElectraSyn vial (equipped with a stirrer bar) was charged with 2-methyl-2-phenylpropanoic acid (**36**; 33 mg, 0.2 mmol, 1 equiv), (*R*)-1-phenylethan-1-ol (**37**; 73 mg, 0.6 mmol, 3 equiv), 2,4,6-collidine (73 mg, 0.6 mmol, 3 equiv), Bu_4NPF_6 (116 mg, 0.3 mmol, 1.5 equiv), 3-Å molecular sieves (150 mg), $AgPF_6$ (76 mg, 0.3 mmol, 1.5 equiv), and CH_2Cl_2 (3.0 mL). The ElectraSyn vial cap, equipped with anode (graphite) and cathode (graphite), was fitted so that the electrodes were in the mixture. The mixture was first stirred for 5 min and then electrolyzed at a constant current of 10 mA for 3 h. The ElectraSyn vial cap was removed, and the electrodes were rinsed with Et_2O (2 mL). The rinse was combined with the crude mixture,

Copyright © 2021 Georg Thieme Verlag KG, Stuttgart, Germany. All rights reserved. This document is for the personal use of – Professor Yiyun Chen – *Chinese Academy of Sciences, Shanghai, China,* only, and may not be distributed to third parties.

which was further diluted with Et_2O (30 mL). The resulting mixture was washed successively with 2 M aq HCl (20 mL) and aq $NaHCO_3$ (20 mL), dried (Na_2SO_4), filtered, and concentrated under reduced pressure. The crude material was purified by flash column chromatography (silica gel, hexanes/Et_2O gradient 50:1 to 5:1); yield: 37 mg (77%).

1.9.1.2.2 α-Oxo Acids

In 2014, the Lei group reported the visible-light-induced decarboxylative amination of α-oxo acids. For example, the reaction of 2-oxo-2-phenylacetic acid (**40**) with 4-toluidine (**41**) in the presence of dichlorotris(1,10-phenanthroline)ruthenium(II) chloride {[Ru(phen)$_3$]Cl$_2$} gives *N*-(4-tolyl)benzamide (**42**) in 85% yield. Mechanistically, the excited ruthenium(II) species is first quenched by the amine to generate ruthenium(I), which then undergoes single-electron transfer (SET) with molecular oxygen to yield the superoxide radical anion and regenerate ruthenium(II). The superoxide radical anion subsequently abstracts an electron from the deprotonated α-oxo acid to generate the oxo acid radical **43**. This radical then undergoes decarboxylation to generate the acyl radical **44** which further reacts with the amine to deliver the amide product after single-electron transfer (Scheme 14).[47]

Scheme 14 Decarboxylative Amination of α-Oxo Acids[47]

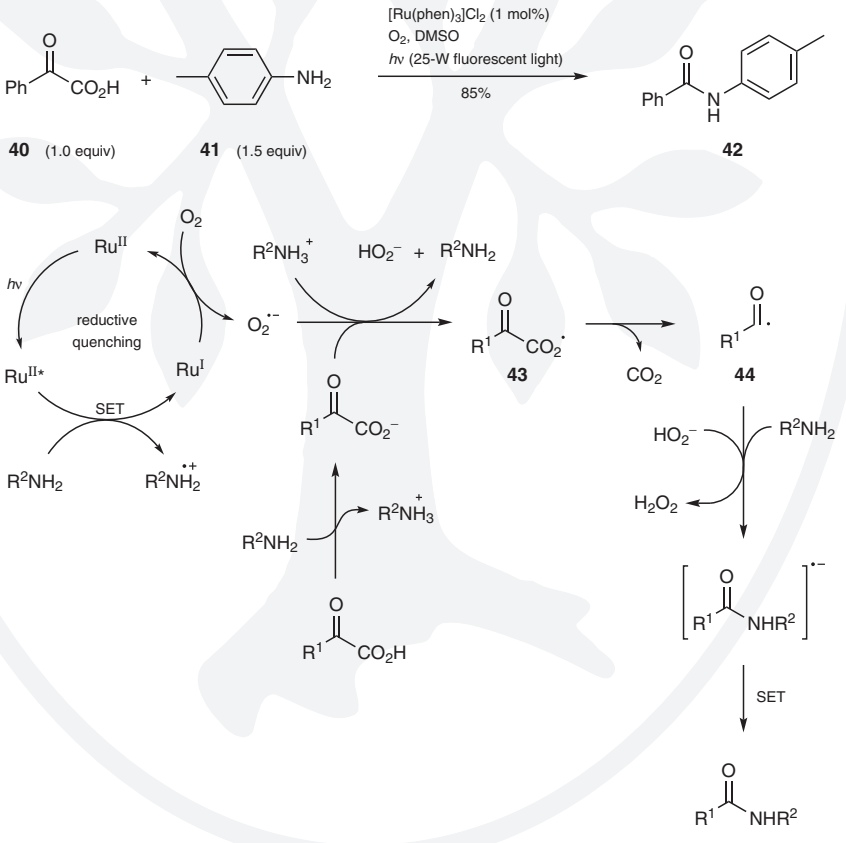

In 2015, the MacMillan group developed a dual-catalytic system involving photoredox and nickel catalysis for the decarboxylative arylation of α-oxo acids with aryl halides. The carboxylate anion is first oxidized by an excited iridium(III) species to generate a nucleophilic acyl radical with formation of an iridium(II) species and carbon dioxide extrusion. Si-

for references see p 377

Copyright © 2021 Georg Thieme Verlag KG, Stuttgart, Germany. All rights reserved. This document is for the personal use of – **Professor Yiyun Chen** – *Chinese Academy of Sciences, Shanghai, China,* only, and may not be distributed to third parties.

multaneously, the nickel catalysis cycle is initiated by oxidative addition of an aryl halide onto nickel(0). The resulting electrophilic arylnickel(II) complex captures the nucleophilic acyl radical to afford an acyl(aryl)nickel(III) complex, which further undergoes reductive elimination to yield the product and the corresponding nickel(I) complex. Finally, the reduced iridium(II) undergoes single-electron transfer to nickel(I) and regenerates both iridium(III) and nickel(0) for the catalytic turnover. For example, the reaction of 2-oxo-2-phenylacetic acid (**40**) with 4-iodotoluene in the presence of iridium complex **20** furnishes phenyl 4-tolyl ketone (**45**) in 88% yield (Scheme 15).[48] Later, the Fu group reported a dual-catalytic system merging photoredox with palladium catalysis for a similar transformation.[49]

Scheme 15 Decarboxylative Arylation of an α-Oxo Acid by Dual Photoredox/Nickel Catalysis[48]

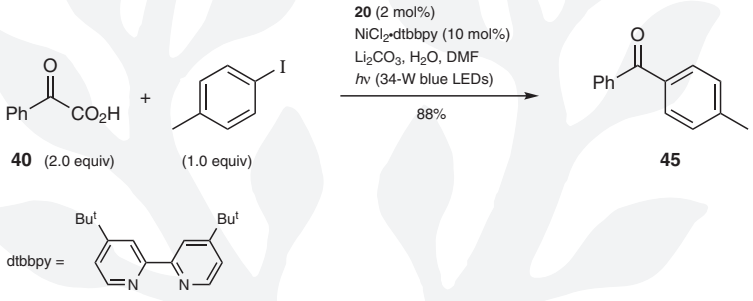

A previously reported palladium-catalyzed decarboxylative *ortho* acylation of *N*-phenylacetamides with α-oxo acids enables the synthesis of aryl ketones, but this transformation requires stoichiometric amounts of oxidants.[50] In 2015, the Wang group developed a dual photocatalytic/palladium system using a catalytic amount of the photocatalyst eosin Y and molecular oxygen to replace the chemical oxidants. For example, *N*-(2-benzoylphenyl)acetamide (**47**) is obtained from 2-oxo-2-phenylacetic acid (**40**) and *N*-phenylacetamide (**46**) in 80% yield (Scheme 16).[51]

Scheme 16 Decarboxylative Acylation with an α-Oxo Acid by Dual Photoredox/Palladium Catalysis[51]

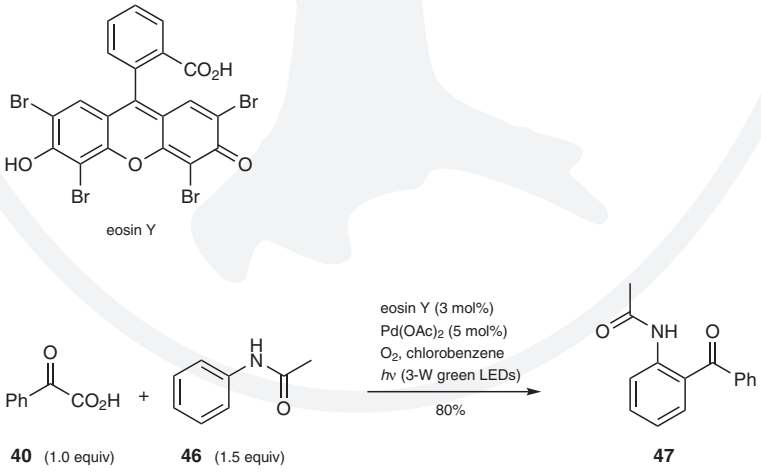

Copyright © 2021 Georg Thieme Verlag KG, Stuttgart, Germany. All rights reserved. This document is for the personal use of – Professor Yiyun Chen – *Chinese Academy of Sciences, Shanghai, China,* only, and may not be distributed to third parties.

Ynones, ynoates, and ynamides are versatile building blocks for the synthesis of heterocyclic compounds and natural products. In 2015, the Chen group synthesized these compounds from α-oxo acids and alkynylbenziodoxoles through a dual hypervalent iodine(III) reagent (HIR)/photoredox catalysis system. For example, in the presence of tris(2,2′-bipyridyl)ruthenium(II) hexafluorophosphate {$[Ru(bipy)_3](PF_6)_2$} and 1-acetoxy-1,2-benziodoxol-3-(1*H*)-one (**49**), the reaction of 2-oxo-2-phenylacetic acid (**40**) with 1-(4-tolylethynyl)-1,2-benziodoxol-3-(1*H*)-one (**48**) gives 1-phenyl-3-(4-tolyl)prop-2-yn-1-one (**50**) in 77% yield. Mechanistically, the reaction is initiated by formation of a benziodoxole–oxo acid complex **51** in situ from the α-oxo acid and 1-acetoxy-1,2-benziodoxol-3-(1*H*)-one (**49**), which is subsequently oxidized by ruthenium(III) to give an acyl radical **52** after decarboxylation. The acyl radical **52** then undergoes α-addition to an alkynylbenziodoxole to yield the ynone product, and the eliminated benziodoxole radical oxidizes the photoexcited ruthenium(II) species to complete the photoredox cycle (Scheme 17).[52] The hypervalent iodine(III) reagent/photoredox dual catalysis is compatible with biomolecular systems such as amino acids, nucleosides, oligosaccharides, nucleic acids, proteins, and cell lysates. Independently, the Wang group reported a decarboxylative alkynylation of α-oxo acids with bromoacetylenes under sunlight irradiation without photocatalysts.[53]

Scheme 17 Decarboxylative Alkynylation of α-Oxo Acids by Dual Photoredox/Hypervalent Iodine(III) Reagent Catalysis[52]

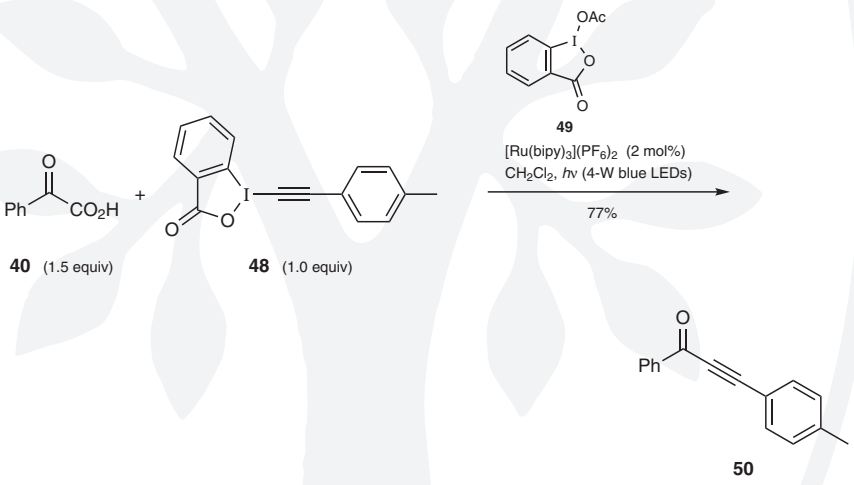

for references see p 377

Copyright © 2021 Georg Thieme Verlag KG, Stuttgart, Germany. All rights reserved. This document is for the personal use of – **Professor Yiyun Chen** – *Chinese Academy of Sciences, Shanghai, China,* only, and may not be distributed to third parties.

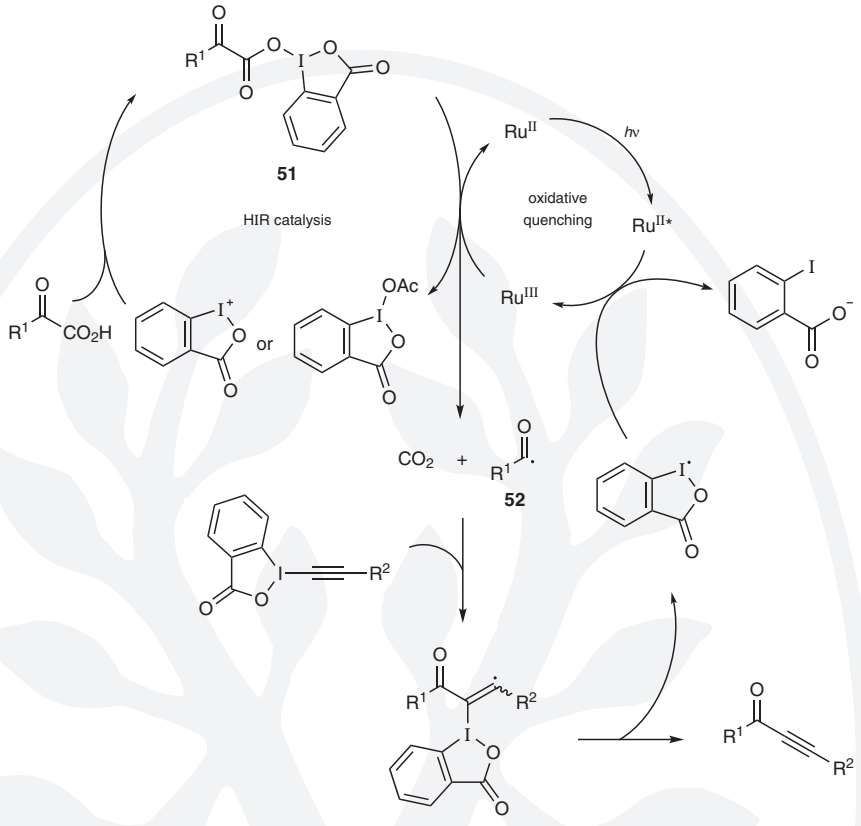

In 2019, the Chen group reported the visible-light-induced acyl radical Smiles rearrangement of α-oxo acids under mild and metal-free conditions. Using the dual catalysis of hypervalent iodine(III) reagent **49** and organophotocatalyst **53**, oxo acids (e.g., **54**) generate acyl radicals after decarboxylation and undergo 1,5-*ipso* addition to afford hydroxybenzophenones (e.g., **55**; Scheme 18).[54]

Scheme 18 Decarboxylative Smiles Rearrangement of an α-Oxo Acid by Dual Photoredox/Hypervalent Iodine(III) Reagent Catalysis[54]

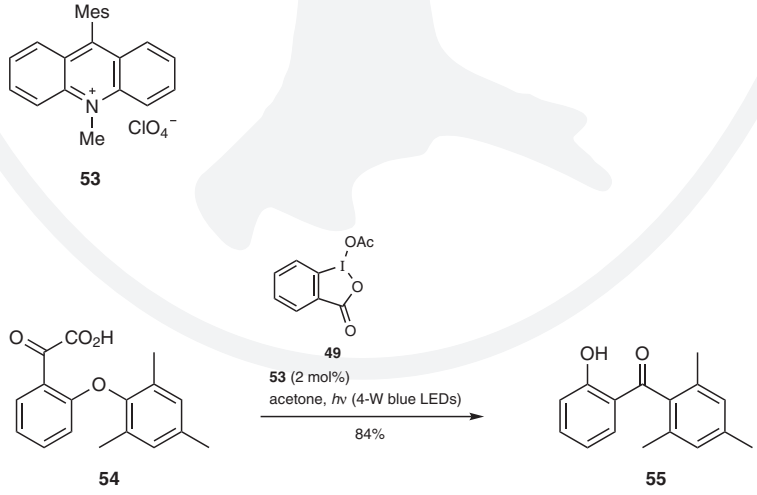

Copyright © 2021 Georg Thieme Verlag KG, Stuttgart, Germany. All rights reserved. This document is for the personal use of – Professor Yiyun Chen – Chinese Academy of Sciences, Shanghai, China, only, and may not be distributed to third parties.

In 2019, the Yu group reported the visible-light-induced radical acylation of imines via electron donor–acceptor (EDA) complexes (Scheme 19).[55] Upon visible-light irradiation, the EDA complex **57** between imine **56** and 2-oxo-2-phenylacetic acid (**40**) is excited and dissociates to a radical pair. After carbon dioxide elimination, the acyl radical **59** couples with the α-aminoalkyl radical **58** to give the coupling product **60**.

Scheme 19 Decarboxylative Acylation of an Imine and an α-Oxo Acid via an Electron Donor–Acceptor Complex[55]

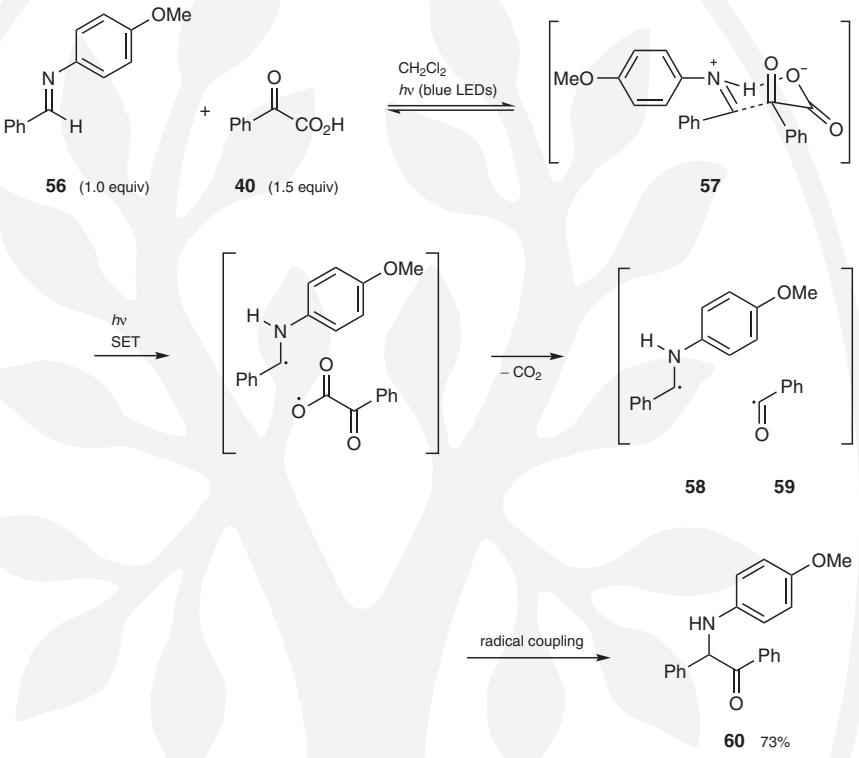

1-Phenyl-3-(4-tolyl)prop-2-yn-1-one (50):[52]

2-Oxo-2-phenylacetic acid (**40**; 45 mg, 0.30 mmol, 1.5 equiv), 1-(4-tolylethynyl)-1,2-benziodoxol-3-(1*H*)-one (**48**; 72 mg, 0.20 mmol), $[Ru(bipy)_3](PF_6)_2$ (3.4 mg, 4 μmol, 2 mol%), and 1-acetoxy-1,2-benziodoxol-3-(1*H*)-one (**49**; 61 mg, 0.20 mmol, 1.0 equiv) were placed in a 5-mL clear glass vial equipped with a magnetic stirrer bar. CH_2Cl_2 (2.0 mL) was added and the vial was sealed. The stirred mixture was then irradiated with blue LEDs (two 4-W LED light bulbs 10-cm away from the vial, 468 nm peak wavelength, 25 nm spectral half-wave width, composed of 55–65 LED units each with 60 mW, 3 V, 20 mA) at rt until TLC indicated complete consumption of the alkynylbenziodoxole **48** (typically 5 h). The mixture was concentrated and the crude product was purified by column chromatography; yield: 34 mg (77%).

for references see p 377

Copyright © 2021 Georg Thieme Verlag KG, Stuttgart, Germany. All rights reserved. This document is for the personal use of – **Professor Yiyun Chen** – *Chinese Academy of Sciences, Shanghai, China,* only, and may not be distributed to third parties.

1.9.1.2.3 Aryl Carboxyl Radicals

The decarboxylation of aryl carboxyl radicals is much slower than that of their aliphatic analogues and usually requires temperatures above 100 °C. In 2015, the Gonzalez-Gomez group reported a dehydrogenative lactonization of 2-arylbenzoic acids (e.g., **61**) at room temperature. The benzoyloxyl radical is generated by the excited photocatalyst **53** via single-electron transfer. This radical undergoes 6-*endo-trig* cyclization to afford a cyclized intermediate, which then yields the lactone (e.g., **62**) either by hydrogen-atom abstraction (HAT) or single-electron transfer/deprotonation processes (Scheme 20).[56]

Scheme 20 Lactonization of a 2-Arylbenzoic Acid[56]

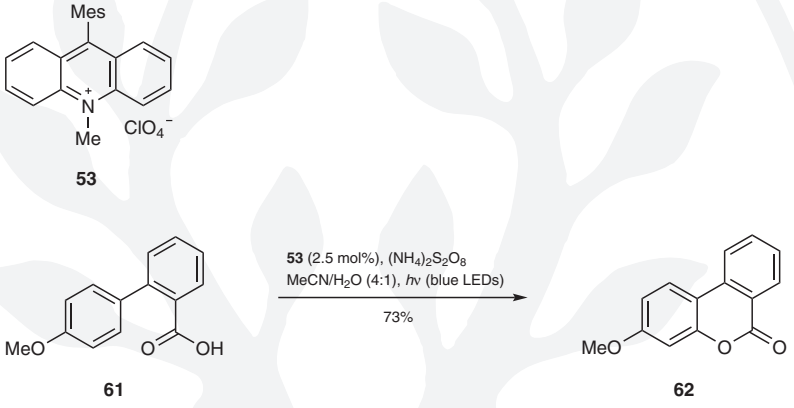

In 2016, the Glorius group reported the benzoyloxyl radical as a hydrogen-atom transfer catalyst for the selective trifluoromethylsulfanylation of unactivated C(sp^3)—H bonds in the presence of iridium photocatalyst **20**. The reaction is initiated by reductive quenching of the excited iridium(III) species by the benzoate anion to afford the benzoyloxyl radical. The electrophilic nature of this radical enables the selective abstraction of a hydrogen atom from the electron-rich C(sp^3)—H bond of substrate **63**. The generated nucleophilic carbon-centered radical **66** then reacts with the electrophilic *N*-[(trifluoromethyl)sulfanyl]phthalimide (**64**) to form the trifluoromethylsulfanylation product **65** (Scheme 21).[57]

Scheme 21 Trifluoromethylsulfanylation of C(sp^3)–H Bonds by Hydrogen-Atom Abstraction of Aryl Carboxyl Radicals[57]

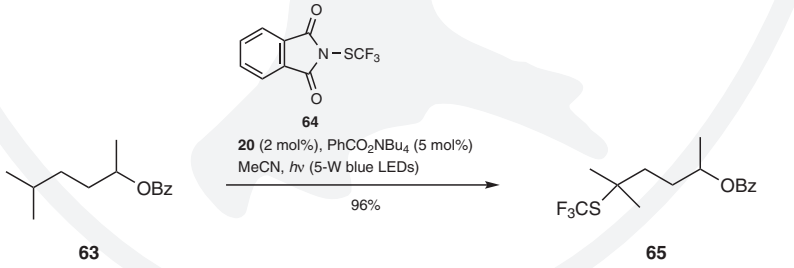

Copyright © 2021 Georg Thieme Verlag KG, Stuttgart, Germany. All rights reserved. This document is for the personal use of – Professor Yiyun Chen – *Chinese Academy of Sciences, Shanghai, China*, only, and may not be distributed to third parties.

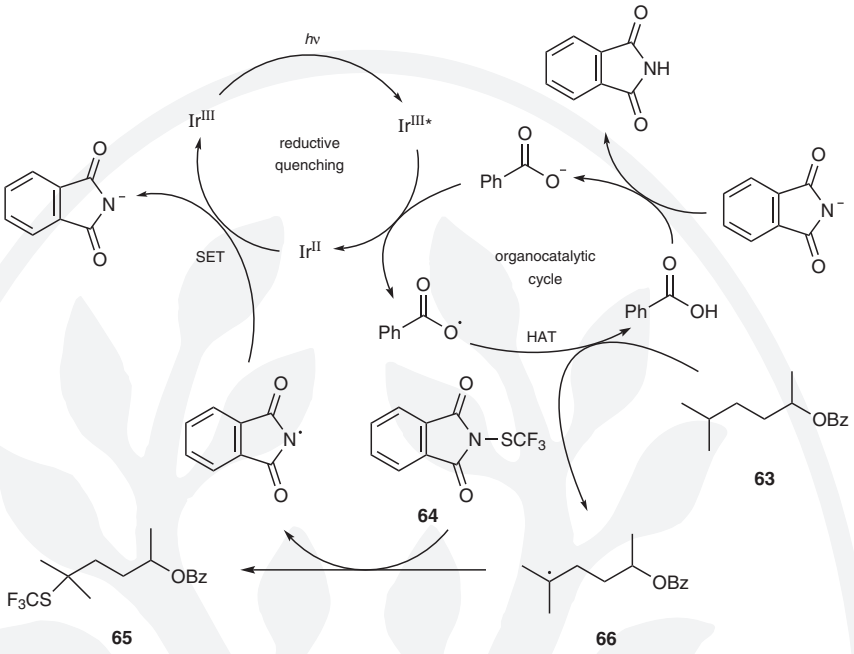

In 2017, the Glorius group reported the visible-light-induced decarboxylation of aryl carboxylic acids via a hypothetical aryl carboxyl radical (Scheme 22).[58,59] For example, the reaction of 2-bromobenzoic acid (**67**) with benzene affords 2-bromo-1,1′-biphenyl (**68**) in 81% yield in the presence of iridium photocatalyst **20** and diethyl 2-bromo-2-methylmalonate. The in situ formation of an acyl hypobromite **70** is proposed as the key to prevent the aroyloxyl radical from unproductive hydrogen-atom abstraction. The reaction is initiated by oxidation of the benzoate anion by the excited iridium(III) species. The resulting aroyloxyl radical **69** generates the hypobromite **70**. The hypobromite **70** then undergoes single-electron transfer with iridium(II) to afford the radical anion **71**, which undergoes decarboxylation to yield the aryl radical **72**. After arene trapping, the cyclohexadienyl radical **73** is oxidized to the aryl cation and deprotonated to afford the biaryl product **68**.

Scheme 22 Decarboxylative Arylation of Aryl Carboxylic Acids[59]



for references see p 377

Copyright © 2021 Georg Thieme Verlag KG, Stuttgart, Germany. All rights reserved. This document is for the personal use of – **Professor Yiyun Chen** – *Chinese Academy of Sciences, Shanghai, China,* only, and may not be distributed to third parties.

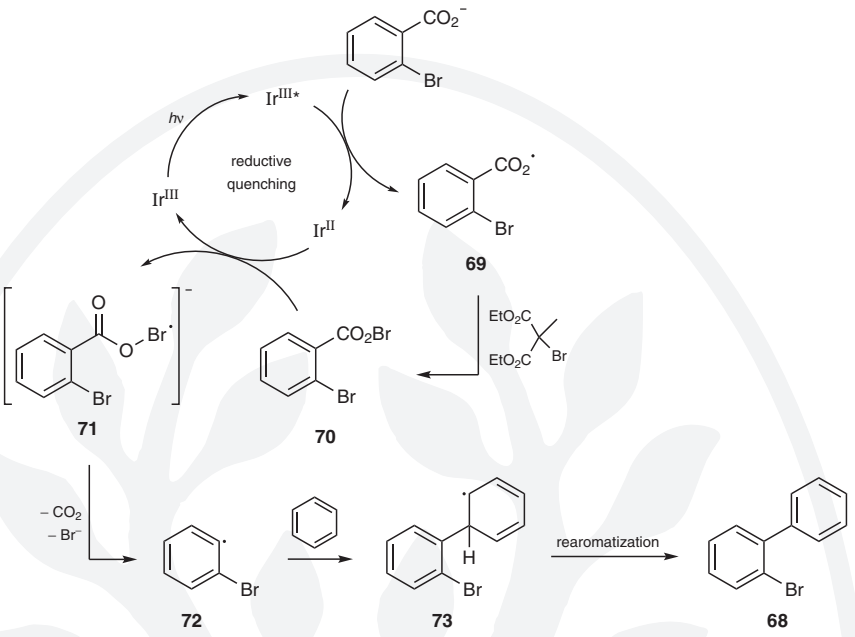

In 2017, the Li group developed an aryl migration strategy from an aryl ether to a carboxylic acid through retro-Smiles rearrangement. For example, the reaction of 2-phenoxybenzoic acid (**75**) in the presence of organic photocatalyst **74** (PDI) gives phenyl 2-hydroxybenzoate (**76**) in 92% yield. Mechanistically, a carboxyl radical **77** is generated from the reductive quench of the excited photocatalyst and yields the intermediate **78** by *ipso* addition. Ring opening subsequently affords the phenoxyl radical **79** for the final aryl ether **76** formation after protonation and single-electron transfer (Scheme 23).[60]

Scheme 23 Retro-Smiles Rearrangement of an Aryl Carboxylic Acid[60]

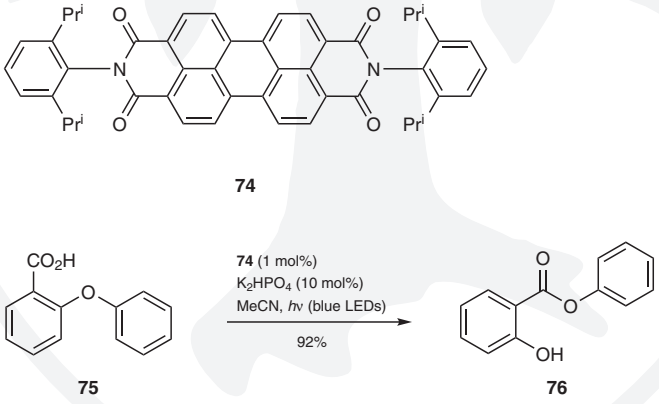

Copyright © 2021 Georg Thieme Verlag KG, Stuttgart, Germany. All rights reserved. This document is for the personal use of – Professor Yiyun Chen – *Chinese Academy of Sciences, Shanghai, China*, only, and may not be distributed to third parties.

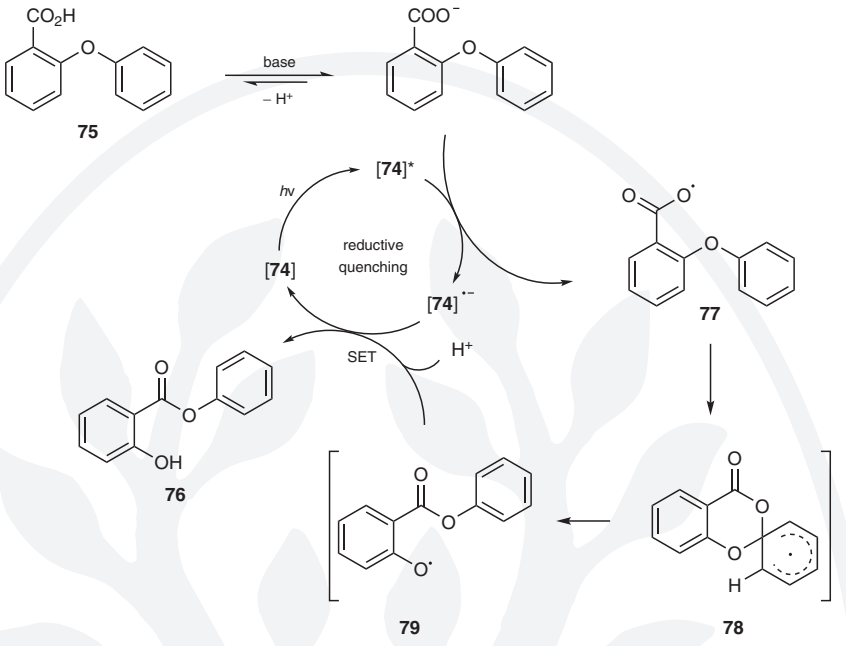

In 2018, the Chen group reported the first regio- and chemoselective C(sp^3)—H bond allylation and alkene difunctionalization enabled by aryl carboxyl radicals (Scheme 24).[61] The reaction is initiated by formation of a donor–acceptor complex between *N*-acyloxyphthalimides and Hantzsch esters. After the visible-light-induced electron transfer, the *N*-acyloxyphthalimide radical anion is formed and eliminates phthalimide to generate the aryl carboxyl radical. Subsequently, the aryl carboxyl radical engages in either 1,5-hydrogen-atom abstraction or 5-*exo* alkene addition to yield the carbon-centered radical for C(sp^3)—H allylation or alkene difunctionalization, and the eliminated sulfone radical is reduced by the Hantzsch ester radical cation.

Scheme 24 C(sp^3)–H Bond Allylation and Alkene Difunctionalization by Hydrogen-Atom Abstraction and Alkene Addition of Aryl Carboxyl Radicals[61]

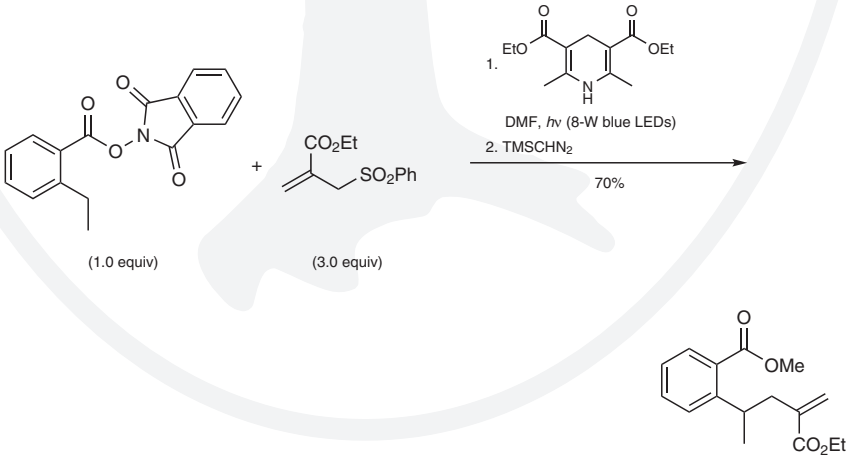

for references see p 377

Copyright © 2021 Georg Thieme Verlag KG, Stuttgart, Germany. All rights reserved. This document is for the personal use of – **Professor Yiyun Chen** – *Chinese Academy of Sciences, Shanghai, China,* only, and may not be distributed to third parties.

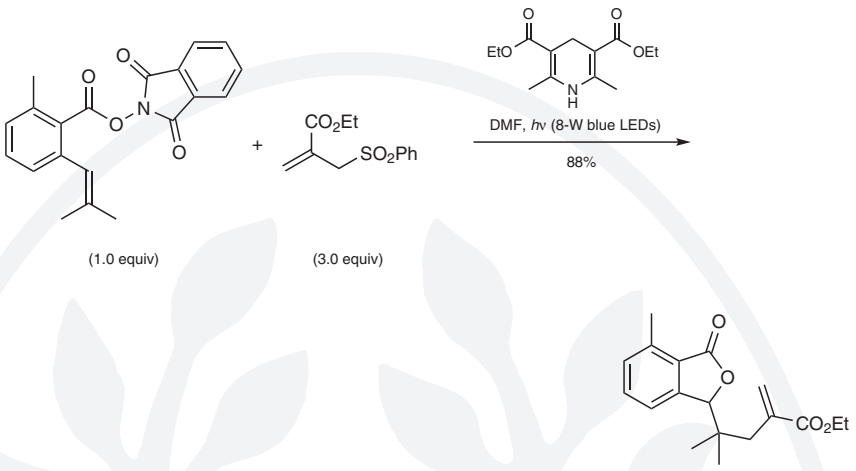

1.9.2 Alkoxyl Radicals

1.9.2.1 Traditional Alkoxyl Radical Generation and Functionalization

Alkoxyl radicals are versatile reactive intermediates with promising synthetic applications. They are traditionally generated from alcohols or alcohol derivatives including nitrites,[62] nitrates,[63] hypohalites,[64] sulfenyl ethers,[65] *N*-alkoxypyridine-2-thiones,[66] and *N*-alkoxyphthalimides.[67] Among these, *N*-alkoxyphthalimides are stable and can be kept without decomposition for several weeks. The classic Barton nitrite ester methodology for alkoxyl radical generation is a powerful reaction for the synthesis of complex molecules (Scheme 25).[62] However, the conventional generation of alkoxyl radicals requires relatively harsh reaction conditions, such as heating with 2,2′-azobisisobutyronitrile/tributyltin hydride, strong oxidants, or UV light irradiation, which compromises synthetic applications and functional-group compatibilities (Scheme 25). In addition, only C(sp^3)—H and C(sp^3)—X bonds can be formed from alkoxyl radicals using traditional reaction conditions, and the formation of C(sp^3)—C(sp^3) bonds, especially intermolecularly, is challenging.

Scheme 25 Traditional Alkoxyl Radical Generation and Functionalization

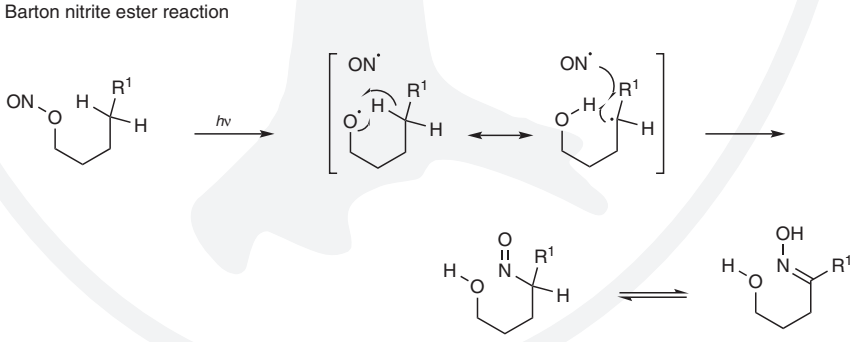

Copyright © 2021 Georg Thieme Verlag KG, Stuttgart, Germany. All rights reserved. This document is for the personal use of – Professor Yiyun Chen – Chinese Academy of Sciences, Shanghai, China, only, and may not be distributed to third parties.

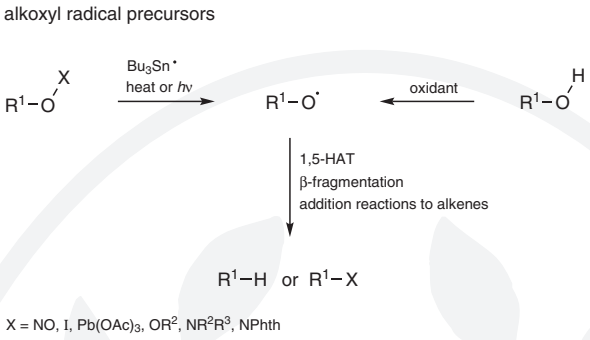

1.9.2.2 Visible-Light-Induced Alkoxyl Radical Generation and Functionalization

In the past decade, visible-light-induced reactions have emerged as a powerful radical initiation method with mild reaction conditions and excellent chemoselectivity, having the potential for biomolecular applications. In general, the photocatalyst (PC) absorbs photons to reach the excited state of the photocatalyst (PC*) under visible-light irradiation. For photooxidative catalysis, the alcohol is oxidized by the excited state of photocatalyst via single-electron transfer (SET) to generate the alkoxyl radical, and the reduced photocatalyst $PC^{\bullet-}$ reduces the electron acceptor A to regenerate the photocatalyst and form a radical anion $A^{\bullet-}$ (Scheme 26). Alternatively, for photoreductive catalysis, the excited photocatalyst is reduced by the electron donor D to generate the radical anion $PC^{\bullet-}$, which subsequently reduces alcohol derivatives to generate alkoxyl radicals. The first examples of visible-light-induced alkoxyl radical generation from alcohols and alcohol derivatives were revealed in 2015.[68,69] Since then, applications of visible-light-induced alkoxyl radical generation for inert chemical bond cleavage and functionalization reactions have been booming.

Scheme 26 Visible-Light-Induced Alkoxyl Radical Generation and Functionalization

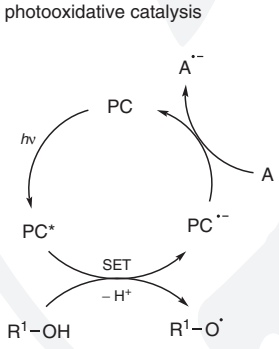

for references see p 377

Copyright © 2021 Georg Thieme Verlag KG, Stuttgart, Germany. All rights reserved. This document is for the personal use of – Professor Yiyun Chen – Chinese Academy of Sciences, Shanghai, China, only, and may not be distributed to third parties.

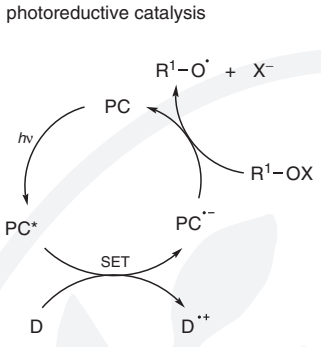

1.9.2.2.1 Inert C(sp³)—H Bond Functionalization

In 2015, the Chen group reported the first visible-light-induced alkoxyl radical generation with *N*-alkoxyphthalimides enabled by diethyl 1,4-dihydro-2,6-dimethylpyridine-3,5-dicarboxylate (**82**, Hantzsch ester). For example, the reaction of phthalimide ester **80** and ethyl 2-[(phenylsulfonyl)methyl]acrylate (**81**) gives allylation product **83** in 90% yield. Mechanistically, the photocatalysis is initiated by photoexcitation of tris[2-(2-pyridyl)-phenyl]iridium(III) [*fac*-Ir(ppy)$_3$] to generate an excited iridium(III) species, which is reduced by Hantzsch ester **82** to yield iridium(II). The reductive iridium(II) undergoes single-electron transfer with an *N*-alkoxyphthalimide to yield the *N*-alkoxyphthalimide radical anion **85**, which is further protonated by the Hantzsch ester radical cation **84** to facilitate formation of alkoxyl radical **86**. Finally, the alkoxyl radical **86** undergoes 1,5-hydrogen-atom transfer (HAT) and subsequent intermolecular alkyl radical trapping to yield the allylation product (Scheme 27).[68] Intermolecular C—C bond formation after 1,5-hydrogen-atom transfer is not applicable under traditional alkoxyl radical reaction conditions due to the facile trapping of carbon-centered radicals by other radical species.[70–75] In 2019, the Smith group reported the generation of dithianyl and dioxolanyl radicals by 1,5- or 1,6-hydrogen-atom transfer of alkoxyl radicals using *N*-alkoxyphthalimides (e.g., **87**) enabled by Hantzsch ester **82** (Scheme 27). The radicals were then engaged in conjugate additions to achieve the total synthesis of danshenspiroketallactones.[76]

Scheme 27 1,5-Hydrogen-Atom Transfer and Allylation of *N*-Alkoxyphthalimides by Hantzsch Esters[68,76]

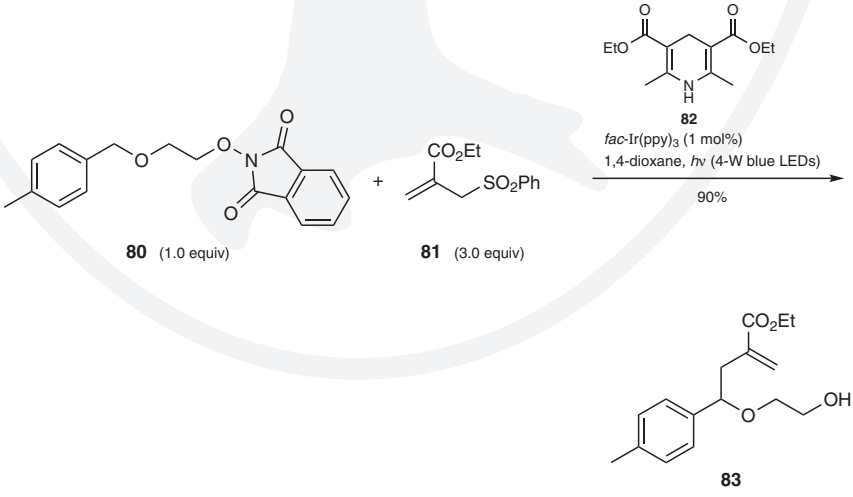

Copyright © 2021 Georg Thieme Verlag KG, Stuttgart, Germany. All rights reserved. This document is for the personal use of – Professor Yiyun Chen – *Chinese Academy of Sciences, Shanghai, China*, only, and may not be distributed to third parties.

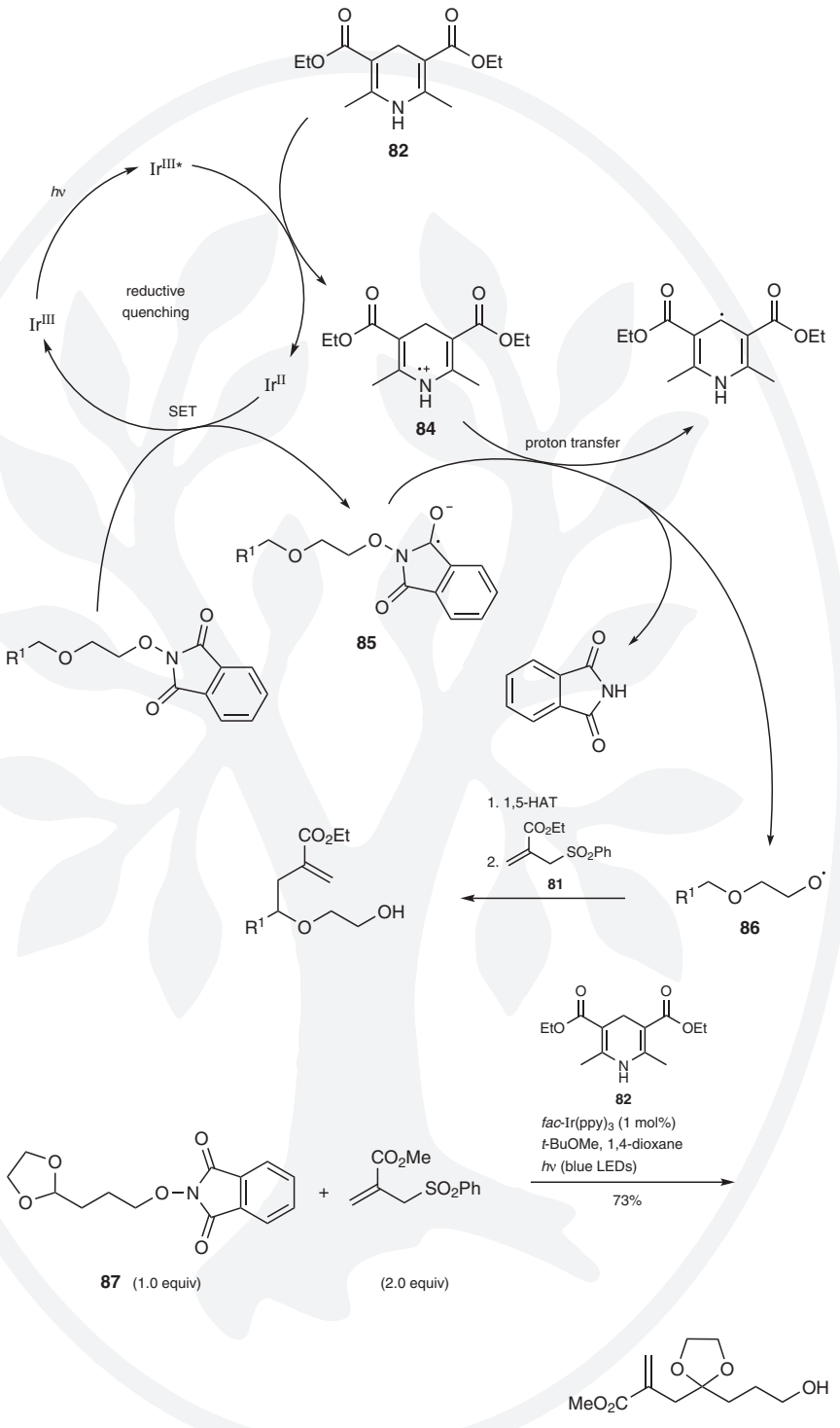

for references see p 377

Copyright © 2021 Georg Thieme Verlag KG, Stuttgart, Germany. All rights reserved. This document is for the personal use of – **Professor Yiyun Chen** – *Chinese Academy of Sciences, Shanghai, China,* only, and may not be distributed to third parties.

In 2016, the Meggers group reported the first asymmetric C(sp^3)—H bond Michael addition by combining visible-light-induced alkoxyl radical generation with catalytic asymmetric C—C bond formation (Scheme 28).[77] The alkoxyl radical is generated from *N*-alkoxyphthalimides facilitated by Hantzsch ester **82**, and the *N*,*O*-rhodium-coordinated *N*-acylpyrazole substrates are ingeniously used for the asymmetric Michael addition. The observed high enantioselectivity demonstrates that the chiral rhodium Lewis acid **88** is compatible with visible-light-induced alkoxyl radical generation conditions and accelerates the radical addition to outcompete the prevailing racemic background reaction. For example, the reaction of (*E*)-1-(3,5-dimethyl-1*H*-pyrazol-1-yl)but-2-en-1-one (**89**) with phthalimide ester **90** furnishes (*R*)-1-(3,5-dimethyl-1*H*-pyrazol-1-yl)-4-(2-hydroxyethoxy)-3-methylbutan-1-one (**91**) in 70% yield and 92% enantiomeric excess using tris[2-(2-pyridyl)phenyl]iridium(III) [*fac*-Ir(ppy)$_3$] as photocatalyst (Scheme 28).

Scheme 28 1,5-Hydrogen-Atom Transfer and Asymmetric Michael Addition of an *N*-Alkoxyphthalimide by Hantzsch Ester and Lewis Acid Catalysis[77]

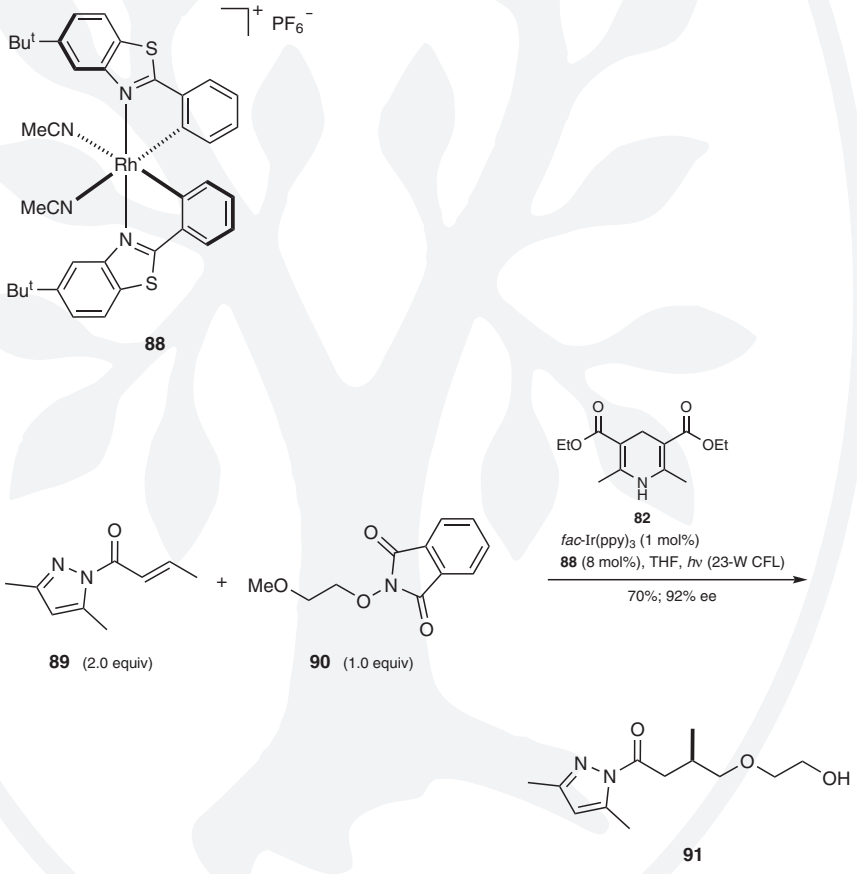

Copyright © 2021 Georg Thieme Verlag KG, Stuttgart, Germany. All rights reserved. This document is for the personal use of – **Professor Yiyun Chen** – *Chinese Academy of Sciences, Shanghai, China,* only, and may not be distributed to third parties.

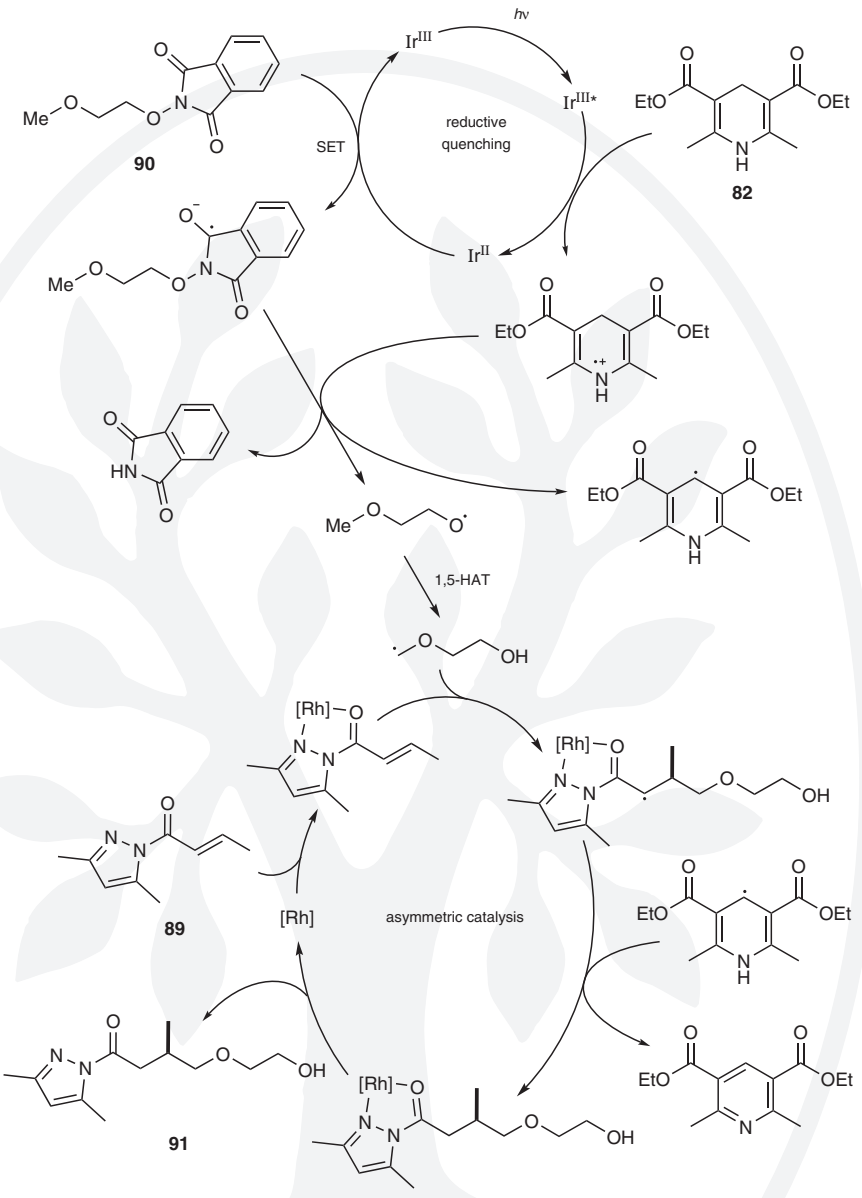

In 2016, the Lakhdar group reported the synthesis of benzophosphole oxides from arylphosphine oxides and alkynes using *N*-ethoxy-2-methylpyridinium tetrafluoroborate as precursor for the ethoxyl radical. For example, the reaction between diphenylacetylene and diphenylphosphine oxide produces benzo[*b*]phosphole oxide **94** using eosin Y (**92**) as photocatalyst. The reaction is initiated by formation of electron donor–acceptor complex **93** between eosin Y and *N*-ethoxy-2-methylpyridinium tetrafluoroborate, which upon absorption of green light generates the ethoxyl radical. The unstable ethoxyl radical abstracts hydrogen from the phosphine oxide to yield the diphenylphosphinoyl radical, which reacts with the alkyne to give radical **95**. Subsequent intramolecular addition onto the arene produces radical **96**, which then undergoes single-electron oxidation, deprotonation, and rearomatization to afford the benzo[*b*]phosphole oxide product **94** (Scheme 29).[78]

for references see p 377

Copyright © 2021 Georg Thieme Verlag KG, Stuttgart, Germany. All rights reserved. This document is for the personal use of – **Professor Yiyun Chen** – *Chinese Academy of Sciences, Shanghai, China*, only, and may not be distributed to third parties.

Scheme 29 Intermolecular Hydrogen-Atom Transfer and Functionalization Using *N*-Ethoxy-2-methylpyridinium Tetrafluoroborate for the Synthesis of a Benzo[*b*]phosphole Oxide[78]

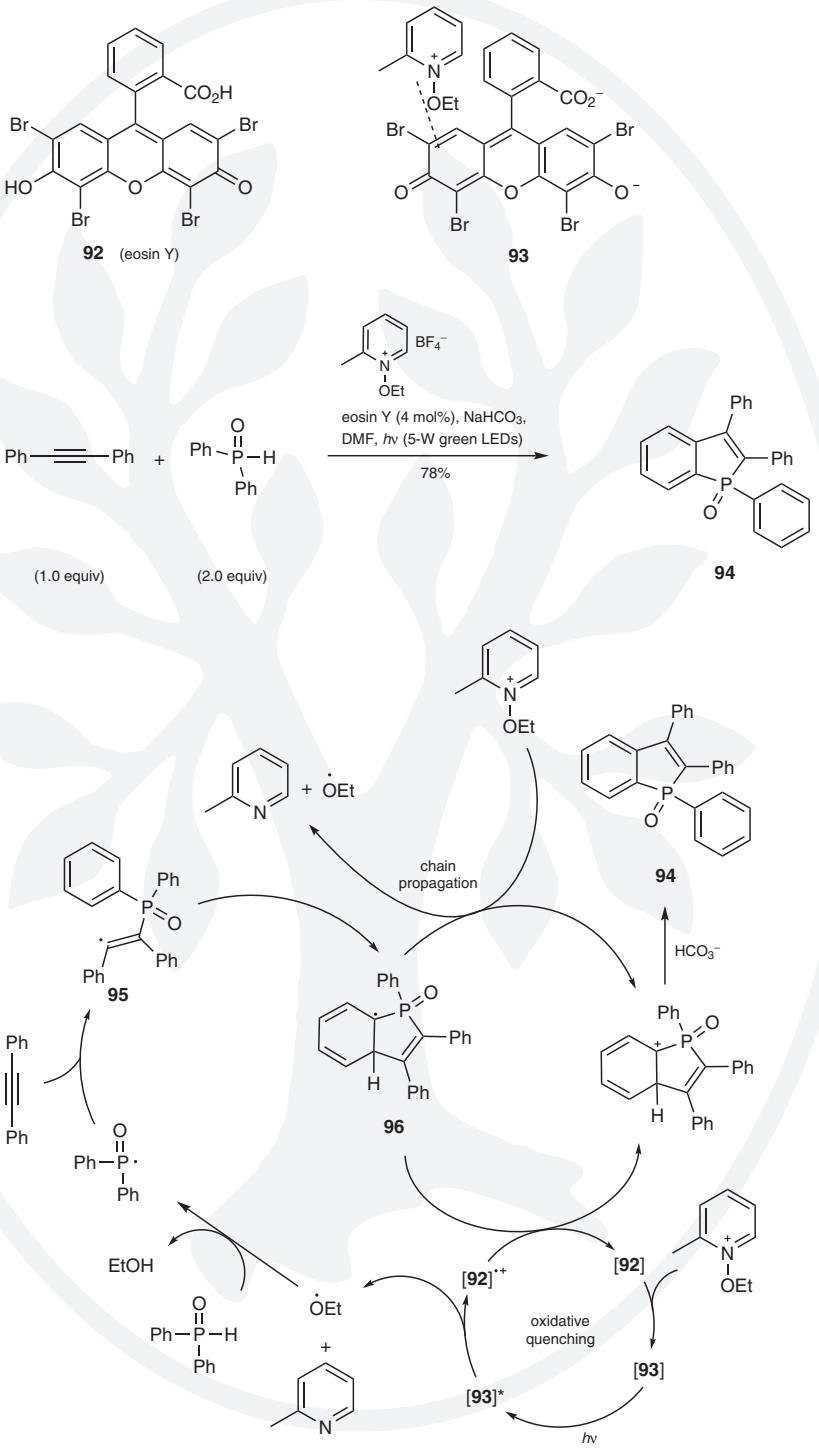

Copyright © 2021 Georg Thieme Verlag KG, Stuttgart, Germany. All rights reserved. This document is for the personal use of – **Professor Yiyun Chen** – *Chinese Academy of Sciences, Shanghai, China*, only, and may not be distributed to third parties.

In 2017, the Zhu group reported the C(sp^3)—H hetarylation of tertiary alcohols using iridium complex **20** as photocatalyst (Scheme 30).[79,80] The photocatalysis may be initiated by the photooxidation of the tertiary alcohols (e.g., **97**) to yield alkoxyl radicals, but the exact oxidative species is unspecified. After 1,5-hydrogen-atom transfer reaction, the resulting carbon-centered radical undergoes *ipso* addition to the heterocycle of **97**, which yields a C(sp^3)—H hetarylation product (e.g., **98**) after hetaryl migration and oxidative elimination. In 2019, the Zhu group reported a similar approach for the C(sp^3)—H bond cyanation of tertiary cyanohydrins (e.g., **99**) using the same iridium complex as photocatalyst (Scheme 30).[81] The alkoxyl radical triggers hydrogen-atom transfer and intramolecular cyano migration, leading to the regioselective cyanation of remote C(sp^3)—H bonds.

Scheme 30 1,5-Hydrogen-Atom Transfer and Hetarylation/Cyanation of Tertiary Alcohols[79–81]

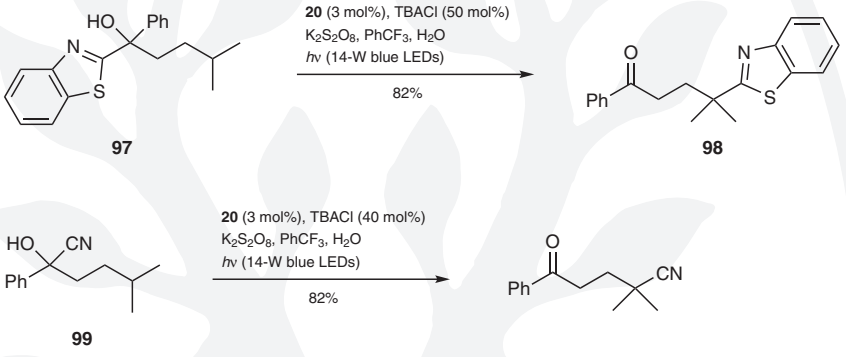

In 2018, the Zuo group reported C(sp^3)—H bond cleavage and C—N bond formation of alcohols (e.g., **100**) by the ligand-to-metal charge transfer (LMCT) homolysis mechanism (Scheme 31).[82] Using cerium(III) chloride as the photocatalyst, the reaction is initiated by formation of the alkoxycerium(III) complex **101** in situ, which is further oxidized to the alkoxycerium(IV) complex **102**. Homolysis of **102** under visible-light irradiation provides the alkoxyl radical and turns over cerium(III). The alkyl radical formed by a 1,5-hydrogen-atom transfer of the alkoxyl radical undergoes radical addition to di-*tert*-butyl azodicarboxylate to yield the radical **103**, which subsequently oxidizes the alkoxycerium(III) complex **101** and forms the product after protonation.

Scheme 31 1,5-Hydrogen-Atom Transfer and C–N Bond Formation of an Alcohol by Cerium Catalysis[82]

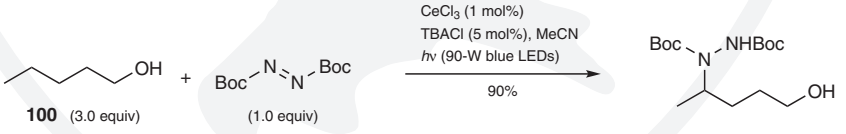

for references see p 377

Copyright © 2021 Georg Thieme Verlag KG, Stuttgart, Germany. All rights reserved. This document is for the personal use of – **Professor Yiyun Chen** – *Chinese Academy of Sciences, Shanghai, China,* only, and may not be distributed to third parties.

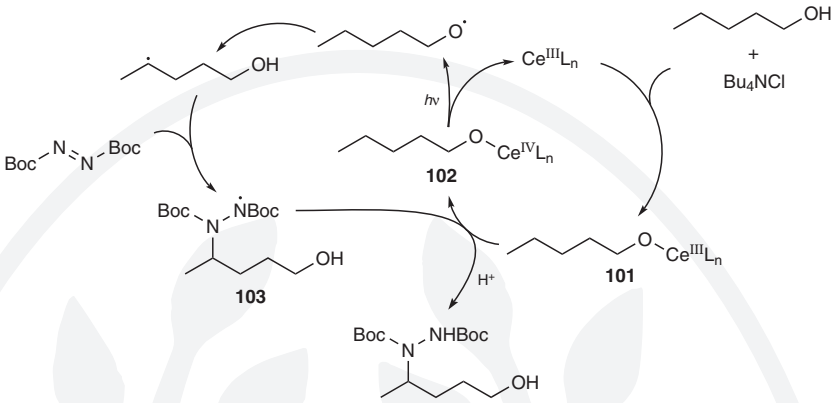

In 2018, the Hong and Baik group reported the site-selective hetarylation of remote C(sp^3)—H bonds using *N*-alkoxyhetarenium salts (e.g., **105**) as both alkoxyl radical precursor and hetaryl source in the presence of quinolinone **104** as organic photocatalyst (Scheme 32).[83] Mechanistically, the alkoxyl radical **106** is generated by single-electron reduction of the *N*-alkoxypyridinium substrate **105** by the photoexcited quinolinone catalyst. Subsequently, the alkoxyl radical **106** undergoes 1,5-hydrogen-atom transfer reaction to form the carbon-centered radical **107**, which then undergoes radical addition to the *N*-alkoxypyridinium substrate **105** at the *para* position. DFT calculations suggest that the pathway forming the *para*-alkylpyridine is more favorable than that forming the *ortho* analogue, and the quantum yield ($\varepsilon = 4.4$) suggests a radical-chain pathway.

Scheme 32 1,5-Hydrogen-Atom Transfer and Hetarylation of an *N*-Alkoxyhetarenium Salt[83]

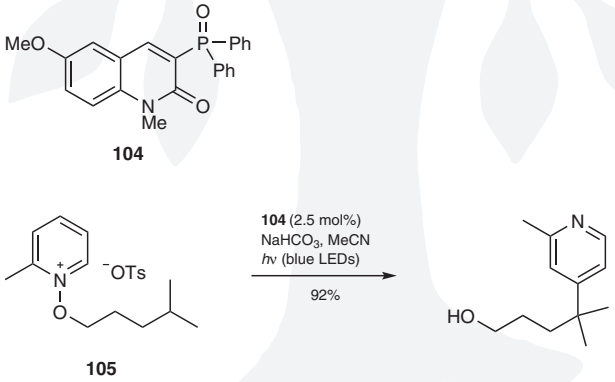

Copyright © 2021 Georg Thieme Verlag KG, Stuttgart, Germany. All rights reserved. This document is for the personal use of – Professor Yiyun Chen – *Chinese Academy of Sciences, Shanghai, China*, only, and may not be distributed to third parties.

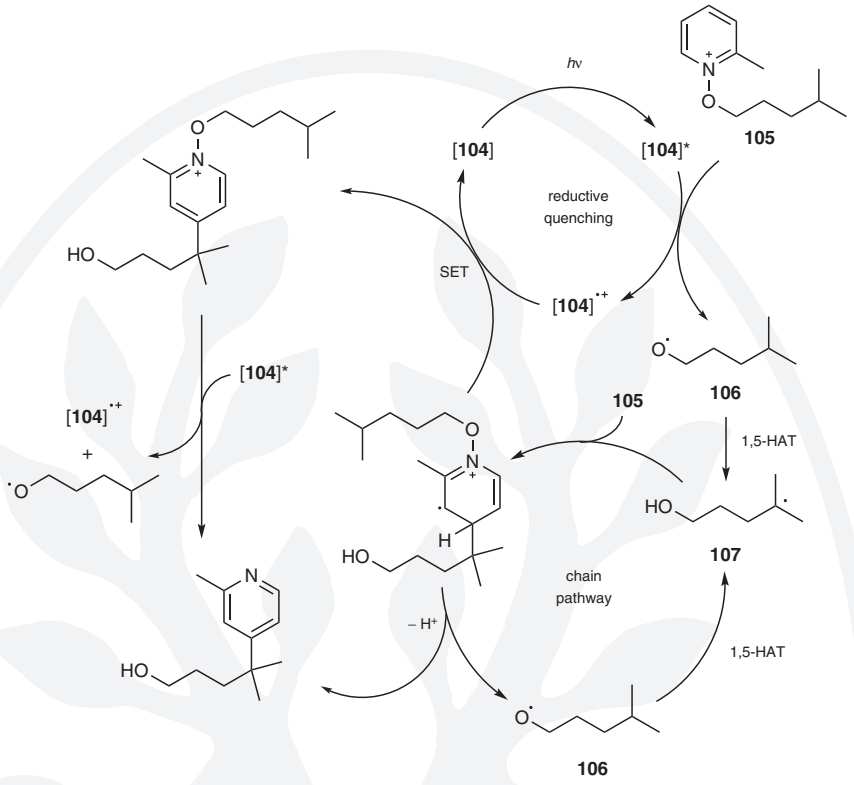

In 2019, the Chen group reported the intermolecular remote δ-C(sp^3)—H hetarylation of free aliphatic alcohols (e.g., **100**) by photoredox catalysis with tris(2,2′-bipyridyl)ruthenium(II) chloride {$[Ru(bipy)_3]Cl_2$} using the hypervalent iodine reagent **108** as oxidant (Scheme 33).[84] The reaction involves in situ alcoholysis of the hypervalent iodine reagent **108** by the alcohol, alkoxyl radical generation by single-electron transfer reduction, 1,5-hydrogen-atom transfer, and Minisci-type hetarylation.

Scheme 33 1,5-Hydrogen-Atom Transfer and Hetarylation of an Alcohol by Dual Photoredox/Hypervalent Iodine Catalysis[84]

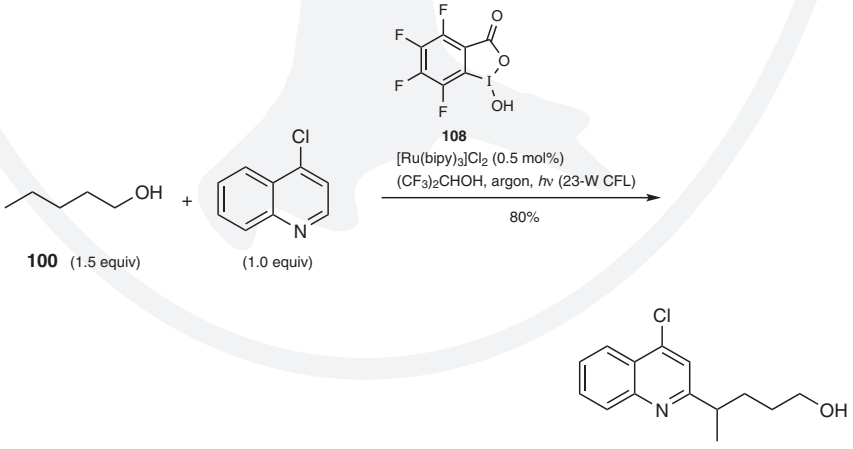

for references see p 377

Copyright © 2021 Georg Thieme Verlag KG, Stuttgart, Germany. All rights reserved. This document is for the personal use of – **Professor Yiyun Chen** – *Chinese Academy of Sciences, Shanghai, China,* only, and may not be distributed to third parties.

In 2019, the Zhu group reported a dual photoredox/copper-catalyzed reaction to afford δ-azido, δ-cyano, and δ-thiocyanato alcohols **111** from *N*-alkoxypyridinium salts (e.g., **109**) and trimethylsilyl reagents **110** using tris[2-(2-pyridyl)phenyl]iridium(III) [*fac*-Ir(ppy)$_3$] as photocatalyst and 1,10-phenanthroline as ligand for copper (Scheme 34).[85] Later, the conversion of *N*-alkoxypyridinium salts (e.g., **109**) with boronic acids **112** into the δ-aryl or δ-vinyl alcohols **113** was reported under similar conditions.[86] The reaction proceeds via reductive generation of alkoxyl radicals and 1,5-hydrogen-atom transfer, followed by a copper-mediated cross-coupling reaction of the resulting translocated carbon-centered radicals with the coupling reagents.

Scheme 34 1,5-Hydrogen-Atom Transfer and Functionalization of an *N*-Alkoxypyridinium Salt by Dual Photoredox/Copper Catalysis[85,86]

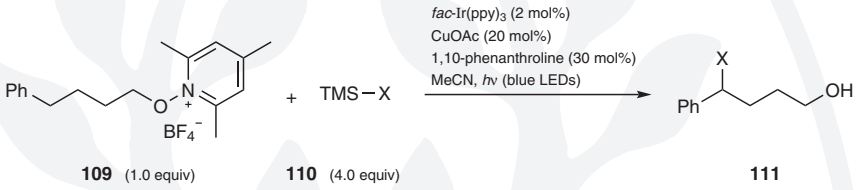

109 (1.0 equiv) **110** (4.0 equiv) **111**

X	Yield (%)	Ref
N_3	72	[85]
CN	72	[85]
NCS	52	[85]

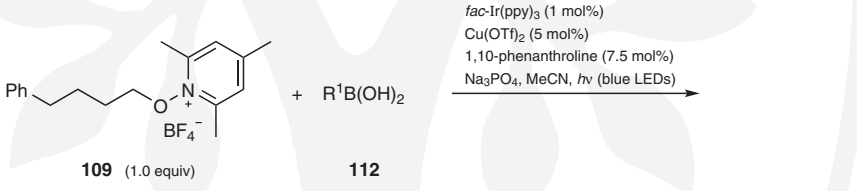

109 (1.0 equiv) **112** **113**

R^1	Yield (%)	Ref
Ph	57	[86]
CH=CHPh	53	[86]

Copyright © 2021 Georg Thieme Verlag KG, Stuttgart, Germany. All rights reserved. This document is for the personal use of – Professor Yiyun Chen – *Chinese Academy of Sciences, Shanghai, China*, only, and may not be distributed to third parties.

When δ-C—H bonds are present within a molecule, the 1,5-hydrogen-atom transfer reaction of alkoxyl radicals preferentially abstracts a hydrogen atom from this δ-position. In contrast, intramolecular hydrogen abstraction at other positions by alkoxyl radicals has been less reported, owing to the unfavorable transition states and high activation energies.[2,3,5,23] There are only a few reports on the 1,2-hydrogen-atom-transfer reactivity of alkoxyl radicals in theoretical or biological studies and, until recently, the synthetic utilization of 1,2-hydrogen-atom transfer for the formation of new C—C bonds remained elusive.[87–92] In 2020, the Chen group reported the first selective 1,2-hydrogen-atom transfer of alkoxyl radicals for α-C(sp^3)—H bond allylation of α-carbonyl, α-cyano, α-trifluoromethyl, and benzylic *N*-alkoxyphthalimides (e.g., **114**) in the presence of tris[2-(2-pyridyl)phenyl]iridium(III) [*fac*-Ir(ppy)$_3$] as photocatalyst and diethyl 1,4-dihydro-2,6-dimethylpyridine-3,5-dicarboxylate (**82**, Hantzsch ester; Scheme 35).[93] Electron paramagnetic resonance (EPR) studies confirmed the presence of the alkoxyl radical with radical spin traps and its 1,2-hydrogen-atom-transfer reactivity. Density functional theory (DFT) calculations suggest that the use of protic solvents lowers the activation energy for 1,2-hydrogen-atom transfer by up to 10.4 kcal/mol to facilitate the α-C(sp^3)—H allylation reaction.

Scheme 35 1,2-Hydrogen-Atom Transfer and Allylation of an *N*-Alkoxyphthalimide by Hantzsch Ester[93]

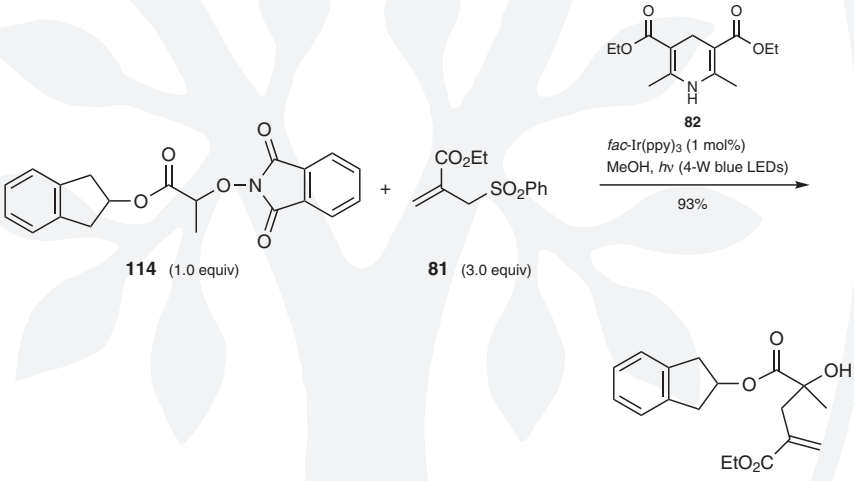

for references see p 377

Copyright © 2021 Georg Thieme Verlag KG, Stuttgart, Germany. All rights reserved. This document is for the personal use of – **Professor Yiyun Chen** – *Chinese Academy of Sciences, Shanghai, China,* only, and may not be distributed to third parties.

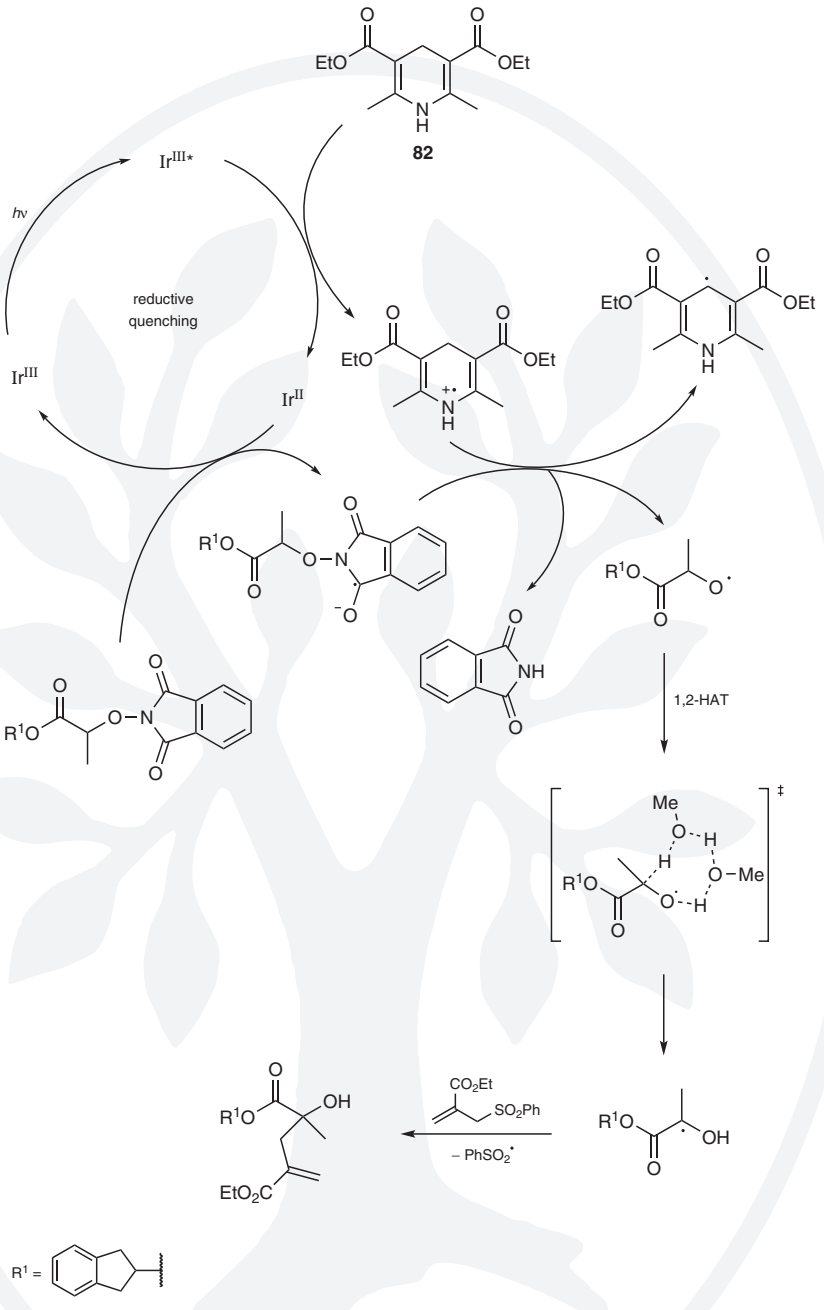

Ethyl 4-(2-Hydroxyethoxy)-2-methylene-4-(4-tolyl)butanoate (83):[68]
A 5-mL clear glass vial was charged with 2-{2-[(4-methylbenzyl)oxy]ethoxy}isoindoline-1,3-dione (**80**; 31 mg, 0.1 mmol), ethyl 2-[(phenylsulfonyl)methyl]acrylate (**81**; 76 mg, 0.3 mmol), *fac*-Ir(ppy)$_3$ (0.7 mg, 1 μmol, 1 mol%), and diethyl 1,4-dihydro-2,6-dimethylpyridine-3,5-dicarboxylate (**82**; 38 mg, 0.15 mmol). 1,4-Dioxane (bubbled with N_2 for 30 min to remove O_2; 1.0 mL) was added and the vial was sealed. The stirred mixture was irradiated with blue LEDs (two 4-W LED light bulbs 10-cm away from the vial, 468 nm peak wavelength, 25 nm spectral half-wave width, composed of 65 LED units each with 60 mW, 3 V, 20 mA) at rt for 3 h and then concentrated. The residue was purified by column chro-

Copyright © 2021 Georg Thieme Verlag KG, Stuttgart, Germany. All rights reserved. This document is for the personal use of – Professor Yiyun Chen – Chinese Academy of Sciences, Shanghai, China, only, and may not be distributed to third parties.

matography (EtOAc/CH_2Cl_2 5:95) to afford the product as a light-yellow oil; yield: 26 mg (90%).

1,2,3-Triphenylphosphindole 1-Oxide (94):[78]
A dry Schlenk flask flushed with argon and equipped with a magnetic stirrer bar and a septum was charged with $NaHCO_3$ (50 mg, 0.6 mmol), *N*-ethoxy-2-methylpyridinium tetrafluoroborate (225 mg, 1.0 mmol), diphenylphosphine oxide (202 mg, 1.0 mmol), diphenylacetylene (89 mg, 0.50 mmol), and eosin Y (**92**; 13 mg, 0.02 mmol, 4 mol%). The solids were dissolved in DMF and the soln was irradiated for 48 h with green LEDs (5 W). Purification by flash chromatography (silica gel, pentane/EtOAc 1:1) afforded the product as a white solid; yield: 147 mg (78%).

1.9.2.2.2 Inert C(sp³)–C(sp³)/C(sp³)–X Bond Functionalization

In 2016, the Chen group reported the first visible-light-induced alkoxyl radical generation from benzyl alcohols using cyclic iodine(III) reagents. The selective C(sp³)–C(sp³) bond cleavage/functionalization is achieved by β-fragmentation of alkoxyl radicals to yield the alkyl radical, followed by the addition to alkynylbenziodoxoles or vinyl carboxylates for the alkynylation/alkenylation. The reaction is initiated by the oxidation of the photoexcited ruthenium(II) species to ruthenium(III) with 1-hydroxy-1,2-benziodoxol-3-(1*H*)-one (**116**) or its resulting benziodoxole radical. The ruthenium(III) then oxidizes the benziodoxole/alcohol complex **118** formed in situ to generate the alkoxyl radical **119**, which then undergoes β-fragmentation to yield the alkyl radical **120** for subsequent alkynylation. For example, the reaction of 1-(4-tolyl)cyclopropan-1-ol (**115**) and 1-(4-tolylethynyl)-1,2-benziodoxol-3-(1*H*)-one (**48**) gives 1,5-di-4-tolylpent-4-yn-1-one (**117**) in 83% yield in the presence of tris(2,2′-bipyridyl)ruthenium(II) hexafluorophosphate {$[Ru(bipy)_3](PF_6)_2$} and 1-hydroxy-1,2-benziodoxol-3-(1*H*)-one (**116**) (Scheme 36).[69] In 2019, the Chen group reported alkoxyl radical generation from aliphatic alcohols (e.g., **122**) using 1-acetoxy-1,2-benziodoxol-3-(1*H*)-one (**49**) and, after β-fragmentation, subsequent Minisci addition to nitrogen-based hetarenes (e.g., **121**). The use of 1,1,1,3,3,3-hexafluoropropan-2-ol as solvent is critical for the oxidation of aliphatic alcohols (Scheme 36).[94]

Scheme 36 β-Fragmentation of Alcohols and Subsequent C–C Bond Formation by Dual Photoredox/Hypervalent Iodine(III) Reagent Catalysis[69,94]

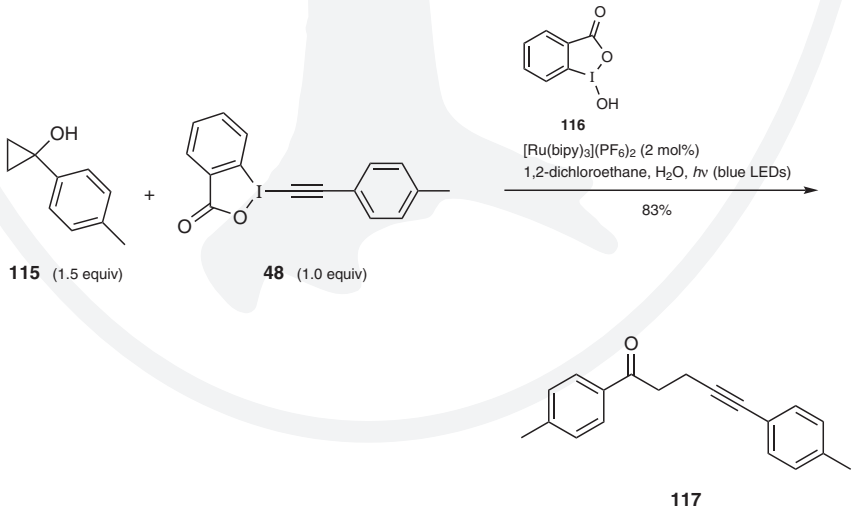

for references see p 377

Copyright © 2021 Georg Thieme Verlag KG, Stuttgart, Germany. All rights reserved. This document is for the personal use of – **Professor Yiyun Chen** – *Chinese Academy of Sciences, Shanghai, China,* only, and may not be distributed to third parties.

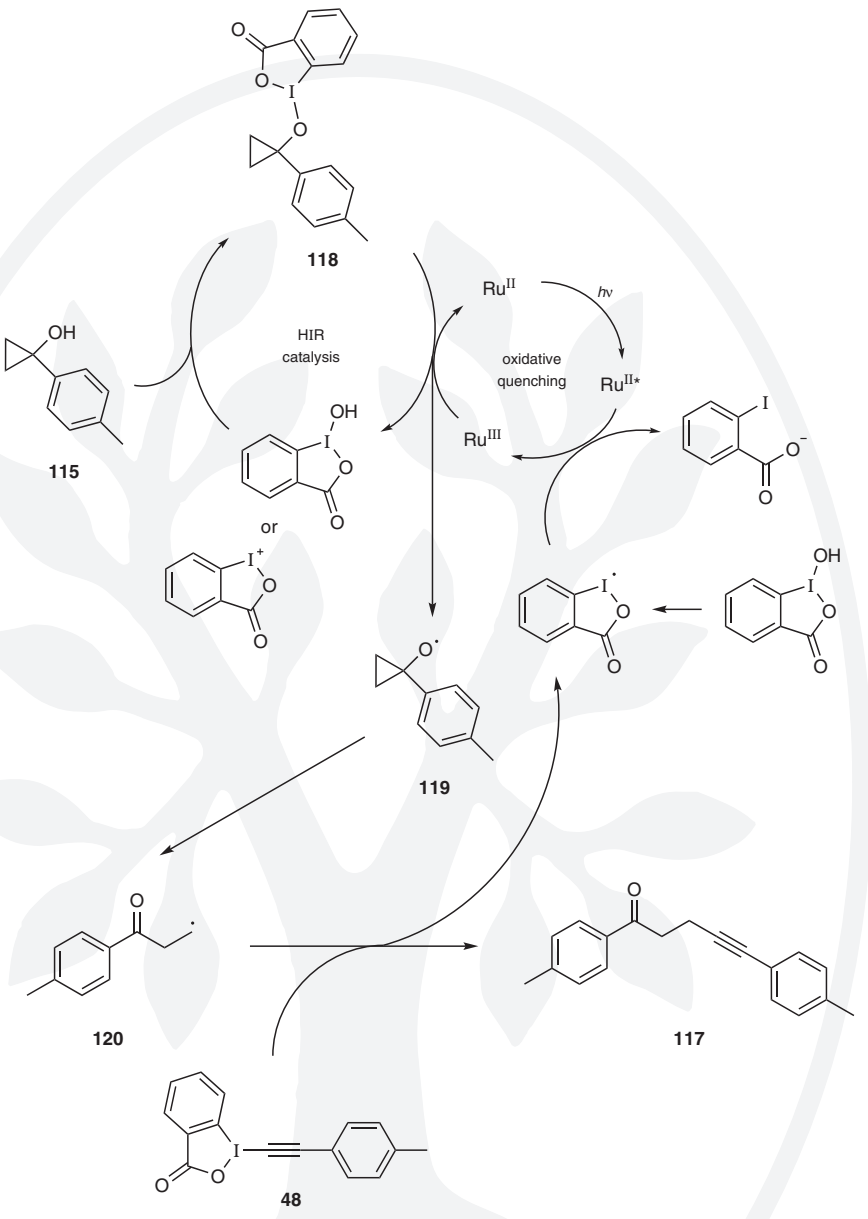

Copyright © 2021 Georg Thieme Verlag KG, Stuttgart, Germany. All rights reserved. This document is for the personal use of – Professor Yiyun Chen – *Chinese Academy of Sciences, Shanghai, China,* only, and may not be distributed to third parties.

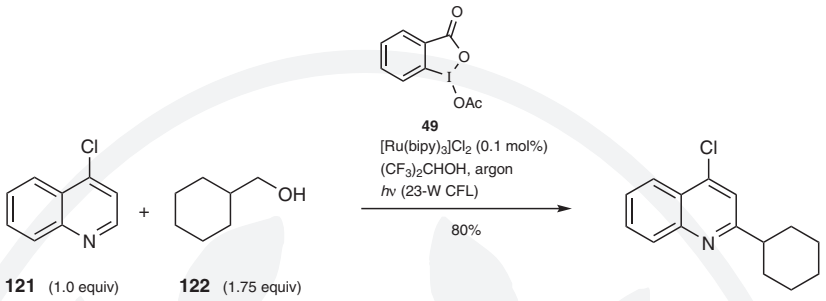

In 2016, the Knowles group reported visible-light-induced alkoxyl radical generation from alcohols by a proton-coupled electron transfer (PCET) mechanism (Scheme 37).[95] The reaction is initiated by oxidation of an electron-rich arene (e.g., **124**) with an excited iridium(III) species derived from iridium complex **123** to give the radical cation **126**, which undergoes one-electron reduction in concert with the Brønsted base catalyst (B) via the intramolecular PCET mechanism. Subsequent β-fragmentation of the alkoxyl radical yields the alkyl radical **127** which reacts with benzenethiol to yield the product **125**.

Scheme 37 β-Fragmentation of a Tertiary Benzyl Alcohol by a Proton-Coupled Electron Transfer Mechanism[95]

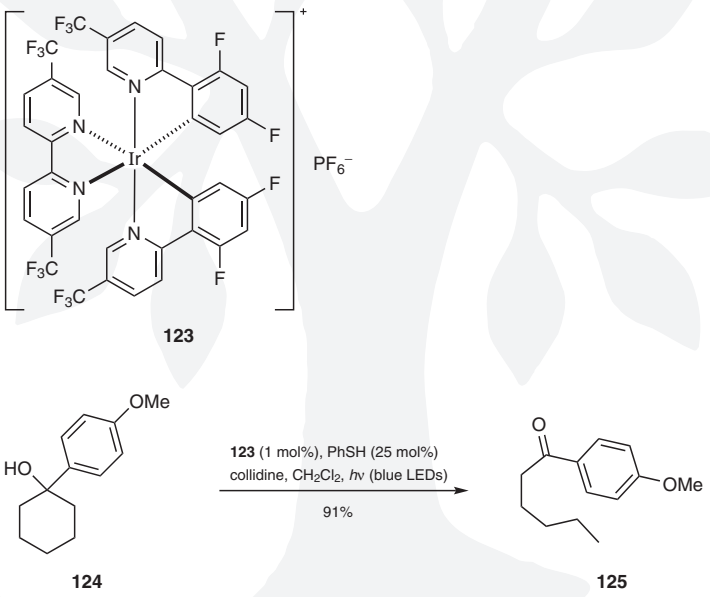

for references see p 377

Copyright © 2021 Georg Thieme Verlag KG, Stuttgart, Germany. All rights reserved. This document is for the personal use of – **Professor Yiyun Chen** – *Chinese Academy of Sciences, Shanghai, China,* only, and may not be distributed to third parties.

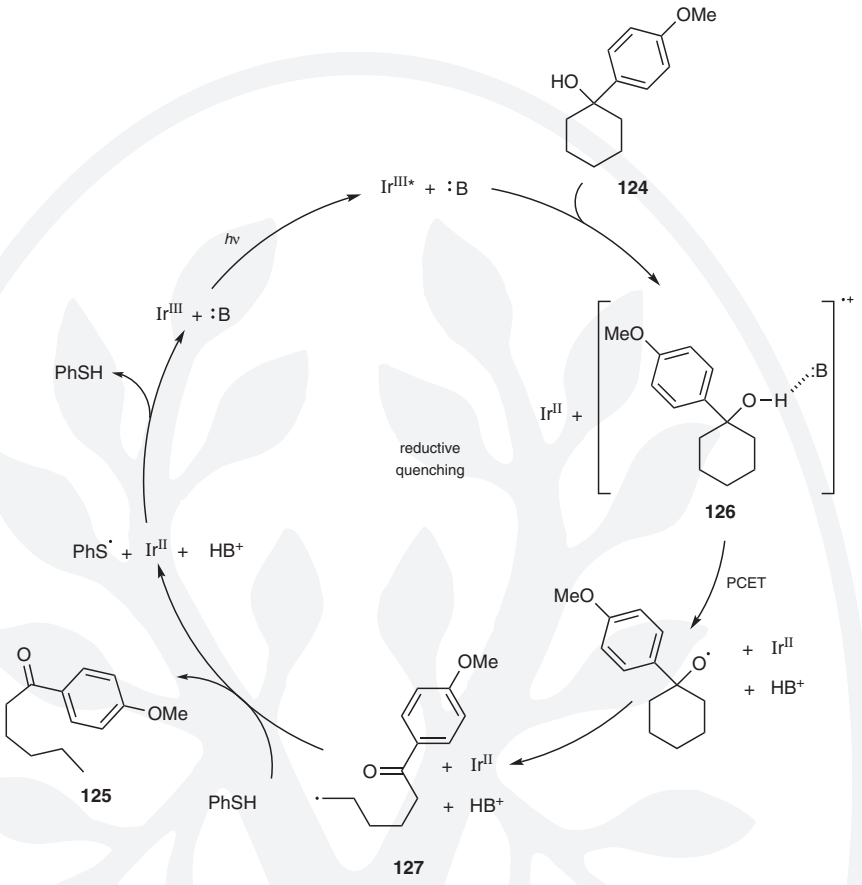

In 2016, the Zuo group reported the visible-light induced oxidation of alcohols to generate alkoxyl radicals from unstrained cycloalkanols (e.g., **128**) by cerium(III) chloride catalysis (Scheme 38).[96] The reaction is initiated by photoexcitation of an alkoxyl cerium(III) complex, which is then oxidized by a nitrogen radical to give an alkoxyl cerium(IV) complex. Decomposition of the alkoxyl cerium(IV) complex provides an alkoxyl radical, which then undergoes β-fragmentation to yield the alkyl radical. This then reacts with di-*tert*-butyl azodicarboxylate to form a new C—N bond. In 2019, the Zuo group reported the visible-light-induced dehydroxymethylative functionalization of alkanols (e.g., **129**) via alkyl radicals generated by β-fragmentation of alkoxyl radicals (Scheme 38).[97]

Scheme 38 β-Fragmentation and Functionalization of Alcohols by Cerium Catalysis[96,97]

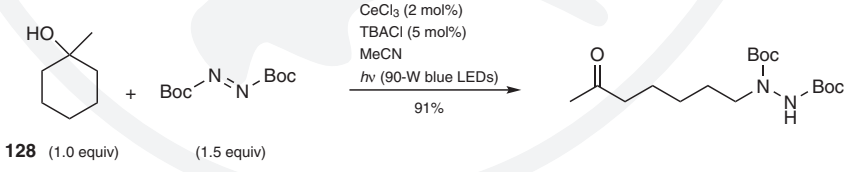

128 (1.0 equiv) (1.5 equiv)

Copyright © 2021 Georg Thieme Verlag KG, Stuttgart, Germany. All rights reserved. This document is for the personal use of – **Professor Yiyun Chen** – *Chinese Academy of Sciences, Shanghai, China,* only, and may not be distributed to third parties.

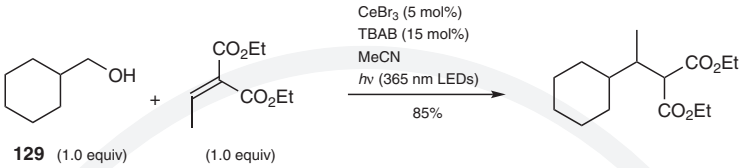

129 (1.0 equiv) (1.0 equiv)

In 2017, the Chen group reported the first visible-light-induced alkoxyl radical generation under metal-free conditions enabled by a donor–acceptor complex (Scheme 39).[98] Selective C(sp^3)—C(sp^3) bond cleavage and allylation/alkenylation were demonstrated with primary, secondary, and tertiary alkyl substituted alkoxyl radicals for the first time. The reaction is initiated by in situ formation of a donor–acceptor complex **131** between Hantzsch ester (HE) **82** and an *N*-alkoxyphthalimide (e.g., **130**), which leads to a red-shift in visible-light absorption. After visible-light-induced electron transfer, an *N*-alkoxyphthalimide radical anion is formed which eliminates phthalimide to generate an alkoxyl radical (e.g., **132**). The resulting alkoxyl radical then undergoes β-fragmentation to yield the alkyl radical, which is trapped by allyl or vinyl sulfones for radical allylation/vinylation. UV/Vis absorption experiments show a red-shift of the donor–acceptor complex, and the Job's plot indicates a 1:1 ratio of the Hantzsch ester and *N*-alkoxyphthalimide for donor–acceptor complex formation. In 2018, the Hari group reported a visible-light-induced deformylative 1,4-addition with a similar strategy, for the synthesis of 5′-carba analogues of nucleoside 5′-phosphates (e.g., **133**) from 2′-deoxy-5′-*O*-phthalimido nucleosides (Scheme 39).[99] In 2019, the Wang group reported ring-opening alkynylation, alkenylation, and allylation of cyclic hemiacetals through β-fragmentation of alkoxyl radicals.[100]

Scheme 39 β-Fragmentation and Allylation/Michael Addition of *N*-Alkoxyphthalimides[98,99]

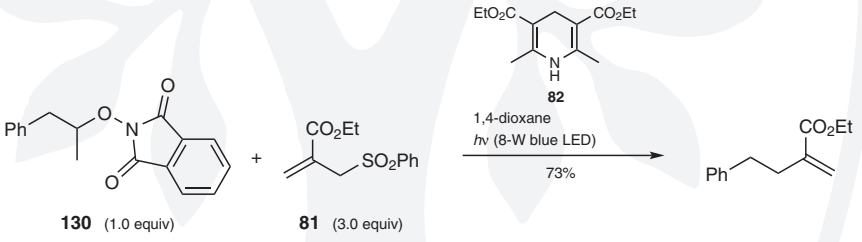

130 (1.0 equiv) **81** (3.0 equiv)

for references see p 377

Copyright © 2021 Georg Thieme Verlag KG, Stuttgart, Germany. All rights reserved. This document is for the personal use of – **Professor Yiyun Chen** – *Chinese Academy of Sciences, Shanghai, China,* only, and may not be distributed to third parties.

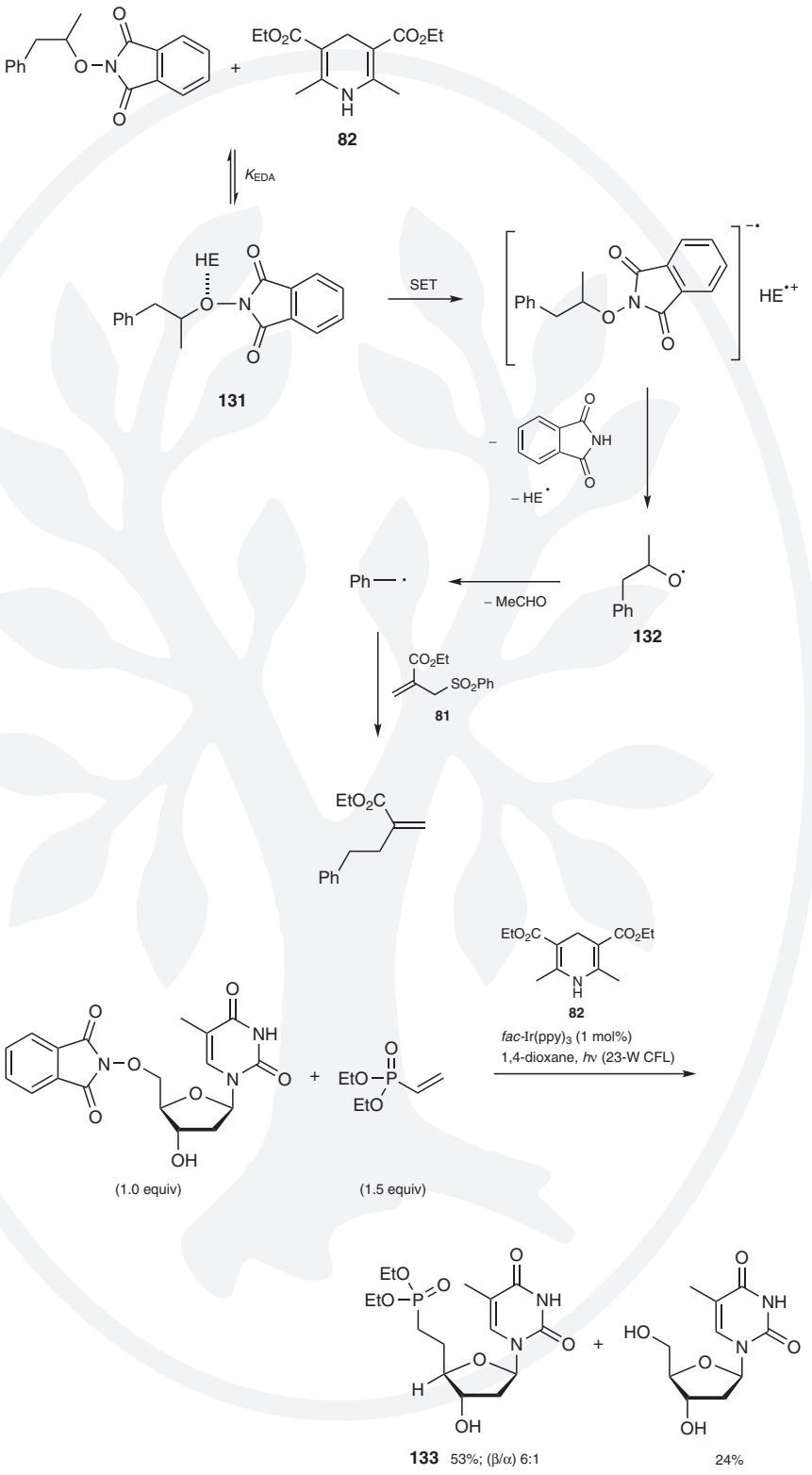

Copyright © 2021 Georg Thieme Verlag KG, Stuttgart, Germany. All rights reserved. This document is for the personal use of – Professor Yiyun Chen – *Chinese Academy of Sciences, Shanghai, China*, only, and may not be distributed to third parties.

Traditional generation of β-carbonyl alkoxyl radicals requires the addition of an alkyl radical to diketones or the homolytic cleavage of peroxide bonds, whereas the formation of α-phosphorus-substituted alkoxyl radicals requires intramolecular alkyl radical addition to acylphosphine oxides.[101–103] In addition, the β-fragmentation of such alkoxyl radicals to yield acyl or phosphoryl radicals for subsequent C—X (X = acyl or POR^1_2) bond formation has not been reported employing traditional alkoxyl radical generation methods.[1,5] In 2017, the Chen group reported the first C(sp^3)—carbonyl bond cleavage/alkynylation reaction involving alkoxyl radicals (Scheme 41).[104] β-Amido (e.g., **139**), β-ester, and β-keto alcohol substrates yield ynamides (e.g., **140**), ynoates, and ynones under mild reaction conditions. The use of novel cyclic iodine(III) reagents (e.g., **134–138**; Scheme 40) is essential for β-carbonyl alkoxyl radical generation from β-carbonyl alcohols. The reaction is initiated by the oxidation of the excited ruthenium(II) species to ruthenium(III) by either the cyclic iodine(III) reagent or its cyclic iodine(III) radical. The ruthenium(III) then oxidizes the β-carbonyl alcohol–cyclic iodine(III) reagent complex formed in situ and releases the cyclic iodine(III) reagent cation for a new catalytic cycle. The alkoxyl radical undergoes β-C(sp^3)—carbonyl bond cleavage to yield a carbamoyl, alkoxycarbonyl, or acyl radical, and yields ynamides, ynoates, or ynones by radical addition to alkynylbenziodoxoles (e.g., **48**). Electron-deficient benziodoxoles are beneficial since they decrease the oxidation potential of the cyclic iodine(III) reagent–alcohol complex, and increase the oxidative quenching efficiency of the photoexcited ruthenium(II) species.

Scheme 40 Cyclic Iodine(III) Reagents

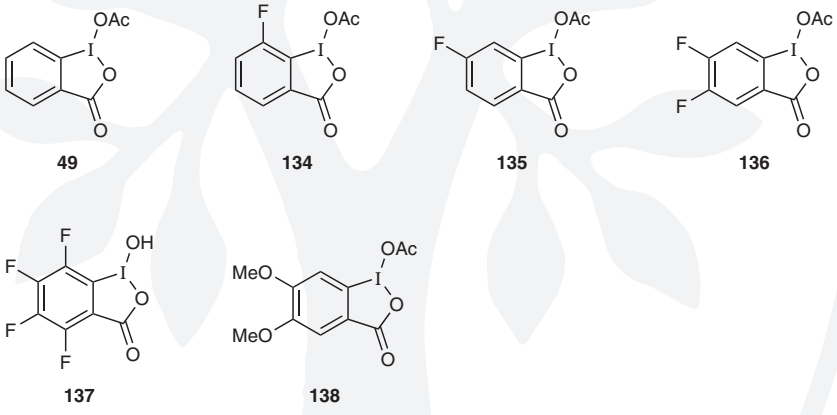

49 **134** **135** **136** **137** **138**

In 2018, the Chen group reported the first C(sp^3)—P bond cleavage reaction by alkoxyl radicals with dual photoredox/cyclic iodine(III) reagent catalysis (Scheme 41).[105] Various α-phosphorus-substituted alcohols, including arylphosphinoyl, alkylphosphinoyl, phosphonate, and phosphonic amide alcohols, undergo C(sp^3)—P bond cleavage and radical alkynylation to generate phosphonoalkynes. The reaction is initiated by formation of a benziodoxole–alcohol complex in situ, which yields the alkoxyl radical upon oxidation by ruthenium(III). The alkoxyl radical undergoes C(sp^3)—P bond cleavage to yield a phosphorus radical, including previously inaccessible phosphonic diamide radicals, which further undergoes radical α-addition to the alkynylbenziodoxoles (e.g., **48**) to yield phosphonoalkynes (e.g., **141**).

for references see p 377

Copyright © 2021 Georg Thieme Verlag KG, Stuttgart, Germany. All rights reserved. This document is for the personal use of – **Professor Yiyun Chen** – *Chinese Academy of Sciences, Shanghai, China,* only, and may not be distributed to third parties.

Scheme 41 β-Fragmentation and Alkynylation of α-Carbonyl or α-Phosphorus Benzylic Alcohols by Dual Photoredox/Cyclic Iodine(III) Reagent Catalysis[104,105]

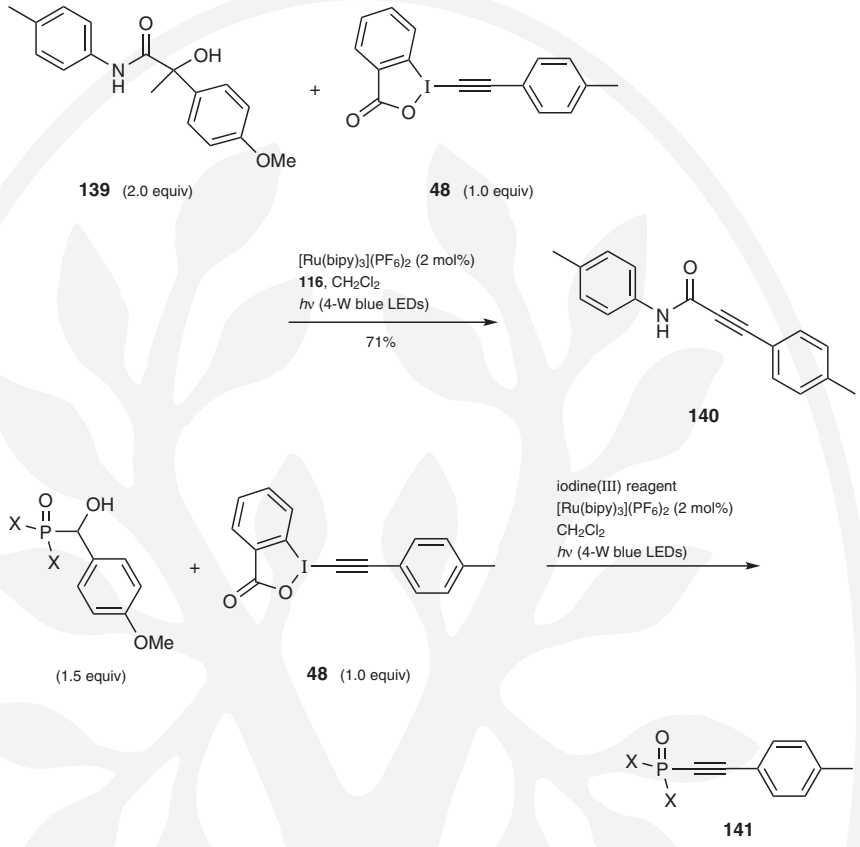

X	Reagent	Yield (%)	Ref
Ph	**49**	78	[105]
OMe	**137**	72	[105]

1,5-Di-4-tolylpent-4-yn-1-one (117**):**[69]

1-(4-Tolyl)cyclopropan-1-ol (**115**; 23 mg, 0.15 mmol), 1-(4-tolylethynyl)-1,2-benziodoxol-3-(1*H*)-one (**48**; 35 mg, 0.10 mmol), $[Ru(bipy)_3](PF_6)_2$ (1.7 mg, 2 μmol, 2 mol%), and 1-hydroxy-1,2-benziodoxol-3-(1*H*)-one (**116**; 39.6 mg, 0.15 mmol, 1.5 equiv) were placed in a 5-mL clear glass vial equipped with a magnetic stirrer bar. 1,2-Dichloroethane (1.0 mL) and H_2O (bubbled with N_2 for 30 min to remove O_2; 1.0 mL) were added and the vial was sealed. The stirred mixture was irradiated with blue LEDs (two 4-W LED light bulbs 10 cm away from the vial, 468 nm peak wavelength, 25 nm spectral half-wave width, composed of 55–65 LED units each with 60 mW, 3 V, 20 mA) at rt. After TLC indicated complete consumption of alkynyl benziodoxole **48**, the mixture was extracted with CH_2Cl_2 and the organic layer was concentrated. The residue was purified by flash chromatography to afford the product as a white solid; yield: 21 mg (83%).

Copyright © 2021 Georg Thieme Verlag KG, Stuttgart, Germany. All rights reserved. This document is for the personal use of – **Professor Yiyun Chen** – *Chinese Academy of Sciences, Shanghai, China,* only, and may not be distributed to third parties.

1.9.2.2.3 Alkoxyl Radical Addition Reactions to Alkenes

In 2018, the Dagousset group reported the first intermolecular alkoxyl radical addition to alkenes with *N*-alkoxypyridinium salts; anti-Markovnikov selective hydroxyalkoxylation, dialkoxylation, and aminoalkoxylation reactions have been demonstrated. For example, the reaction of (4-chlorophenyl)ethene and 4-cyano-1-methoxypyridin-1-ium tetrafluoroborate (**142**) gives 1-(4-chlorophenyl)-2-methoxyethan-1-ol (**143**) in 65% yield in the presence of tris[2-(2-pyridyl)phenyl]iridium(III) [*fac*-Ir(ppy)$_3$] as photocatalyst. Mechanistically, the *N*-methoxypyridinium salts is reduced by the excited iridium(III) species to generate a methoxyl radical, as confirmed by EPR detection. The alkoxyl radical further adds to 4-(chlorophenyl)ethene to yield the benzylic radical **144**. This radical is oxidized by single-electron transfer with the iridium(IV) species to generate carbocation **145**, which is subsequently trapped by water, alcohol, or acetonitrile (Scheme 42).[106] In 2019, the Hong group reported the alkoxyl radical cyclization and pyridylation using alkene-tethered *N*-alkoxypyridinium salts to afford various pyridine-tethered tetrahydrofuran products (e.g., **146**) using phosphine oxide **104** as organic photocatalyst (Scheme 42).[107]

Scheme 42 Alkene Additions of *N*-Alkoxyhetarenium Salts[106,107]

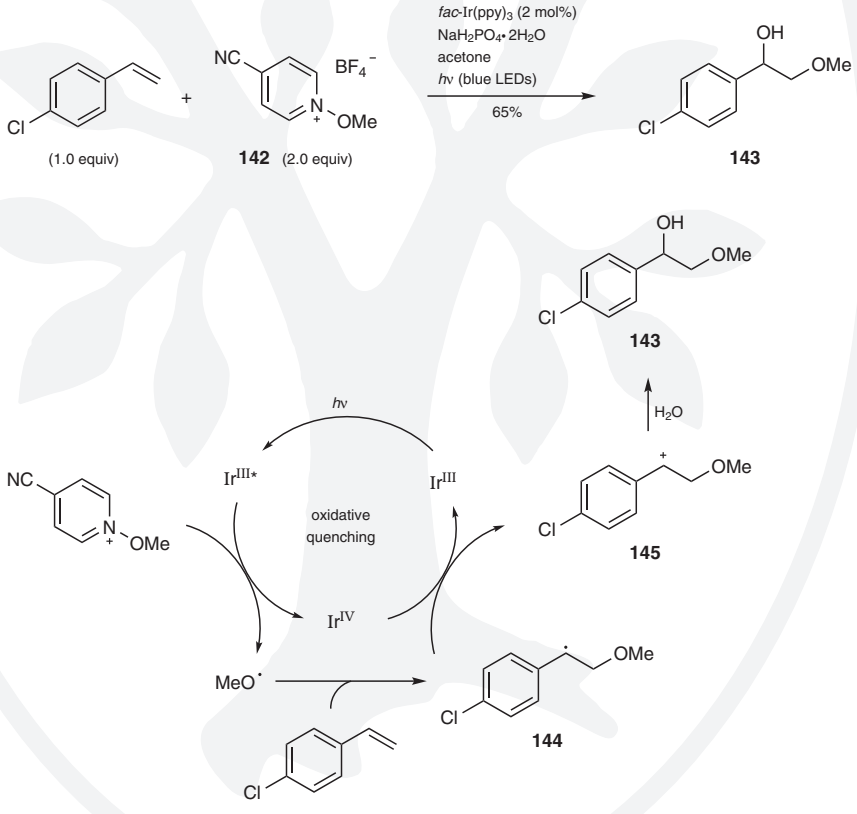

for references see p 377

Copyright © 2021 Georg Thieme Verlag KG, Stuttgart, Germany. All rights reserved. This document is for the personal use of – **Professor Yiyun Chen** – *Chinese Academy of Sciences, Shanghai, China*, only, and may not be distributed to third parties.

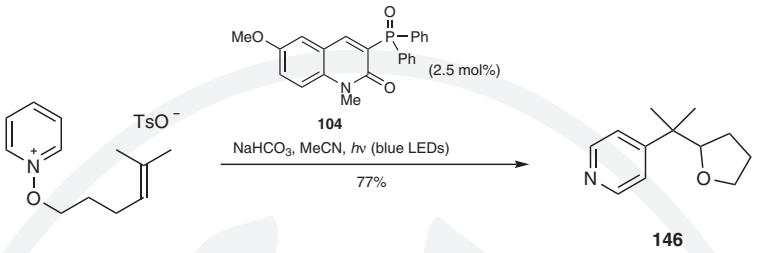

1.9.3 Other Oxygen-Centered Radicals

The reactivity of acyclic aminoxyl, trifluoromethoxyl, difluoromethoxyl, phenoxyl, and vinyloxyl radicals are discussed here, especially the recently emerged photoredox catalytic and electrochemical pathways.

1.9.3.1 Acyclic Aminoxyl Radicals

1.9.3.1.1 Traditional Aminoxyl Radical Generation and Functionalization

The most well-known aminoxyl radicals (nitroxide radicals) are stable N-heterocyclic radicals in which surrounding bulky alkyl groups increase the chemical stability. Among them 2,2,6,6-tetramethylpiperidin-1-oxyl (TEMPO) is the most frequently studied and shows excellent chemical stability at room temperature. It can be employed to capture reactive intermediates to verify radical reaction mechanisms and is widely used in electron paramagnetic resonance (EPR) experiments.[108] The reactivity of cyclic aminoxyl radical is discussed in Section 1.2. The current section covers acyclic aminoxyl radicals, including iminoxyl and amidoxyl radicals.

Iminoxyl radicals were first identified in 1964 by EPR spectroscopy.[109] Either 2,2,6,6-tetramethylpiperidin-1-oxyl or diethyl azodicarboxylate can initiate the formation of iminoxyl radicals from ketoximes. In the case of β,γ-unsaturated ketoximes, the iminoxyl radicals can be further captured intramolecularly by alkenes to form 4,5-dihydroisoxazoles (Scheme 43).[110] EPR studies indicate that iminoxyl radicals can be represented by the resonance structures **147A** and **147B** (Scheme 43). Computational studies show that the spin densities on the oxygen and nitrogen atoms are similar, which indicates that the iminoxyl radicals can behave as both nitrogen-centered and oxygen-centered radicals, depending on the substituents.[111] Using oxidative radical initiators, amidoxyl radicals can be generated from hydroxamic acids and undergo intramolecular alkene additions to produce heterocyclic compounds (Scheme 43).[112–114]

Scheme 43 Traditional Aminoxyl Radical Generation and Functionalization[110–114]

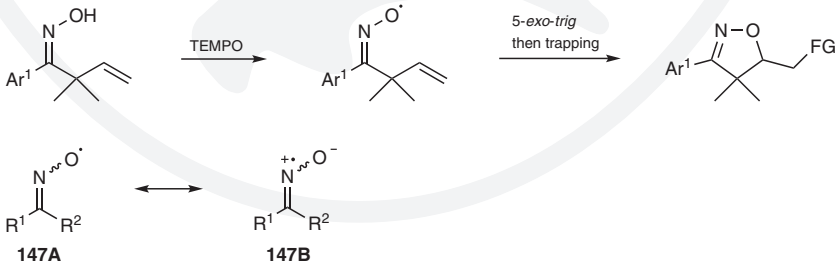

Copyright © 2021 Georg Thieme Verlag KG, Stuttgart, Germany. All rights reserved. This document is for the personal use of – Professor Yiyun Chen – Chinese Academy of Sciences, Shanghai, China, only, and may not be distributed to third parties.

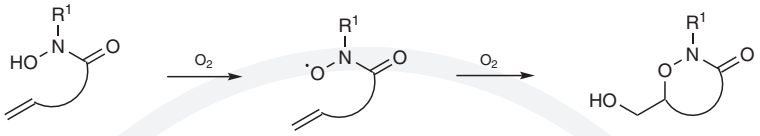

1.9.3.1.2 Visible-Light-Induced Iminoxyl Radical Generation and Functionalization

Recently emerged visible-light photoredox catalysis approaches enable the generation of iminoxyl radicals under mild reaction conditions. In 2016, the Xiao group reported the first photocatalytic iminoxyl radical generation for the synthesis of isoxazoline derivatives. For example, the reaction of 1-phenylbut-3-en-1-one oxime (**148**) in the presence of 9-mesityl-10-methylacridinium perchlorate (**53**) as photocatalyst gives (3-phenyl-4,5-dihydroisoxazol-5-yl)methanol (**149**) in 97% yield. Mechanistically, the excited photocatalyst ([**53**]*) oxidizes the 2,2,6,6-tetramethylpiperidin-1-oxyl (TEMPO) radical to the 2,2,6,6-tetramethyl-1-oxopiperidin-1-ium cation, which then oxidizes the β,γ-unsaturated ketoxime **148** via single-electron transfer (SET) to give the iminoxyl radical **151** after deprotonation of intermediate **150**. The iminoxyl radical then undergoes 5-*exo* radical cyclization to afford the carbon-centered radical **152**, which yields the peroxyl radical **153** after trapping of molecular oxygen. The peroxyl radical then produces the final isoxazoline product **149** after hydrogen-atom transfer and reduction with triphenylphosphine (Scheme 44).[115] In 2020, the Li group reported the sulfonylation of β,γ-unsaturated ketoximes (e.g., **148**) with sulfonylhydrazines (e.g., **154**) by photoredox catalysis using eosin Y as catalyst. Preliminary mechanistic experiments suggest that the hydroxy group of the oxime is essential and that iminoxyl radicals are involved (Scheme 44).[116]

Scheme 44 Visible-Light-Induced Transformation of Oximes via Iminoxyl Radicals[115,116]

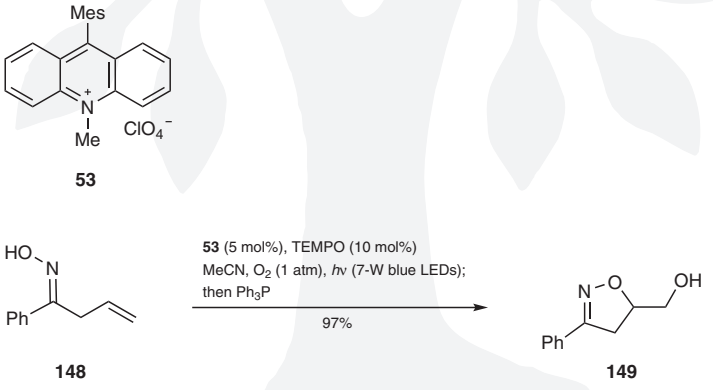

for references see p 377

Copyright © 2021 Georg Thieme Verlag KG, Stuttgart, Germany. All rights reserved. This document is for the personal use of – **Professor Yiyun Chen** – *Chinese Academy of Sciences, Shanghai, China,* only, and may not be distributed to third parties.

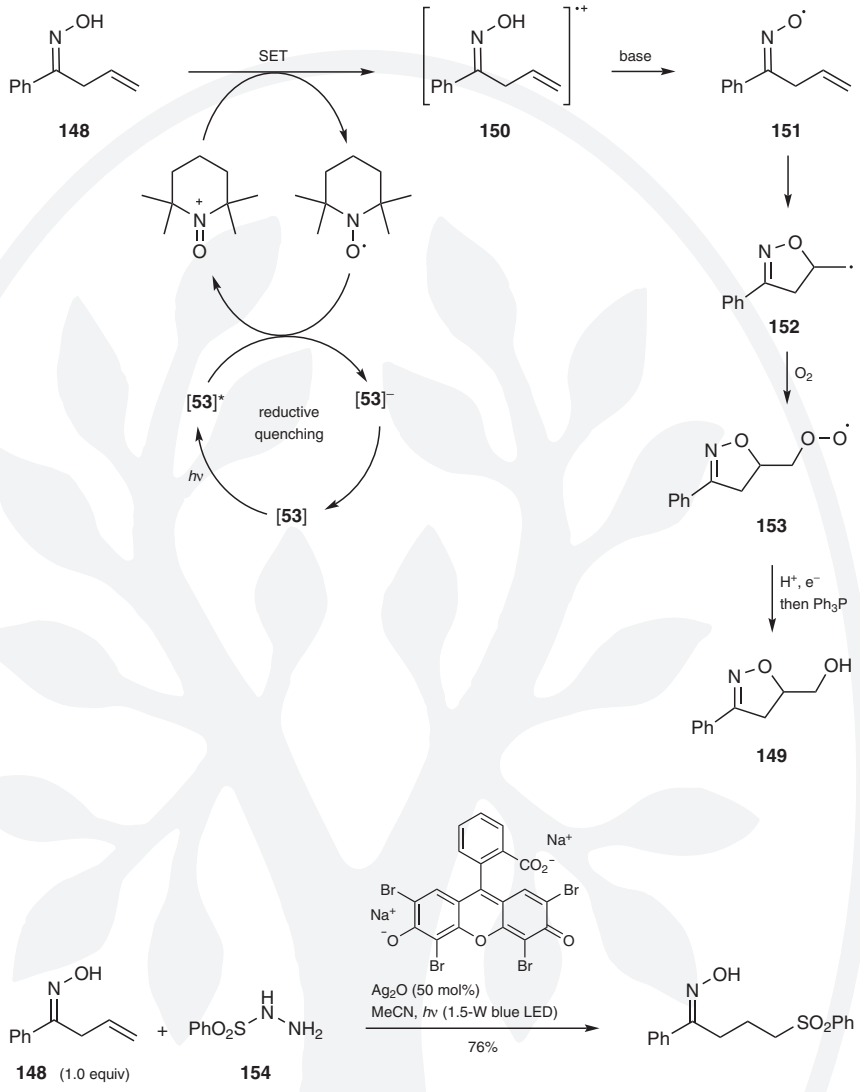

(3-Phenyl-4,5-dihydroisoxazol-5-yl)methanol (149):[115]
1-Phenylbut-3-en-1-one oxime (**148**; 48 mg, 0.3 mmol), 9-mesityl-10-methylacridinium perchlorate (**53**; 5 mol%), and TEMPO (10 mol%) were dissolved in MeCN (6.0 mL) under O_2 (balloon). The stirred soln was irradiated by 7-W blue LEDs (450–460 nm) at a distance of ~5 cm at rt for about 24 h until the reaction was completed as monitored by TLC analysis. Ph_3P (1.0 equiv) was added and the mixture was stirred at rt for another 10 min. The crude product was purified by flash chromatography (silica gel, petroleum ether/EtOAc 10:1 to 2:1); yield: 97%.

1.9.3.2 Trifluoromethoxyl and Difluoromethoxyl Radicals

1.9.3.2.1 Traditional Trifluoromethoxyl and Difluoromethoxyl Radical Generation

Trifluoromethoxy and difluoromethoxy groups are prevalent in medicinal chemistry and drug discovery processes because these fluorinated groups enhance the biological activities and the pharmacokinetic properties of drug candidates.[117,118] In 2010 and 2012, the

Copyright © 2021 Georg Thieme Verlag KG, Stuttgart, Germany. All rights reserved. This document is for the personal use of – Professor Yiyun Chen – Chinese Academy of Sciences, Shanghai, China, only, and may not be distributed to third parties.

Aruguello and Navarrini groups independently reported the generation of the trifluoromethoxyl radical from bis(trifluoromethyl) peroxide and trifluoromethyl hypofluorite, respectively.[119,120] These gaseous reagents are highly reactive and toxic, and the resulting radicals can only add to structurally simple thiophenes and arenes with poor chemoselectivity (Scheme 45).

Scheme 45 Traditional Trifluoromethoxyl Radical Generation and Functionalization[119,120]

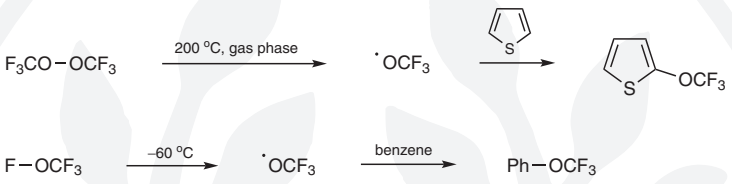

1.9.3.2.2 Visible-Light-Induced Trifluoromethoxyl and Difluoromethoxyl Radical Generation and Functionalization

Until recently, the incorporation of trifluoromethoxy and difluoromethoxy groups required harsh conditions and was thus only possible at the early stages of multistep syntheses.[121] In 2018, the Ngai group reported the generation of trifluoromethoxyl radicals from trifluoromethoxylating reagent **155** under violet LED irradiation to achieve the intermolecular aryl C(sp^2)—H trifluoromethoxylation of arenes such as benzene (Scheme 46).[122] Later, in 2018, they reported the second-generation trifluoromethoxylating reagent **156** with better substrate scope, where the use of high-energy violet LEDs is not required. For example, the reaction of 1,3,5-trichlorobenzene with this reagent in the presence of tris(2,2′-bipyridyl)ruthenium(II) hexafluorophosphate {[$Ru(bipy)_3$](PF_6)$_2$} furnishes 1,3,5-trichloro-2-(trifluoromethoxy)benzene (**157**) in 80% yield. Mechanistically, the trifluoromethoxylation reagent **156** is first reduced by the excited ruthenium(II) species to liberate the trifluoromethoxyl radical, which is trapped by the arene. The resulting carbon-centered radical is oxidized by ruthenium(III) to give the trifluoromethoxylation product after deprotonation (Scheme 46).[123]

In the same year, the Togni group reported the pyridinium-based trifluoromethoxylating reagent **158**, which can be synthesized in one step from Togni reagent I [3,3-dimethyl-1-(trifluoromethyl)-1,3-dihydro-1λ^3-benzo[*d*][1,2]iodaoxole], for the intermolecular aryl C(sp^2)—H trifluoromethoxylation of arenes.[124] DFT calculations and cyclic voltammetry measurements indicate that reagent **158** is reduced by the excited ruthenium(II) species, and the trifluoromethoxyl radical was detected by EPR spectroscopy at cryogenic temperature with the release of 4-cyanopyridine (Scheme 46). Due to the high reactivity of the trifluoromethoxyl radical, a large excess of arenes is typically required.

Scheme 46 Visible-Light-Induced Trifluoromethoxylation of Arenes[122–124]

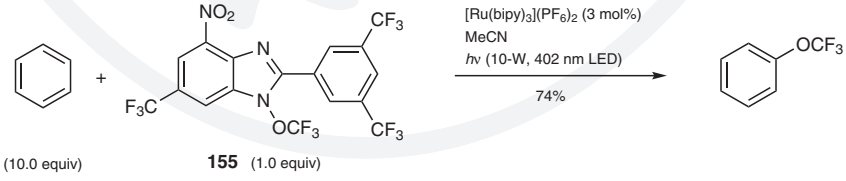

for references see p 377

Copyright © 2021 Georg Thieme Verlag KG, Stuttgart, Germany. All rights reserved. This document is for the personal use of – **Professor Yiyun Chen** – *Chinese Academy of Sciences, Shanghai, China,* only, and may not be distributed to third parties.

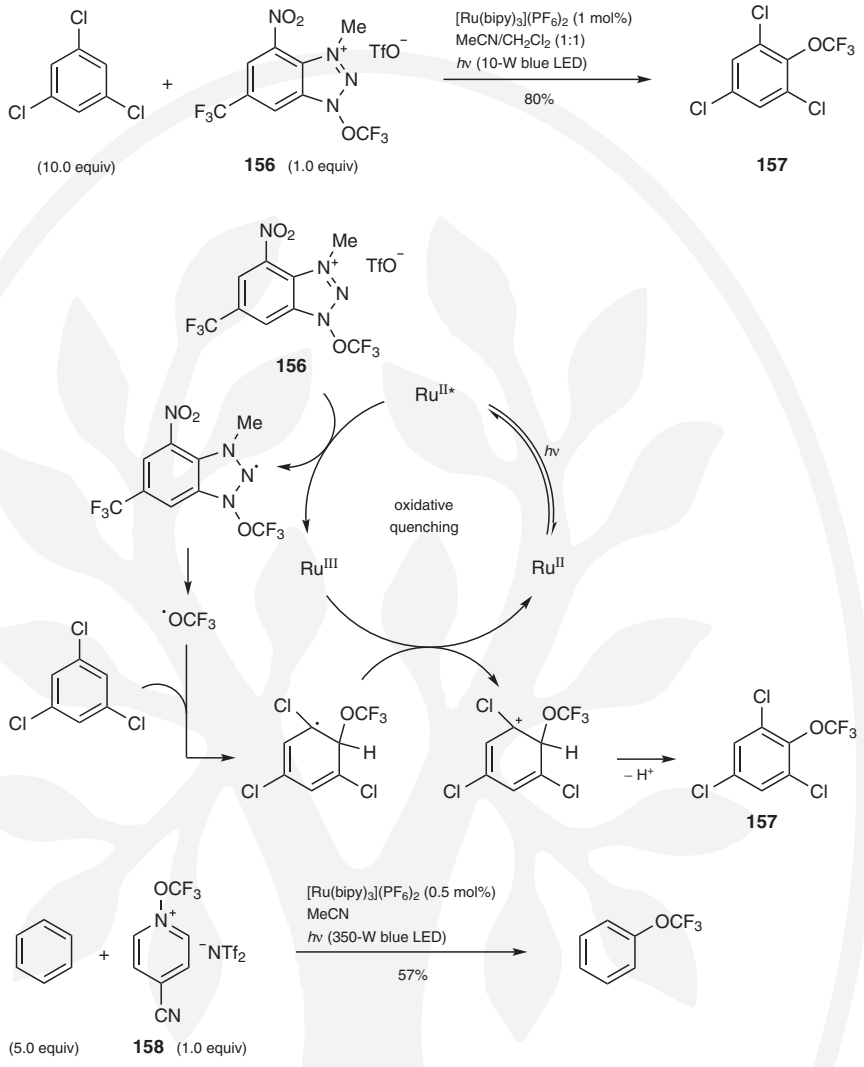

In 2019, the Ngai group developed the difluoromethoxylation of arenes using the difluoromethoxylating reagent **159**, which is analogous to trifluoromethoxylating reagent **156** (Scheme 47).[125] The reaction mechanism is similar to that of the trifluoromethoxylation depicted in Scheme 46.

Scheme 47 Visible-Light-Induced Difluoromethoxylation of Arenes[125]

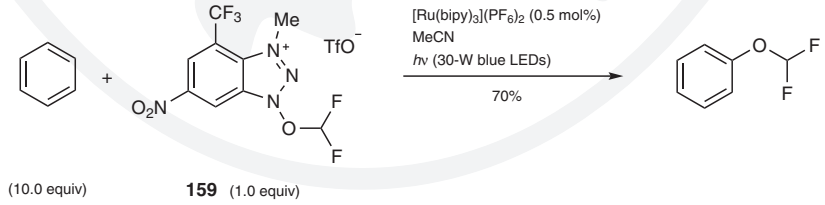

Copyright © 2021 Georg Thieme Verlag KG, Stuttgart, Germany. All rights reserved. This document is for the personal use of – Professor Yiyun Chen – Chinese Academy of Sciences, Shanghai, China, only, and may not be distributed to third parties.

1,3,5-Trichloro-2-(trifluoromethoxy)benzene (157):[123]
In a glovebox, 1-(trifluoromethoxy)-1*H*-benzo[*d*][1,2,3]triazol-3-ium trifluoromethanesulfonate **156** (98 mg, 0.20 mmol, 1.0 equiv), 1,3,5-trichlorobenzene (2.0 mmol, 10.0 equiv), and $[Ru(bipy)_3](PF_6)_2$ (1.72 mg, 2.0 μmol, 1.0 mol%) were added to an oven-dried 20-mL screw-cap vial. MeCN (0.5 mL), CH_2Cl_2 (0.5 mL), and a magnetic stirrer bar were added. The vial was capped and taken out of the glovebox. The mixture was then stirred and irradiated with two 10-W LEDs (λ_{max} = 447 nm) at rt for 16 h. The solvent was removed under reduced pressure and the crude material was purified by HPLC [Luna PFP(2) preparative column (250 × 21.2 mm), MeCN/H_2O 65:35, flow rate 10 mL/min, t_R 35 min]; yield: 80%.

1.9.3.3 Phenoxyl Radicals

1.9.3.3.1 Traditional Phenoxyl Radical Generation and Functionalization

Phenol derivatives are widely utilized as free-radical scavengers in living organisms, in which antioxidant activity is reflected as the effective hydrogen-atom transfer (HAT) from the oxidants.[126] Phenols undergo hydrogen abstraction with nitroxides,[127] peroxyl,[128] alkoxyl,[129] nitrogen-centered,[130] and carbon-centered radicals[131] to generate the phenoxyl radicals (Scheme 48). However, harsh reaction conditions are usually required, which makes the subsequent functionalization of phenoxyl radicals difficult. Recently, phenoxyl radicals have been proposed as reactive intermediates for intramolecular imine additions[132] and intermolecular radical/radical coupling reactions (Scheme 48).[133–135]

Scheme 48 Traditional Phenoxyl Radical Generation

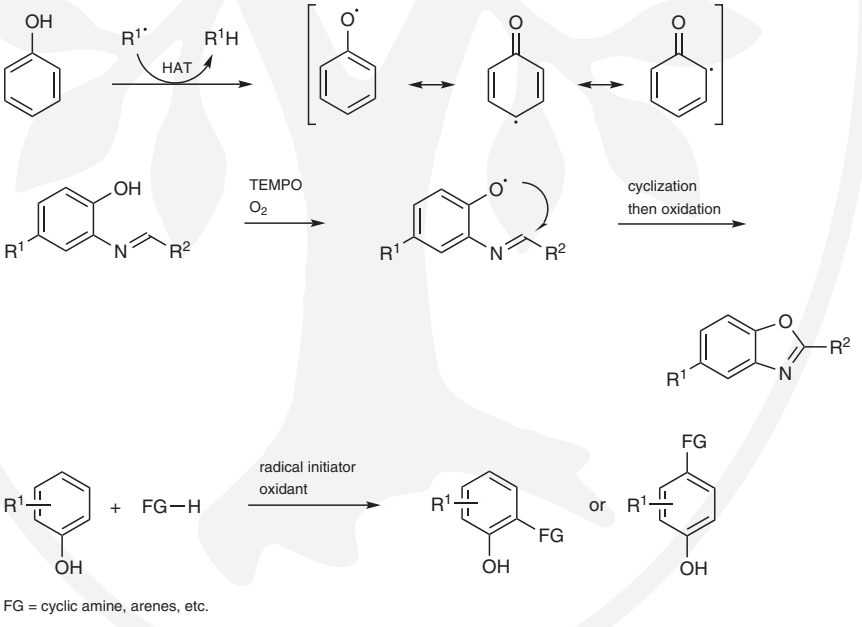

1.9.3.3.2 Electrochemical Phenoxyl Radical Generation and Functionalization

The use of electrochemical methods enables generation of phenoxyl radicals and subsequent formation of C—C and C—X bonds. In 2009, the Waldvogel group reported anodic phenol/arene cross-coupling reactions on boron-doped diamond (BDD) electrodes, albeit in low yields and with poor selectivity (Scheme 49).[136] In 2012, they optimized the solvent

for references see p 377

Copyright © 2021 Georg Thieme Verlag KG, Stuttgart, Germany. All rights reserved. This document is for the personal use of – **Professor Yiyun Chen** – *Chinese Academy of Sciences, Shanghai, China,* only, and may not be distributed to third parties.

to a mixture of 1,1,1,3,3,3-hexafluoropropan-2-ol and methanol, which significantly decreased the formation of homocoupling byproducts (Scheme 49).[137] Subsequently, they found that the ratio of the mixed solvent affected the oxidation potentials of the substrates to facilitate the formation of the polar-matched intermediates for better regioselectivity.[138] They later reported the electrochemical cross coupling of phenols with thiophenes[139] and benzothiophenes[140] by conducting the reaction in a single undivided cell, in a process which is scalable and inherently safe (Scheme 49).

In 2019, the Chen group reported the electrochemical regioselective coupling between phenols and aniline derivatives with excellent scalability. For example, the reaction of 4-methoxyphenol and 1*H*-pyrazole produces 4-methoxy-2-(1*H*-pyrazol-1-yl)phenol (**160**) in 97% yield. Mechanistic studies indicated that a radical/radical combination is involved (Scheme 49).[141]

Scheme 49 Electrochemical Cross Coupling of Phenols and Arenes[136–141]

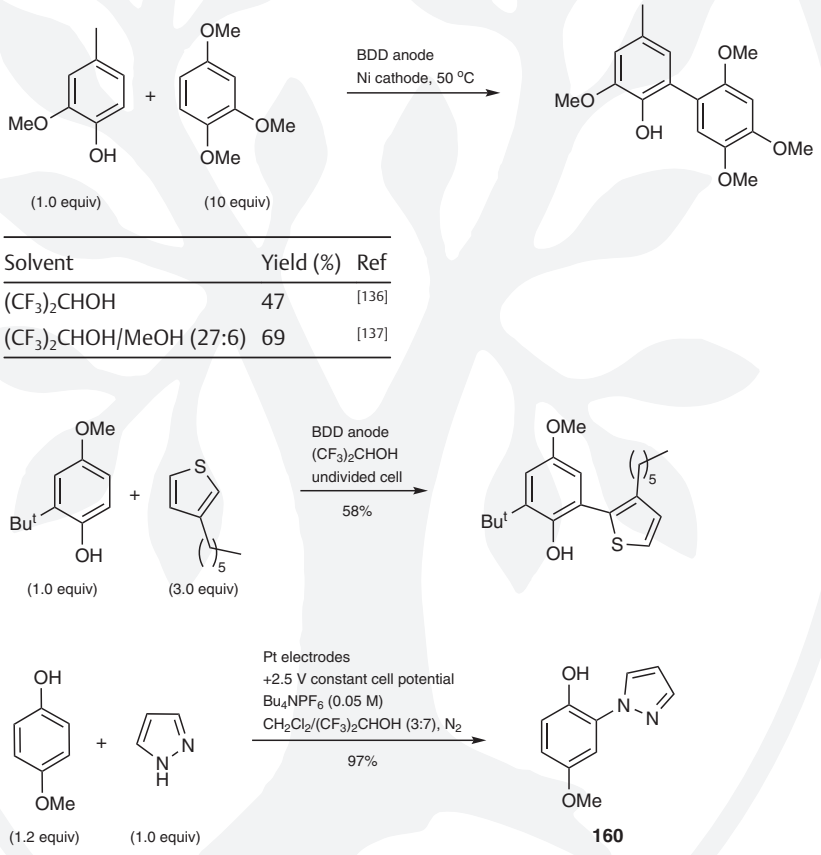

Solvent	Yield (%)	Ref
$(CF_3)_2CHOH$	47	[136]
$(CF_3)_2CHOH$/MeOH (27:6)	69	[137]

4-Methoxy-2-(1*H*-pyrazol-1-yl)phenol (160):[141]
A soln of 4-methoxyphenol (0.6 mmol), 1*H*-pyrazole (0.5 mmol), and Bu_4NPF_6 (0.5 mmol) in $(CF_3)_2CHOH/CH_2Cl_2$ (7:3; 10.0 mL) was stirred at 23 °C under N_2 in a three-necked bottle equipped with platinum plate electrodes (1.0 cm × 1.0 cm × 0.1 mm) as both the anode and cathode. The mixture was stirred and electrolyzed at a constant cell potential of 2.5 V until the disappearance of 1*H*-pyrazole (TLC plate under UV lamp or using I_2 staining). The mixture was directly concentrated under reduced pressure and the residue was purified by chromatography (silica gel, petroleum ether/EtOAc) to afford the pure product; yield: 97%.

Copyright © 2021 Georg Thieme Verlag KG, Stuttgart, Germany. All rights reserved. This document is for the personal use of – Professor Yiyun Chen – *Chinese Academy of Sciences, Shanghai, China,* only, and may not be distributed to third parties.

1.9.3.3.3 Visible-Light-Induced Phenoxyl Radical Generation and Functionalization

In 2016, the Xia group reported the visible-light-induced cross-dehydrogenative coupling reaction of phenols (e.g., **162**) and cyclic anilines (e.g., **161**).[142] Potassium persulfate serves as an external oxidant after light excitation for the radical/radical cross-coupling reaction (Scheme 50).

In 2017, they extended the scope of acyclic anilines by using organic photocatalysts (e.g., **163**) and improved the coupling efficiency of electron-deficient substrates. For example, 2-(di-4-tolylamino)-4-methoxyphenol (**164**) is obtained in 32% yield (62% based on recovered starting material) with 2,4,6-triphenylpyrylium tetrafluoroborate (**163**) as photocatalyst (Scheme 50).[143] A radical reaction pathway was confirmed by electron paramagnetic resonance experiments.

Scheme 50 Visible-Light-Induced Cross Coupling of Phenols and Anilines[142,143]

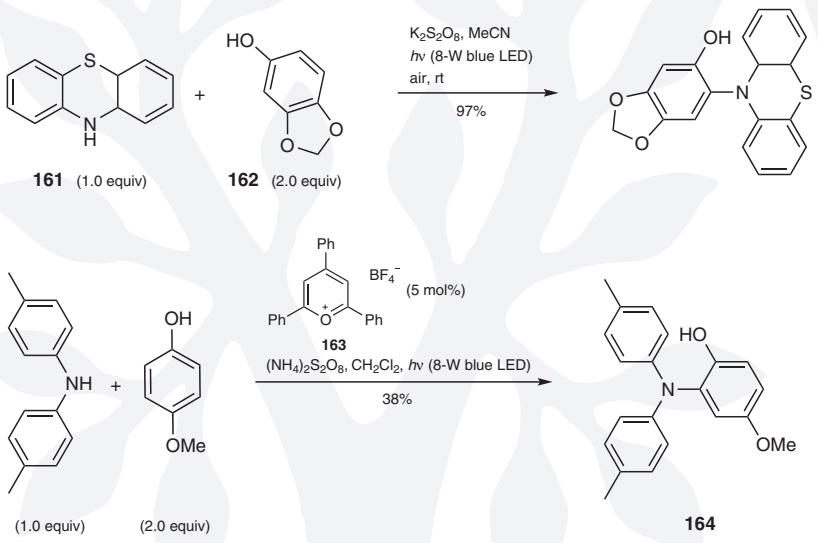

1.9.3.4 Vinyloxyl Radicals

Vinyloxyl radicals are similar to phenoxyl radicals regarding the resonance structure and typically behave like α-carbonyl methylene radicals. In 2018, the Feng group reported the radical transfer addition of *O*-vinylhydroxylamine derivatives (e.g., **166**) with unactivated alkenes in the presence of iridium complex **165**.[144] The excited iridium(III) species undergoes triplet energy transfer with the *O*-vinylhydroxylamine **166**, which subsequently undergoes N—O bond cleavage to yield the O- and N-centered radicals. The N-centered radical undergoes addition to ethyl vinyl ether to give carbon-centered radical **168**, which reacts with another molecule of *O*-vinylhydroxylamine **166**. The formed carbon-centered radical **169** then releases additional N-centered radical to continue the chain reaction while also producing the ketone product **167** (Scheme 51).

In 2019, the Hong group reported *N*-vinyloxypyridinum salts (e.g., **170**) for the generation of α-carbonyl methylene radicals (e.g., **173**).[145] The *N*-vinyloxypyridinum salt **170** is reduced by an excited iridium(III)* species to give the vinyloxyl radical **172**, which resonates to the α-carbonyl methylene radical **173** and then reacts with an alkene. The resulting carbon-centered radical **174** reacts with another molecule of *N*-vinyloxypyridinum salt **170** to give the γ-pyridinyl ketone product **171** after deprotonation and release of the O-centered radical **172** for the chain reaction (Scheme 51).

for references see p 377

Copyright © 2021 Georg Thieme Verlag KG, Stuttgart, Germany. All rights reserved. This document is for the personal use of – **Professor Yiyun Chen** – *Chinese Academy of Sciences, Shanghai, China,* only, and may not be distributed to third parties.

Scheme 51 Visible-Light-Induced Vinyloxyl Radical Reactions[144,145]

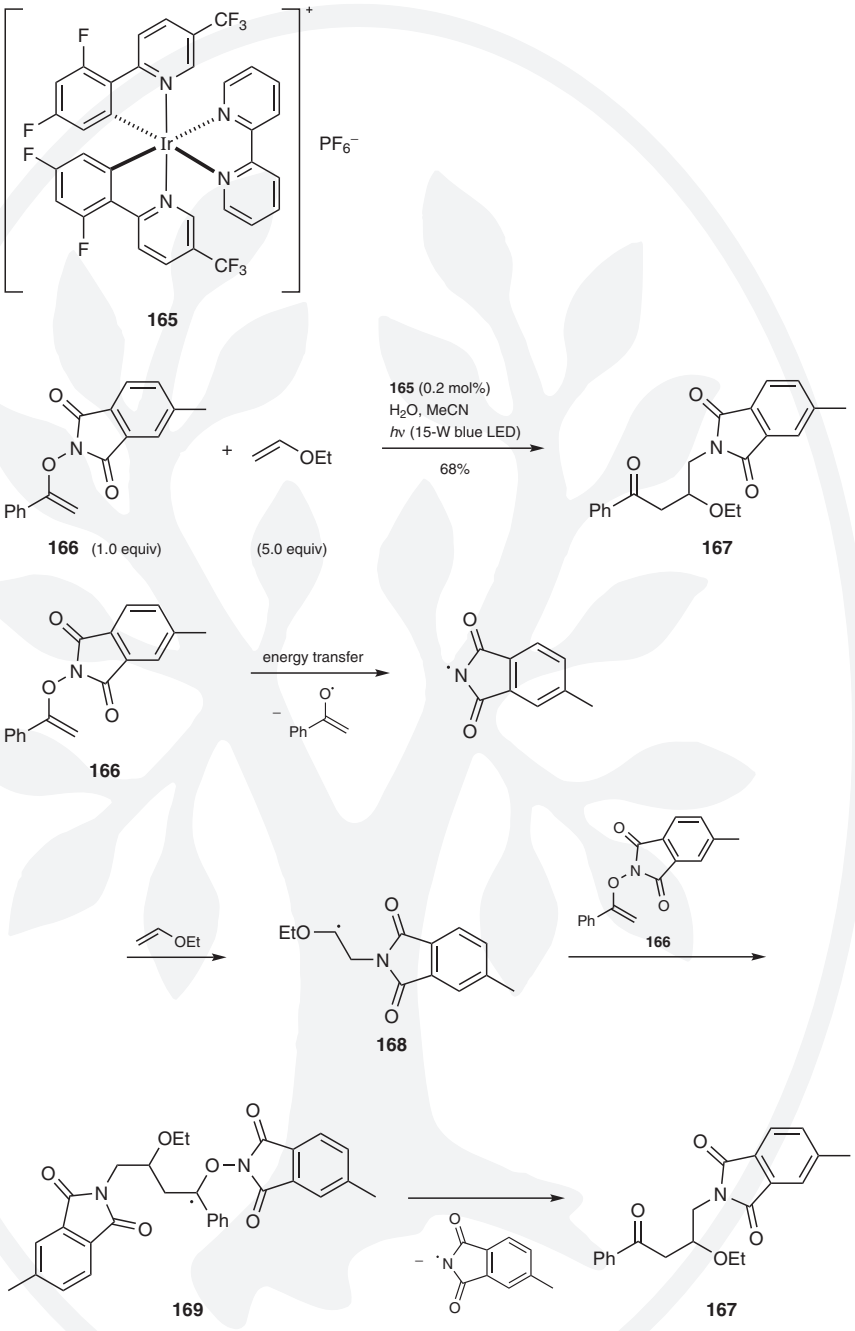

Copyright © 2021 Georg Thieme Verlag KG, Stuttgart, Germany. All rights reserved. This document is for the personal use of – **Professor Yiyun Chen** – *Chinese Academy of Sciences, Shanghai, China*, only, and may not be distributed to third parties.

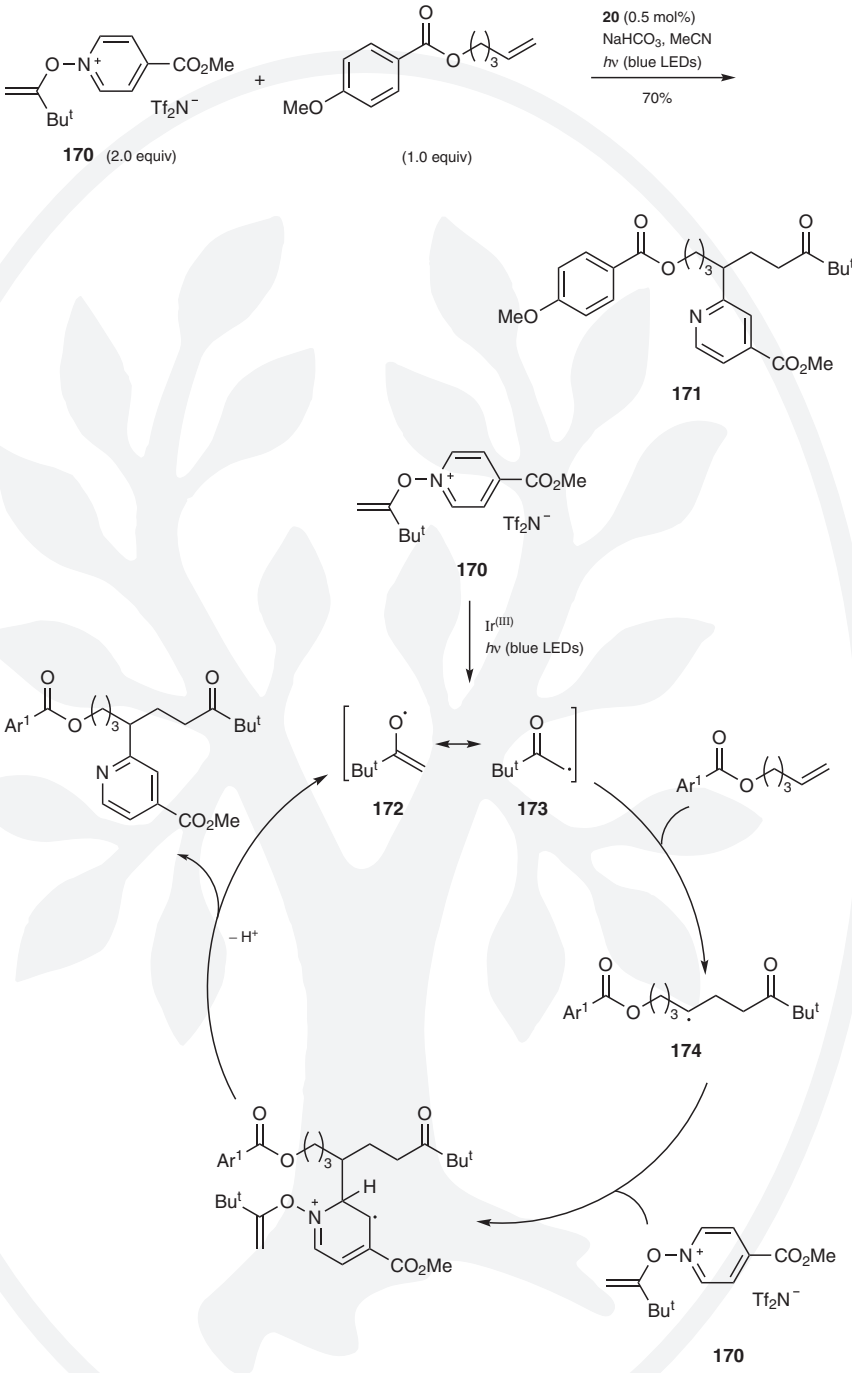

for references see p 377

Copyright © 2021 Georg Thieme Verlag KG, Stuttgart, Germany. All rights reserved. This document is for the personal use of – **Professor Yiyun Chen** – *Chinese Academy of Sciences, Shanghai, China*, only, and may not be distributed to third parties.

1.9.4 Conclusion

Significant progress has recently been reported regarding the generation and reactivity of oxygen-centered radicals. The hydrogen-atom transfer (HAT) and β-fragmentation reactivity demonstrated by carboxyl and alkoxyl radicals yields stable carbon-centered radicals, and the new visible-light photocatalysis reaction conditions have thereafter enabled many new carbon—carbon and carbon—heteroatom bond formations. It is anticipated that the mild reaction conditions of visible-light photocatalysis will inspire new reactivity of oxygen-centered radicals in the near future.

Copyright © 2021 Georg Thieme Verlag KG, Stuttgart, Germany. All rights reserved. This document is for the personal use of – **Professor Yiyun Chen** – *Chinese Academy of Sciences, Shanghai, China,* only, and may not be distributed to third parties.

References

[1] Hartung, J.; Gottwald, T.; Špehar, K., *Synthesis*, (2002), 1469.
[2] Čeković, Ž., *J. Serb. Chem. Soc.*, (2005) **70**, 287.
[3] Chiba, S.; Chen, H., *Org. Biomol. Chem.*, (2014) **12**, 4051.
[4] Guo, S. R.; Kumar, P. S.; Yang, M. H., *Adv. Synth. Catal.*, (2017) **359**, 2.
[5] Hartung, J., *Eur. J. Org. Chem.*, (2001), 619.
[6] Stateman, L. M.; Nakafuku, K. M.; Nagib, D. A., *Synthesis*, (2018) **50**, 1569.
[7] Motherwell, W. B.; Crich, D., *Free Radical Chain Reactions in Organic Synthesis*, Academic: London, (1992).
[8] *Oxygen Radicals in Chemistry and Biology*, Bors, W.; Saran, M.; Tait, D., Eds., de Gruyter: Berlin, (1984).
[9] Blanksby, S. J.; Ellison, G. B., *Acc. Chem. Res.*, (2003) **36**, 255.
[10] Togo, H.; Katohgi, M., *Synlett*, (2001), 565.
[11] Narayanam, J. M. R.; Stephenson, C. R. J., *Chem. Soc. Rev.*, (2011) **40**, 102.
[12] Prier, C. K.; Rankic, D. A.; MacMillan, D. W. C., *Chem. Rev.*, (2013) **113**, 5322.
[13] Reckenthaler, M.; Griesbeck, A. G., *Adv. Synth. Catal.*, (2013) **355**, 2727.
[14] Staveness, D.; Bosque, I.; Stephenson, C. R. J., *Acc. Chem. Res.*, (2016) **49**, 2295.
[15] Xuan, J.; Xiao, W. J., *Angew. Chem. Int. Ed.*, (2012) **51**, 6828.
[16] Xuan, J.; Zhang, Z. G.; Xiao, W. J., *Angew. Chem. Int. Ed.*, (2015) **54**, 15632.
[17] Guo, J.-J.; Hu, A. H.; Zuo, Z. W., *Tetrahedron Lett.*, (2018) **59**, 2103.
[18] Roslin, S.; Odell, L. R., *Eur. J. Org. Chem.*, (2017), 1993.
[19] Jia, K. F.; Chen, Y. Y., *Chem. Commun. (Cambridge)*, (2018) **54**, 6105.
[20] Guo, L.-N.; Wang, H.; Duan, X.-H., *Org. Biomol. Chem.*, (2016) **14**, 7380.
[21] Yan, M.; Kawamata, Y.; Baran, P. S., *Chem. Rev.*, (2017) **117**, 13230.
[22] Rowlands, G. J., *Tetrahedron*, (2010) **66**, 1593.
[23] Čeković, Ž., *Tetrahedron*, (2003) **59**, 8073.
[24] Francisco, C. G.; Herrera, A. J.; Suárez, E., *J. Org. Chem.*, (2002) **67**, 7439.
[25] Serguchev, Y. A.; Beletskaya, I. P., *Russ. Chem. Rev. (Engl. Transl.)*, (1980) **49**, 1119.
[26] Hunsdiecker, H.; Hunsdiecker, C.; Vogt, E., US 2176181, (1939).
[27] Hunsdiecker, H.; Hunsdiecker, C.; Vogt, E., *Chem. Abstr.*, (1940) **34**, 1685.
[28] Hunsdiecker, C.; Hunsdiecker, H., *Ber. Dtsch. Chem. Ges. B*, (1942) **75**, 291.
[29] Barton, D. H. R.; Crich, D.; Motherwell, W. B., *J. Chem. Soc., Chem. Commun.*, (1983), 939.
[30] Barton, D. H. R.; Crich, D.; Motherwell, W. B., *Tetrahedron Lett.*, (1983) **24**, 4979.
[31] Barton, D. H. R.; Serebryakov, E. P., *Proc. Chem. Soc., London*, (1962), 309.
[32] Okada, K.; Okamoto, K.; Morita, N.; Okubo, K.; Oda, M., *J. Am. Chem. Soc.*, (1991) **113**, 9401.
[33] Schnermann, M. J.; Overman, L. E., *Angew. Chem. Int. Ed.*, (2012) **51**, 9576.
[34] Xie, J.; Xu, P.; Li, H. M.; Xue, Q. C.; Jin, H. M.; Cheng, Y. X.; Zhu, C. J., *Chem. Commun. (Cambridge)*, (2013) **49**, 5672.
[35] Yang, J.; Zhang, J.; Qi, L.; Hu, C. C.; Chen, Y. Y., *Chem. Commun. (Cambridge)*, (2015) **51**, 5275.
[36] Hu, C. C.; Chen, Y. Y., *Org. Chem. Front.*, (2015) **2**, 1352.
[37] Li, J. J.; Tian, H.; Jiang, M.; Yang, H. J.; Zhao, Y. F.; Fu, H., *Chem. Commun. (Cambridge)*, (2016) **52**, 8862.
[38] Zuo, Z. W.; Ahneman, D. T.; Chu, L. L.; Terrett, J. A.; Doyle, A. G.; MacMillan, D. W. C., *Science (Washington, D. C.)*, (2014) **345**, 437.
[39] Noble, A.; McCarver, S. J.; MacMillan, D. W. C., *J. Am. Chem. Soc.*, (2015) **137**, 624.
[40] Johnston, C. P.; Smith, R. T.; Allmendinger, S.; MacMillan, D. W. C., *Nature (London)*, (2016) **536**, 322.
[41] Zhou, Q. Q.; Guo, W.; Ding, W.; Wu, X.; Chen, X.; Lu, L. Q.; Xiao, W. J., *Angew. Chem. Int. Ed.*, (2015) **54**, 11196.
[42] Le Vaillant, F.; Courant, T.; Waser, J., *Angew. Chem. Int. Ed.*, (2015) **54**, 11200.
[43] Griffin, J. D.; Zeller, M. A.; Nicewicz, D. A., *J. Am. Chem. Soc.*, (2015) **137**, 11340.
[44] Ventre, S.; Petronijevic, F. R.; MacMillan, D. W. C., *J. Am. Chem. Soc.*, (2015) **137**, 5654.
[45] Candish, L.; Standley, E. A.; Gómez-Suárez, A.; Mukherjee, S.; Glorius, F., *Chem.–Eur. J.*, (2016) **22**, 9971.
[46] Xiang, J. B.; Shang, M.; Kawamata, Y.; Lundberg, H.; Reisberg, S. H.; Chen, M.; Mykhailiuk, P.; Beutner, G.; Collins, M. R.; Davies, A.; Del Bel, M.; Gallego, G. M.; Spangler, J. E.; Starr, J.; Yang, S. L.; Blackmond, D. G.; Baran, P. S., *Nature (London)*, (2019) **573**, 398.

Copyright © 2021 Georg Thieme Verlag KG, Stuttgart, Germany. All rights reserved. This document is for the personal use of – **Professor Yiyun Chen** – *Chinese Academy of Sciences, Shanghai, China,* only, and may not be distributed to third parties.

[47] Liu, J.; Liu, Q.; Yi, H.; Qin, C.; Bai, R. P.; Qi, X. T.; Lan, Y.; Lei, A. W., *Angew. Chem. Int. Ed.*, (2014) **53**, 502.
[48] Chu, L. L.; Lipshultz, J. M.; MacMillan, D. W. C., *Angew. Chem. Int. Ed.*, (2015) **54**, 7929.
[49] Cheng, W. M.; Shang, R.; Yu, H. Z.; Fu, Y., *Chem.–Eur. J.*, (2015) **21**, 13191.
[50] Fang, P.; Li, M. Z.; Ge, H. B., *J. Am. Chem. Soc.*, (2010) **132**, 11898.
[51] Zhou, C.; Li, P. H.; Zhu, X. J.; Wang, L., *Org. Lett.*, (2015) **17**, 6198.
[52] Huang, H. C.; Zhang, G. J.; Chen, Y. Y., *Angew. Chem. Int. Ed.*, (2015) **54**, 7872.
[53] Tan, H.; Li, H. J.; Ji, W. Q.; Wang, L., *Angew. Chem. Int. Ed.*, (2015) **54**, 8374.
[54] Li, J. Z.; Liu, Z. Y.; Wu, S.; Chen, Y. Y., *Org. Lett.*, (2019) **21**, 2077.
[55] Zhang, H. H.; Yu, S. Y., *Org. Lett.*, (2019) **21**, 3711.
[56] Ramirez, N. P.; Bosque, I.; Gonzalez-Gomez, J. C., *Org. Lett.*, (2015) **17**, 4550.
[57] Mukherjee, S.; Maji, B.; Tlahuext-Aca, A.; Glorius, F., *J. Am. Chem. Soc.*, (2016) **138**, 16200.
[58] Chateauneuf, J.; Lusztyk, J.; Ingold, K. U., *J. Am. Chem. Soc.*, (1988) **110**, 2886.
[59] Candish, L.; Freitag, M.; Gensch, T.; Glorius, F., *Chem. Sci.*, (2017) **8**, 3618.
[60] Wang, S. F.; Cao, X. P.; Li, Y., *Angew. Chem. Int. Ed.*, (2017) **56**, 13809.
[61] Li, Y.; Zhang, J.; Li, D. F.; Chen, Y. Y., *Org. Lett.*, (2018) **20**, 3296.
[62] Barton, D. H. R.; Beaton, J. M.; Geller, L. E.; Pechet, M. M., *J. Am. Chem. Soc.*, (1960) **82**, 2640.
[63] Vite, G. D.; Fraserreid, B., *Synth. Commun.*, (1988) **18**, 1339.
[64] Walling, C.; Clark, R. T., *J. Am. Chem. Soc.*, (1974) **96**, 4530.
[65] Beckwith, A. L. J.; Hay, B. P.; Williams, G. M., *J. Chem. Soc., Chem. Commun.*, (1989), 1202.
[66] Beckwith, A. L. J.; Hay, B. P., *J. Am. Chem. Soc.*, (1988) **110**, 4415.
[67] Kim, S.; Lee, T. A.; Song, Y., *Synlett*, (1998), 471.
[68] Zhang, J.; Li, Y.; Zhang, F. Y.; Hu, C. C.; Chen, Y. Y., *Angew. Chem. Int. Ed.*, (2016) **55**, 1872.
[69] Jia, K. F.; Zhang, F. Y.; Huang, H. C.; Chen, Y. Y., *J. Am. Chem. Soc.*, (2016) **138**, 1514.
[70] Curran, D. P.; Shen, W., *J. Am. Chem. Soc.*, (1993) **115**, 6051.
[71] Francisco, C. G.; Freire, R.; Herrera, A. J.; Perez-Martin, I.; Suárez, E., *Org. Lett.*, (2002) **4**, 1959.
[72] Francisco, C. G.; Freire, R.; Herrera, A. J.; Perez-Martin, I.; Suárez, E., *Tetrahedron*, (2007) **63**, 8910.
[73] Leon, E. I.; Martin, A.; Perez-Martin, I.; Quintanal, L. M.; Suárez, E., *Eur. J. Org. Chem.*, (2012), 3818.
[74] Martin, A.; Perez-Martin, I.; Quintanal, L. M.; Suárez, E., *Tetrahedron Lett.*, (2008) **49**, 5179.
[75] Petrović, G.; Čeković, Ž., *Tetrahedron Lett.*, (1997) **38**, 627.
[76] Deng, Y. F.; Nguyen, M. D.; Zou, Y. K.; Houk, K. N.; Smith, A. B., III, *Org. Lett.*, (2019) **21**, 1708.
[77] Wang, C. Y.; Harms, K.; Meggers, E., *Angew. Chem. Int. Ed.*, (2016) **55**, 13495.
[78] Quint, V.; Morlet-Savary, F.; Lohier, J.-F.; Lalevée, J.; Gaumont, A.-C.; Lakhdar, S., *J. Am. Chem. Soc.*, (2016) **138**, 7436.
[79] Wu, X. X.; Wang, M. Y.; Huan, L. T.; Wang, D. P.; Wang, J. W.; Zhu, C., *Angew. Chem. Int. Ed.*, (2018) **57**, 1640.
[80] Wu, X. X.; Zhang, H.; Tang, N. N.; Wu, Z.; Wang, D. P.; Ji, M. S.; Xu, Y.; Wang, M.; Zhu, C., *Nat. Commun.*, (2018) **9**, 3343.
[81] Wang, M.; Huan, L. T.; Zhu, C., *Org. Lett.*, (2019) **21**, 821.
[82] Hu, A. H.; Guo, J.-J.; Pan, H.; Tang, H. M.; Gao, Z. B.; Zuo, Z. W., *J. Am. Chem. Soc.*, (2018) **140**, 1612.
[83] Kim, I.; Park, B.; Kang, G.; Kim, J.; Jung, H.; Lee, H.; Baik, M.-H.; Hong, S., *Angew. Chem. Int. Ed.*, (2018) **57**, 15517.
[84] Li, G. X.; Hu, X. F.; He, G.; Chen, G., *Chem. Sci.*, (2019) **10**, 688.
[85] Bao, X.; Wang, Q.; Zhu, J. P., *Angew. Chem. Int. Ed.*, (2019) **58**, 2139.
[86] Bao, X.; Wang, Q.; Zhu, J. P., *Chem.–Eur. J.*, (2019) **25**, 11630.
[87] Buszek, R. J.; Sinha, A.; Francisco, J. S., *J. Am. Chem. Soc.*, (2011) **133**, 2013.
[88] Elford, P. E.; Roberts, B. P., *J. Chem. Soc., Perkin Trans. 2*, (1996), 2247.
[89] Fernández-Ramos, A.; Zgierski, M. Z., *J. Phys. Chem. A*, (2002) **106**, 10578.
[90] Konya, K. G.; Paul, T.; Lin, S. Q.; Lusztyk, J.; Ingold, K. U., *J. Am. Chem. Soc.*, (2000) **122**, 7518.
[91] Gilbert, B. C.; Holmes, R. G. G.; Laue, H. A. H.; Norman, R. O. C., *J. Chem. Soc., Perkin Trans. 2*, (1976), 1047.
[92] Che, C.; Qian, Z. S.; Wu, M. C.; Zhao, Y.; Zhu, G. G., *J. Org. Chem.*, (2018) **83**, 5665.
[93] Zhang, J.; Liu, D.; Liu, S.; Ge, Y. Y.; Lan, Y.; Chen, Y. Y., *iScience*, (2020) **23**, 100755.
[94] Hu, X. F.; Li, G. X.; He, G.; Chen, G., *Org. Chem. Front.*, (2019) **6**, 3205.
[95] Yayla, H. G.; Wang, H. J.; Tarantino, K. T.; Orbe, H. S.; Knowles, R. R., *J. Am. Chem. Soc.*, (2016) **138**, 10794.
[96] Guo, J.-J.; Hu, A. H.; Chen, Y. L.; Sun, J. F.; Tang, H. M.; Zuo, Z. W., *Angew. Chem. Int. Ed.*, (2016) **55**, 15319.

Copyright © 2021 Georg Thieme Verlag KG, Stuttgart, Germany. All rights reserved. This document is for the personal use of – **Professor Yiyun Chen** – *Chinese Academy of Sciences, Shanghai, China,* only, and may not be distributed to third parties.

[97] Zhang, K. N.; Chang, L.; An, Q.; Wang, X.; Zuo, Z., *J. Am. Chem. Soc.*, (2019) **141**, 10556.
[98] Zhang, J.; Li, Y.; Xu, R. Y.; Chen, Y. Y., *Angew. Chem. Int. Ed.*, (2017) **56**, 12619.
[99] Ito, Y.; Kimura, A.; Osawa, T.; Hari, Y., *J. Org. Chem.*, (2018) **83**, 10701.
[100] Shi, J. L.; Wang, Z. X.; Zhang, R.; Wang, Y. K.; Wang, J. B., *Chem.–Eur. J.*, (2019) **25**, 8992.
[101] Bentrude, W. G.; Darnall, K. R., *J. Am. Chem. Soc.*, (1968) **90**, 3588.
[102] Sawaki, Y.; Ogata, Y., *J. Am. Chem. Soc.*, (1976) **98**, 7324.
[103] Kim, S.; Cho, C. H.; Lim, C. J., *J. Am. Chem. Soc.*, (2003) **125**, 9574.
[104] Jia, K. F.; Pan, Y.; Chen, Y. Y., *Angew. Chem. Int. Ed.*, (2017) **56**, 2478.
[105] Jia, K. F.; Li, J. Z.; Chen, Y. Y., *Chem.–Eur. J.*, (2018) **24**, 3174.
[106] Barthelemy, A. L.; Tuccio, B.; Magnier, E.; Dagousset, G., *Angew. Chem. Int. Ed.*, (2018) **57**, 13790.
[107] Kim, Y.; Lee, K.; Mathi, G. R.; Kim, I.; Hong, S., *Green Chem.*, (2019) **21**, 2082.
[108] Tebben, L.; Studer, A., *Angew. Chem. Int. Ed.*, (2011) **50**, 5034.
[109] Thomas, J. R., *J. Am. Chem. Soc.*, (1964) **86**, 1446.
[110] Han, B.; Yang, X. L.; Fang, R.; Yu, W.; Wang, C.; Duan, X. Y.; Liu, S., *Angew. Chem. Int. Ed.*, (2012) **51**, 8816.
[111] Pratt, D. A.; Blake, J. A.; Mulder, P.; Walton, J. C.; Korth, H. G.; Ingold, K. U., *J. Am. Chem. Soc.*, (2004) **126**, 10667.
[112] Berti, C.; Grierson, L.; Grimes, J. A. M.; Perkins, M. J.; Terem, B., *Angew. Chem. Int. Ed. Engl.*, (1990) **29**, 653.
[113] Schmidt, V. A.; Alexanian, E. J., *Angew. Chem. Int. Ed.*, (2010) **49**, 4491.
[114] Schmidt, V. A.; Alexanian, E. J., *J. Am. Chem. Soc.*, (2011) **133**, 11402.
[115] Hu, X.-Q.; Chen, J.; Chen, J.-R.; Yan, D.-M.; Xiao, W.-J., *Chem.–Eur. J.*, (2016) **22**, 14141.
[116] Yang, S.; Wang, L.; Wang, L.; Li, H., *J. Org. Chem.*, (2020) **85**, 564.
[117] Jeschke, P.; Baston, E.; Leroux, F. R., *Mini-Rev. Med. Chem.*, (2007), 1027.
[118] Leroux, F.; Jeschke, P.; Schlosser, M., *Chem. Rev.*, (2005) **105**, 827.
[119] Peláez, W. J.; Argüello, G. A., *Tetrahedron Lett.*, (2010) **51**, 5242.
[120] Venturini, F.; Navarrini, W.; Famulari, A.; Sansotera, M.; Dardani, P.; Tortelli, V., *J. Fluorine Chem.*, (2012) **140**, 43.
[121] Lee, J. W.; Lee, K. N.; Ngai, M.-Y., *Angew. Chem. Int. Ed.*, (2019) **58**, 11171.
[122] Zheng, W.; Morales-Rivera, C. A.; Lee, J. W.; Liu, P.; Ngai, M.-Y., *Angew. Chem. Int. Ed.*, (2018) **57**, 9645.
[123] Zheng, W.; Lee, J. W.; Morales-Rivera, C. A.; Liu, P.; Ngai, M.-Y., *Angew. Chem. Int. Ed.*, (2018) **57**, 13795.
[124] Jelier, B. J.; Tripet, P. F.; Pietrasiak, E.; Franzoni, I.; Jeschke, G.; Togni, A., *Angew. Chem. Int. Ed.*, (2018) **57**, 13784.
[125] Lee, J. W.; Zheng, W.; Morales-Rivera, C. A.; Liu, P.; Ngai, M.-Y., *Chem. Sci.*, (2019) **10**, 3217.
[126] Burton, G. W.; Ingold, K. U., *Acc. Chem. Res.*, (1986) **19**, 194.
[127] Aliaga, C.; Aspee, A.; Scaiano, J. C., *Org. Lett.*, (2003) **5**, 4145.
[128] Burton, G. W.; Doba, T.; Gabe, E.; Hughes, L.; Lee, F. L.; Prasad, L.; Ingold, K. U., *J. Am. Chem. Soc.*, (1985) **107**, 7053.
[129] Das, P. K.; Encinas, M. V.; Steenken, S.; Scaiano, J. C., *J. Am. Chem. Soc.*, (1981) **103**, 4162.
[130] Ingold, K. U., In *Landolt Börnstein: Group II Molecules and Radicals: Radical Reaction Rates in Liquids*, Fisher, H., Ed.; Springer: Berlin, (1984); Vol. 13C.
[131] Franchi, P.; Lucarini, M.; Pedulli, G. F.; Valgimigli, L.; Lunelli, B., *J. Am. Chem. Soc.*, (1999) **121**, 507.
[132] Chen, Y. X.; Qian, L. F.; Zhang, W.; Han, B., *Angew. Chem. Int. Ed.*, (2008) **47**, 9330.
[133] Libman, A.; Shalit, H.; Vainer, Y.; Narute, S.; Kozuch, S.; Pappo, D., *J. Am. Chem. Soc.*, (2015) **137**, 11453.
[134] Goswami, M.; Konkel, A.; Rahimi, M.; Louillat-Habermeyer, M. L.; Kelm, H.; Jin, R.; de Bruin, B.; Patureau, F. W., *Chem.–Eur. J.*, (2018) **24**, 11936.
[135] Bering, L.; D'Ottavio, L.; Sirvinskaite, G.; Antonchick, A. P., *Chem. Commun. (Cambridge)*, (2018) **54**, 13022.
[136] Kirste, A.; Schnakenburg, G.; Stecker, F.; Fischer, A.; Waldvogel, S. R., *Angew. Chem. Int. Ed.*, (2009) **49**, 971.
[137] Kirste, A.; Elsler, B.; Schnakenburg, G.; Waldvogel, S. R., *J. Am. Chem. Soc.*, (2012) **134**, 3571.
[138] Elsler, B.; Wiebe, A.; Schollmeyer, D.; Dyballa, K. M.; Franke, R.; Waldvogel, S. R., *Chem.–Eur. J.*, (2015) **21**, 12321.
[139] Wiebe, A.; Lips, S.; Schollmeyer, D.; Franke, R.; Waldvogel, S. R., *Angew. Chem. Int. Ed.*, (2017) **56**, 14727.

Copyright © 2021 Georg Thieme Verlag KG, Stuttgart, Germany. All rights reserved. This document is for the personal use of – **Professor Yiyun Chen** – *Chinese Academy of Sciences, Shanghai, China,* only, and may not be distributed to third parties.

[140] Lips, S.; Schollmeyer, D.; Franke, R.; Waldvogel, S. R., *Angew. Chem. Int. Ed.*, (2018) **57**, 13325.
[141] Feng, P.; Ma, G.; Chen, X.; Wu, X.; Lin, L.; Liu, P.; Chen, T., *Angew. Chem. Int. Ed.*, (2019) **58**, 8400.
[142] Zhao, Y.; Huang, B.; Yang, C.; Xia, W., *Org. Lett.*, (2016) **18**, 3326.
[143] Zhao, Y.; Huang, B.; Yang, C.; Li, B.; Gou, B.; Xia, W., *ACS Catal.*, (2017) **7**, 2446.
[144] Zhang, Y.; Liu, H.; Tang, L.; Tang, H. J.; Wang, L.; Zhu, C.; Feng, C., *J. Am. Chem. Soc.*, (2018) **140**, 10695.
[145] Mathi, G. R.; Jeong, Y.; Moon, Y.; Hong, S., *Angew. Chem. Int. Ed.*, (2020) **59**, 2049.

Copyright © 2021 Georg Thieme Verlag KG, Stuttgart, Germany. All rights reserved. This document is for the personal use of – **Professor Yiyun Chen** – *Chinese Academy of Sciences, Shanghai, China,* only, and may not be distributed to third parties.